Review

Organoactinides in catalysis

Eyal Barnea, Moris S. Eisen *

Department of Chemistry and Institute of Catalysis Science and Technology, Technion-Israel Institute of Technology, Haifa 32000, Israel

Contents

* Corresponding author. Tel.: +972 48292680; fax: +972 48295703.
  E-mail address: chmoris@technix.technion.ac.il (M.S. Eisen).

Abstract

During the last three decades, organoactinide chemistry has flourished, reaching a high level of sophistication. The use of organoactinide complexes as stoichiometric or catalytic compounds to promote synthetically important organic transformation has grown-up due to their rich, complex, unique and highly informative organometallic chemistry. In many instances the regio- and chemo-selectivities displayed by organoactinide complexes are complementary to those observed for other transition-metal complexes. The reactivity of organoactinide complexes is based on their ability to perform unique bond-breaking and bond-forming reactions of distinct moieties. The factors influencing such processes are the steric and electronic effects. This review is aimed at a brief and selective survey of the catalytic chemistry of organoactinide complexes in homogeneous and heterogeneous catalytic reactions. A comprehensive review for the reactivities of actinide compounds has been published covering the literature until 1992. This review covers the new literature of the last decade, and will focus on the reactivity of organoactinide complexes as catalysts for demanding organic transformations. In the beginning the synthesis and characterization of organoactinide based complexes and catalysts will be presented, followed by a survey of organic transformation catalyzed by these organoactinides, including oligomerization, dimerization, hydrosilylation and hydroamination of terminal alkynes, coupling of isonitriles with terminal alkynes, polymerization of α-olefins, heterogeneous hydrogenation of arenes and more. For each reaction, the scope, kinetic, thermodynamic and mechanistic aspects are presented.
© 2006 Elsevier B.V. All rights reserved.

1. Introduction

During the last three decades, organoactinide chemistry has reached a high level of sophistication. The use of organoactinide complexes as stoichiometric or catalytic compounds to promote synthetically important organic transformations has grown-up due to their rich, complex, unique and highly informative organometallic chemistry. Among the unique features exhibited by actinides the first that should be pointed out is their very sizeable ionic radii, which give rise to large formal coordination numbers and unusual coordination geometries. The presence of 5f valence orbitals is another characteristic of actinides that differs distinctly from d-block elements. Taking into account these differences, when compared to early or late transition-metal complexes, the actinides exhibit parallel but mostly different reactivities for similar organic processes, sometimes challenging the activities of transition metals and shedding light on their unique reactivities. In many instances the regio- and chemo-selectivities displayed by organoactinide complexes are complementary to that observed for other transition-metal complexes. Several recent review articles [1–7] dealing mostly

with the synthesis of new actinide complexes confirm the broad and rapidly expanding scope of this field. One of the first examples for this type of unique catalytic activity was set in 1974 [8] when the homogeneous polymerization of butadiene catalyzed by U(η³-allyl)₃Cl in combination with Al(C₂H₅)Cl was carried out. This reaction produced poly-1,4-butadiene with higher *cis*-1,4 content (>98.5%) than was previously produced by conventional transition-metal organometallic catalysts. Polymer produced in this reaction had far superior mechanical and processing characteristics, due to the high *cis*-1,4 content. This review is aimed at a brief and selective survey of the catalytic chemistry of organoactinide complexes in homogeneous and heterogeneous catalytic reactions. A comprehensive review for the reactivities of actinide compounds has been published covering the literature until 1992 [9].

This review covers the new literature for the last decade, and will focus on the reactivity of organoactinide complexes as catalysts for demanding organic transformations. In the beginning the synthesis of the organoactinide catalysts will be presented, followed by a survey of organic transformation catalyzed by these organoactinides.

The reactivity of organoactinide complexes is based on their ability to perform bond-breaking and bond-forming reactions of distinct functional groups. The factors influencing such processes are the steric and electronic effects. With reference to steric hindrance, a number of articles have been devoted on the geometric control in organo-5f-complexes. Xing-Fu has developed a rule for a packaging saturation, indicating that the stability of a complex is governed by the sum of the ligand cone angles [10–12]. In this model highly coordinative "over-saturated" complexes will display low stability. An additional

model regarding steric environments has been proposed by Pires de Matos [13]. This model assumes pure ionic bonding, and is based on cone angles defining the term "steric coordination number". A more important and unique approach to the reactivity of organo-5f-complexes regards the utilization of thermochemical studies. The knowledge of the metal–ligand bond enthalpies is of fundamental importance to allow the estimation of new reaction pathways [14–21]. In addition, neutral organoactinides have been shown to follow a four-center transition state (Eq. (1)) due to the high-energy orbital impediment to undergo oxidative addition and reductive elimination. Such a transition state allows the predictions of new actinide reactivities, when taking into account the negative entropies of activation [22].

$$(1)$$
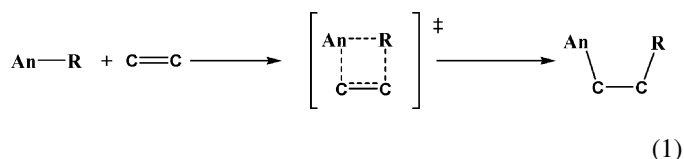
2. Synthesis of organoactinide catalysts

2.1. Synthesis of actinide (An(IV)) based complexes

In this review we will focus on the catalytic activity of several organoactinide complexes: the neutral metallocene–alkyl

complexes $Cp_2^*AnMe_2$ (An = Th (**1**) or U (**2**), $Cp^* = C_5Me_5$), $Me_2Si(C_5Me_4)_2AnR_2$ (**3**, An = Th, R = ^nBu; **4**, An = U, R = Me; **5**, An = U, R = $CH_2C_6H_5$), the cationic trisamido complex $[(NEt_2)_3U][BPh_4]$ (**6**).

The synthesis of the metallocene-like complexes **1** and **2** (Eq. (2)) was reported by Fagan et al. [23] and includes two major steps: (i) the reaction of the actinide chloride with two equivalent of Cp^*MgCl to yield the corresponding dichloride complex and (ii) reaction of the latter with two equivalent of MeLi to form the dimethyl complex. Despite the ease of the synthesis, the crystal structure for complex **2** was reported only recently [24].

$$An = Th\ (\mathbf{1}),\ U\ (\mathbf{2}) \qquad (2)$$

Since the stoichiometric and catalytic properties of organo-f-element complexes are profoundly influenced by the nature of the π ancillary ligands [25–29], opening the metal coordination sphere (frontier orbitals) [30] at the equatorial girdle where the σ-ligation is disposed was performed by using a bridge ligation as in the complex $ansa$-$Me_2Si(C_5Me_4)_2MR_2$ [31–34]. The effect of opening the coordination sphere in some catalytic processes can be observed for organolanthanides allowing an increase (10–100-fold) in rates for the olefin insertion into the M−R bond [32,33,35,36] and in organoactinides, this modification was shown to cause an increase (10^3-fold) in their catalytic activity for the hydrogenation of 1-hexene [34,36]. The complete syntheses of the complexes $Me_2Si(C_5Me_4)_2ThCl_2$ (**7**) and $Me_2Si(C_5Me_4)_2Th^nBu$ (**3**) have been performed as presented in Eq. (3) [36,37]. The complex $Me_2Si(C_5Me_4)_2ThCl_2$ was isolated in 82% yield with the salt lithium chloride as an adduct. Single crystal X-ray diffraction revealed a typical bent metallocene complex. The ring centroid–Th centroid angle (113.3°), is smaller than that observed in unhindered bis(pentamethylcyclopentadienyl) thorium complexes (130–138°) [38], and slightly smaller to the angle determined for the bridged thorium dialkyl complex $[Me_2Si(C_5Me_4)_2Th(CH_2SiMe_3)_2]$ (118.4°) [34]. The thorium–carbon (carbon = C_5Me_4 ring carbons) bond lengths are not equidistant having the shorter distance between the metal and the first carbon adjacent to the silicon bridge because of the strain generated by the Me_2Si-bridge as reported for other $ansa$ type of complexes [39].

$$(3)$$
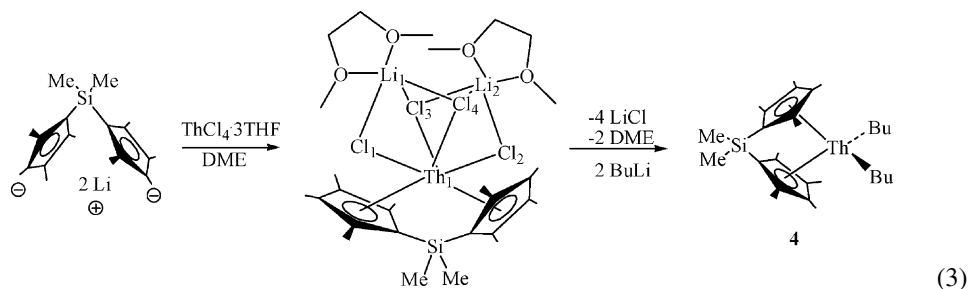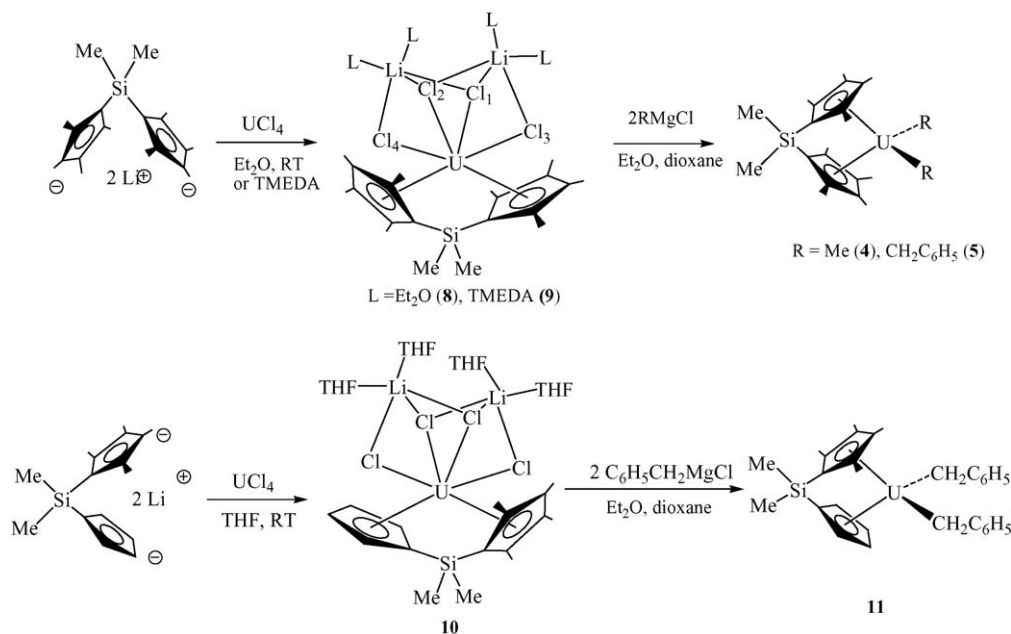
Scheme 1. Synthetic pathway for the preparation of *ansa*-organouranium complexes [40].

The X-ray analysis of complex **3** showed that two of the thorium–chloride bonds are shorter than the other two Th(1)–Cl(1) = 2.770(2) Å, Th(1)–Cl(2) = 2.661(2) Å, Th(1)–Cl(3) = 2.950(2) Å and Th(1)–Cl(4) = 2.918(2) Å. The longer Th–Cl distances are those corresponding to the chlorine atoms disposed in the three-fold bridging positions and coordinated to both lithium atoms. Each of the other two chlorine atoms is coordinated only to one lithium atom. All the Th–Cl distances are longer than those observed for terminal Th–Cl distances (Th–Cl = 2.601 Å for $Cp_2^*ThCl_2$ or 2.65 Å for $Cp_2^*Th(Cl)Me$). *Ansa*-chelating bis(cyclopentadienyl) complexes of uranium have been prepared as presented in Scheme 1. Burns et al. have described an effective high yield procedure for these desired U(IV) complexes [40].

The uranium complexes **8–10** were obtained as dark-red air and moisture sensitive materials. The complexes are soluble in aromatic solvents but insoluble in hexane. In solution, these complexes have shown no dynamic behavior. The molecular structure of complex **8** exposed a normal bent metallocene with an angle of 114.1° for the ring centroid–metal–ring centroid. This angle is smaller as compared to the non-bridge uranium complexes (133–138°) [23,41–44]. The uranium atom is bonded to four bridg-

ing chloride ligands for which two bonds are much longer than the others U–(Cl(1)) = 2.885(3), U–(Cl(2)) = 2.853(3), U–(Cl(3)) = 2.760(3) and U–(Cl(4)) = 2.746(3) Å, when the chlorine ligations that are closely associated to the metal center, only bridge one lithium atom. For the preparation of the dialkyl complexes, the corresponding chloride-TMEDA complex (**9**) was used as a precursor. The alkylation of the halo-precursors with Grignard reagents produced the corresponding alkyl complexes using large excess of dioxane as the solvent. Interestingly, complex **4** is very stable as compared to the instability of the corresponding dimethyl thorium complex [34]. The dimethyl complex of the mixed cyclopentadienyl precursor (**10**) was not formed rather there was precipitation of insoluble material and the evolution of gas. On the other hand, the dibenzyl complexes **5** and **11** were obtained in high yields. The mixed benzyl-chloride complex **12** was obtained by protonation of the dibenzyl complex **5** with [HNMe₃]Cl as described in Eq. (4).
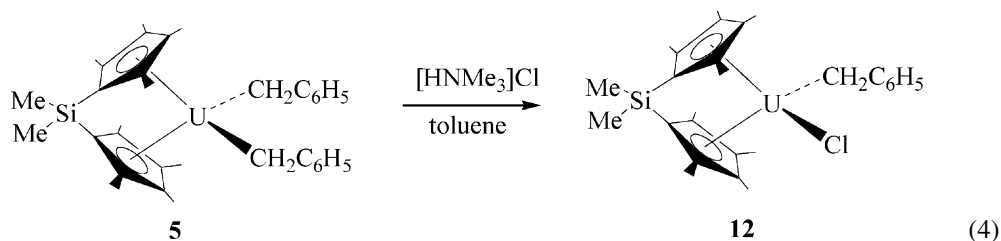
(4)

solution, these complexes have shown no dynamic behavior. The molecular structure of complex **8** exposed a normal bent metallocene with an angle of 114.1° for the ring centroid–metal–ring centroid. This angle is smaller as compared to the non-bridge uranium complexes (133–138°) [23,41–44]. The uranium atom is bonded to four bridg-

As will be presented in the course of this review, a large amount of work has been dedicated towards catalytic reactions using the cationic complex [(Et₂N)₃U][BPh₄] (**6**) [45]. The syntheses of this and other cationic complexes, reported by Berthet et al., are based on the reaction of U(NEt₂)₄ with [NHEt₃][BPh₄] in THF.
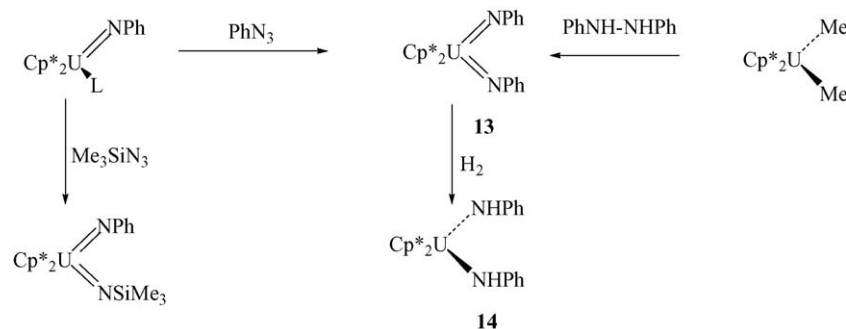
Scheme 2. Alternative synthetic pathways for the preparation of high-valent organouranium imido complexes and their reactivity with dihydrogen [47].

2.2. Synthesis of high-valent organouranium complexes

Since the reactivity of organoactinide(IV) complexes towards unsaturated organic substrates such as olefin, alkynes and nitriles follows a four-center transition state as described in Eq. (1), the synthesis, characterization and reactivity studies of high-valent organouranium complexes are of primordial importance. The ability to transform U(IV)–U(VI) and vice versa can originate complementary modes of activation inducing unique and novel reactivities. The first high-valent organouranium(VI) bis imido complex (**13**) was prepared by Burns et al. by the oxidation of a lithium salt of an organoimido uranium chloride complex with phenylazide (Eq. (5)) [46].
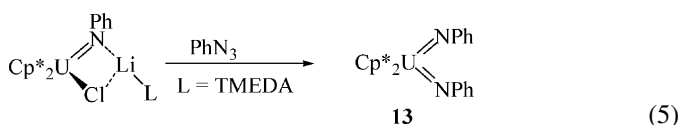
Other bis(imido) organouranium(VI) complexes have been prepared as described in Scheme 2. The reactions involve the oxidation of uranium(IV) bis alkyl or uranium(IV) imido complexes with the two-electron atom transfer reagents, in high yield [47].

A very elegant and simple procedure for the generation of the high-valent bis(imido) organouranium(VI) complexes **13**, and **15** has been described starting from an organometallic uranium(III) complex (**16**). The reaction involves the direct reduction of diazenes or azides (Eq. (6)) [48].
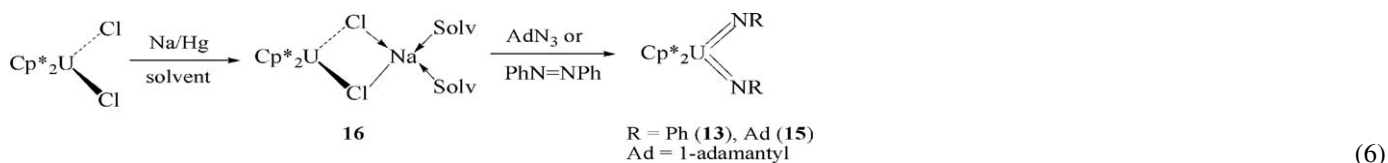
3. Oligomerization of terminal alkynes

3.1. Introduction

Metal-mediated oligomerization of terminal alkynes is of substantial current interest, since it can lead to a diversity of organic enynes and oligoacetylene products that are valuable synthetic precursors for the synthesis of natural products and also a diversity of organic conducting polymers.

The last decade has witnessed an intense investigation in the chemistry of electrophilic d^0/f^n lanthanide and actinide metallocenes [25]. Substantial success was obtained in diverse catalytic areas, where the key step is an insertion of an olefinic (alkene or alkyne) functionality into a metal–alkyl, metal–hydride or metal–heteroatom moiety (Eq. (7); X = alkyl, H, NR_2).
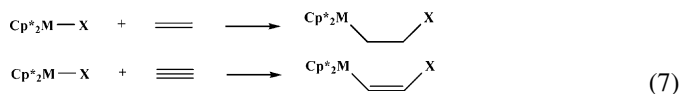
For organolanthanides, such processes include oligomerization/polymerization [49–55], hydrogenation [35,56–60], dimerization [61] and other related processes, whereas for organoactinides, until 1991, only C−H activation [31,39,62] and hydrogenation [31,63,64] were reported. Mechanistically, these insertion processes are not in general well-understood and are certainly efficient in very different metal–ligand environments than the more extensively studied analogues of the middle and late transition metals [65–67]. Hence, the d^0/f^n metal ions are likely to be in a formal high oxidation state, and in neutral complexes are expected to be electronically unsuitable for π-back-donation. In addition, these complexes are unlikely to form stable olefin/alkyne complexes. However, they will be involved in relatively polar metal–ligand bonding with a strong affinity for "hard" ligands, and are likely to feature highly unexpected M−C/M−H bond disruption enthalpy patterns when compared with those of the late transition elements [20,68–70].

Organolanthanide chemistry has developed greatly with the aid of acetylide–organometallic complexes [71–74]. Comprehensively applicable synthetic routes to this class of compounds have been developed. Such routes include the salt metathesis between lanthanide halides with main group acetylides, and the σ-bond metathesis between lanthanide alkyl or hydrides and terminal alkynes.

As already mentioned, mechanistically, the relatively polar metal–ligand bonds, the absence of energetically accessible
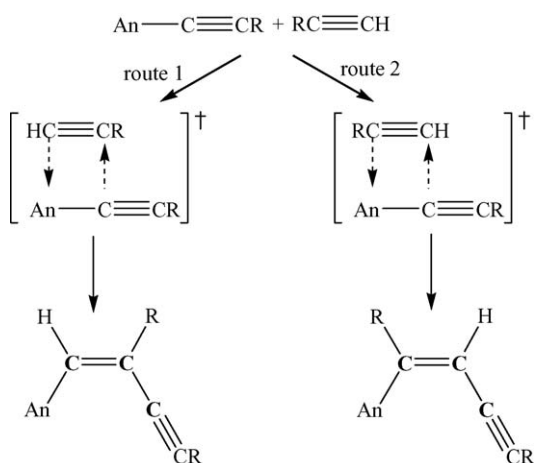
Scheme 3. Insertion of an alkyne into actinide–acetylide bond through a *syn* four-centered transition state pathway towards the formation of the two possible regioisomers.

metal oxidation states for oxidative addition/reductive elimination processes and the presence of relatively low-lying empty σ-bonding orbitals, implicates a "four-center" heterolytic transition state in the metal–carbon bond cleavage [22,75]. The reaction of the actinide acetylide with a terminal alkyne will be governed in a *syn* mode and the σ-bond protonolysis of the alkenyl complex obtained will be expected to maintain the *cis*-stereochemistry at the product (Scheme 3).

3.2. Stoichiometric reaction—bis(acetylide) organoactinide complexes

The bis(acetylide) organoactinide complexes $Cp_2^*An(C\equiv CR)_2$ (**18**, An = Th; **19**, An = U) can be synthesized
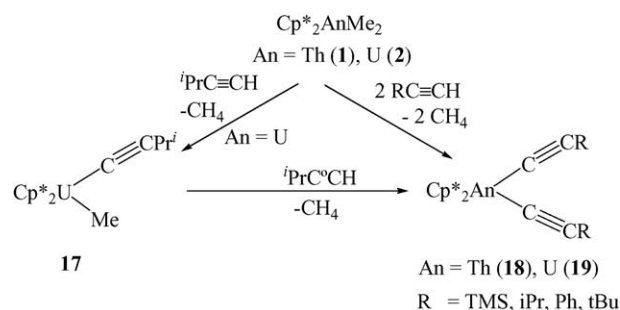
Scheme 4. Stoichiometric reactivity of the organoactinide complexes **1** and **2** with terminal alkynes [76].

center and the rapid electron spin-lattice relaxation times, magnetically non-equivalent ligand protons (methyl versus isopropyl) were found generally sharp, well-separated and readily resolved.

3.3. Oligomerization of terminal alkynes catalyzed by neutral complexes $Cp_2^*AnMe_2$ (An = Th (1) or U (2))

3.3.1. Scope of the reaction

The reaction of $Cp_2^*AnMe_2$ (An = Th (**1**), U (**2**)) with an excess of *tert*-butylacetylene yielded the regio-selective catalytic formation of the head-to-tail geminal dimer, 2,4-di-*tert*-butyl-1-butene-3-yne (Th = 99%; U = 95%), whereas with trimethylsilylacetylene the head-to-tail geminal dimer, 2,4-bis(trimethylsilyl)-1-butene-3-yne (Th = 10%; U = 5%) and the head-to-tail-to-head trimer, (*E*,*E*)-1,4,6-tris(trimethylsilyl)-1-3-hexadiene-5-yne (Th = 90%; U = 95%), were the exclusive products (Eq. (8)) [76].

(8)
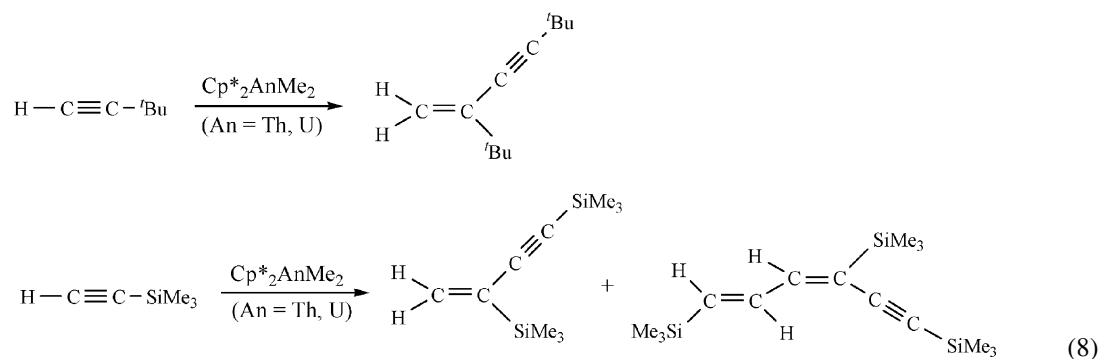
at room temperature by the reaction of $Cp_2^*AnMe_2$ (An = Th, U) with either stoichiometric or excess amounts of the corresponding terminal alkynes (Scheme 4). The reaction is faster for the uranium complex than for the corresponding thorium complex. The bis(acetylide) complexes were the sole product in all cases but the formation of the uranium isopropyl acetylide complex (**17**) indicated that the metathesis substitution of the second methyl ligand by the terminal alkyne is normally much faster than the first σ-bond metathesis. Characterization of complex **17** was achieved by ^1H NMR spectra. Due to the paramagnetic chemical shifts of the $5f^2$ uranium(IV)

For other terminal alkynes such as HC≡CPh, HC≡CPr^i and HC≡CC$_5$H$_9$ (cyclopentyl), both $Cp_2^*AnMe_2$ complexes produced mixtures of the head-to-head and head-to-tail dimers and higher oligomers with no specific regio- and chemo-selectivity. For the bulky 4-Me-PhC≡CH, a different reactivity was found for the different organoactinide complexes. Whereas $Cp_2^*ThMe_2$ generated a mixture of dimers and trimers, the corresponding $Cp_2^*UMe_2$ afforded *only* the head-to-head *trans*-dimer. In contrast to the reactivity of lanthanide complexes, the organoactinides did not induced the formation of allenic compounds. Although the turnover frequencies for both of the organoactinide
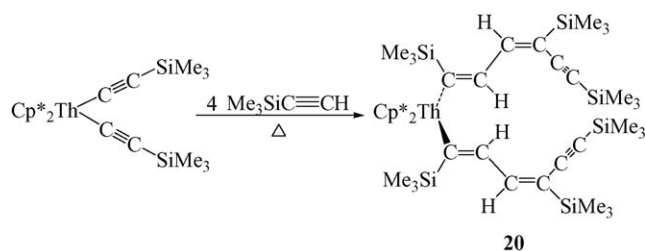
Scheme 5. Formation of the bis(dienyne) organoactinide complex **20** [76].

complexes were in the range of the $1–10\,h^{-1}$, the turnover number were found to be high in the range of 200–400. The key intermediate complexes in the oligomerization reaction were found when the reaction of $Me_3SiC{\equiv}CH$ with $Cp_2^*ThMe_2$ was followed spectroscopically. The first compound was observed at room temperature and characterized as the bis(acetylide) complex. The oligomerization reaction started only by heating the reaction mixture to 70 °C where the bis(acetylide) complex disappeared and the new complex **20** was obtained, indicating that both acetylide positions at the metal center were active sites (Scheme 5).

3.3.2. Kinetic, thermodynamic and thermochemical data

The kinetic study for the trimerization of $Me_3SiC{\equiv}CH$ with $Cp_2^*UMe_2$ was conducted by in situ ^1H NMR spectroscopy. From the kinetic plots the empirical rate law for the organoactinide-catalyzed oligomerization of $Me_3SiC{\equiv}CH$ is given by Eq. (9). The derived rate constant for the production of the corresponding trimer was found to be at 70 °C, $k = 7.6 \times 10^{-4}$ (6) s^{-1}.

$$v = k[\text{alkyne}]^1[\text{cat}]^1 \tag{9}$$

Similar kinetic dependence of alkyne and catalyst concentration was observed over a temperature range allowing the deriva-

tion of the activation parameters from the corresponding Eyring analysis. The values measured were $E_a = 11.8(3)\,\text{kcal mol}^{-1}$, $\Delta H^{\ddagger} = 11.1(3)\,\text{kcal mol}^{-1}$ and $\Delta S^{\ddagger} = -45.2(6)$ e.u., respectively [77].

Thermodynamically, higher oligomers and even polymers were expected [78,79]. The reaction of either organoactinide complex with acetylene (HC≡CH) produced the precipitation of black *cis*-polyacetylene. The *cis*-polyacetylene was thermally converted to the corresponding *trans*-polyacetylene at 80 °C. As calculated for the enthalpy of the reaction, for the addition of triple bonds in a conjugated manner (Scheme 6), the ΔH_{calc} for the dimer formation is exothermic by $27\,\text{kcal mol}^{-1}$, whereas every additional insertion is calculated to be exothermic by an additional $20\,\text{kcal mol}^{-1}$. Thus, ΔH_{calc} for the trimer formation is exothermic by $47\,\text{kcal mol}^{-1}$, corroborating the results in which unhindered terminal alkynes were oligomerized with no chemo-selectivity.

A plausible pathway for the organoactinide–oligomerization of terminal alkynes was proposed (Scheme 7). The mechanism is based on a sequence of well-defined reactions such as insertion of an alkyne into a M−C σ-bond and σ-bond metathesis. The first step in the catalytic cycle involves the protonation of the alkyl groups in the organoactinide precatalyst at room temperature, yielding the bis(acetylide) complexes $Cp_2^*An(C{\equiv}CR)_2$ (**18**), with elimination of methane (step 1). In general, this is a very rapid reaction extremely exothermic as calculated for the reaction of the organoactinides with PHC≡CH (Eq. (10)).

The 1,2-head-to-tail-insertion of the alkyne into the actinide-carbon σ-bond was proposed to yield the bisalkenyl actinide complex **21** (step 2). **21** Can undergo either a σ-bond metathesis with another alkyne to liberate the geminal dimer and regenerate **18** (step 3), or an additional 2,1-tail-to-head-insertion of an alkyne, with the expected regio-selectivity (for $Me_3SiC{\equiv}CH$), into the actinide alkenyl bond, yielding the bis(dienyl)organoactinide complex **20** (step 4). The metathesis
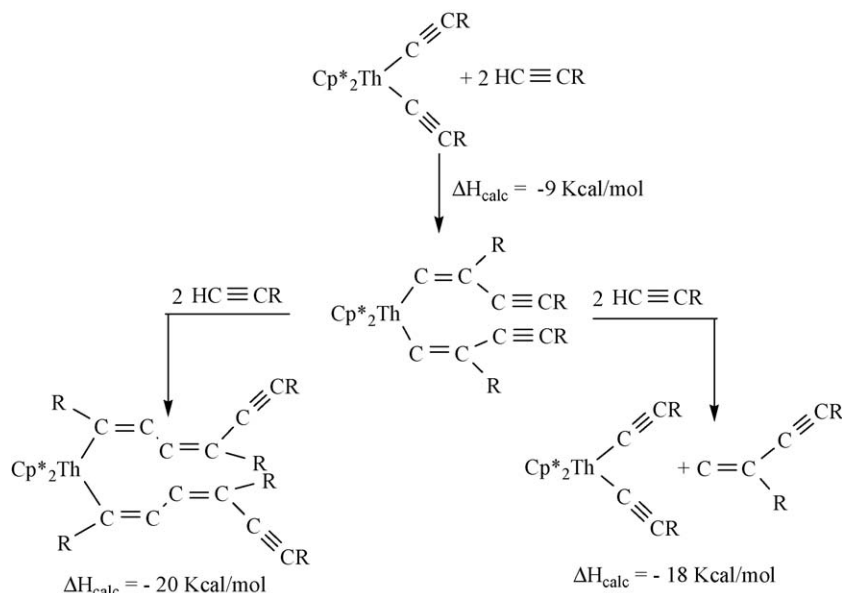
Scheme 6. Calculated enthalpies of reaction for the oligomerization of terminal alkynes.
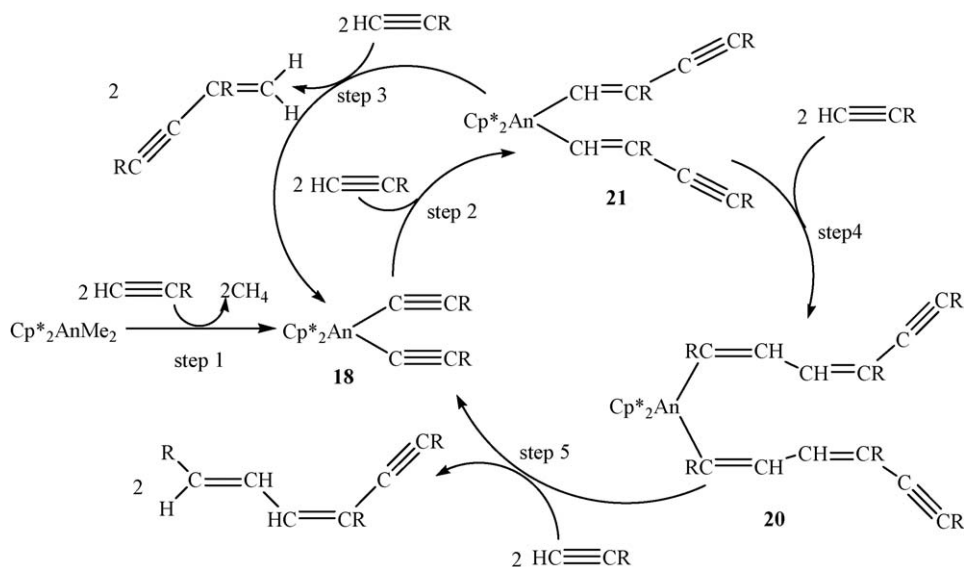
Scheme 7. Plausible mechanism for the linear oligomerization of terminal alkynes catalyzed by organoactinide bis(acetylide) complexes [77].

of **20** with another alkyne yields the corresponding trimer and the active actinide bis(acetylide) complex **18** (step 5). The turnover-limiting step for the catalytic trimerization was identified to be the elimination of the organic trimer from the organometallic complex **20**. This result indicated that the rate for σ-bond metathesis between the actinide-carbyl and the alkyne and the rate of insertion of the alkyne into the metal–acetylide (steps 1 and 2) were much faster than the rate for σ-bond metathesis of the alkyne with the metal–dialkenyl bond in the catalytic cycle (step 5).

$$\Delta H_{\text{Th (calc)}} = -18 \text{ kcal mol}^{-1}$$
$$\Delta H_{\text{U (calc)}} = -48 \text{ kcal mol}^{-1}$$

(10)
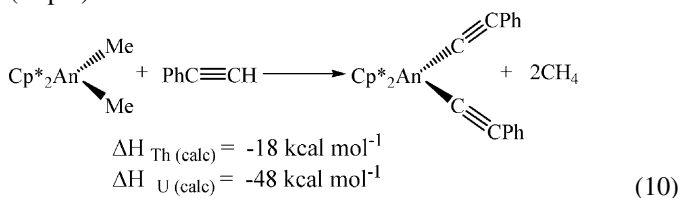
3.4. Cross oligomerization of $^{t}BuC{\equiv}CH$ and $Me_3SiC{\equiv}CH$ promoted by $Cp_2^*UMe_2$

In the oligomerization of $^{t}BuC{\equiv}CH$ with $Cp_2^*UMe_2$ the geminal dimer was found to be the major product, indicating that the

addition of the alkyne to the metal acetylide was regio-selective with the bulky group pointing away from the cyclopentadienyl groups (which resembles path 1 in Scheme 3).

The catalytic reaction of equimolar amounts of $^{t}BuC{\equiv}CH$ and $Me_3SiC{\equiv}CH$ with $Cp_2^*UMe_2$ produced two dimers (14%) and three specific trimers (86%). The dimers obtained were characterized to be the geminal dimer **22** (10%) and the cross geminal dimer **23** (4%), resulting from the insertion of $^{t}BuC{\equiv}CH$ into the uranium bis(trimethylsilyl)acetylide complex. The trimers obtained were the head-to-tail-to-head trimer, (E,E)-1,4,6-tris(trimethylsilyl)-1-3-hexadiene-5-yne (**24**), as the major product (43%), the trimer **25** (15%), resulting from the insertions of two $Me_3SiC{\equiv}CH$ into the *tert*-butylacetylide complex, and the unexpected trimer **26** (27%) (Eq. (11)). Trimer **26** was formed by the consecutive insertion of $^{t}BuC{\equiv}CH$ after the second $Me_3SiC{\equiv}CH$ insertion. These results indicated that in the formation of trimers, the last insertion rate must be fast and competitive for both alkynes, and that the metathesis of the free alkyne with the metal–dialkenyl bond is the rate-determining step, as was proposed in Scheme 7.

(11)
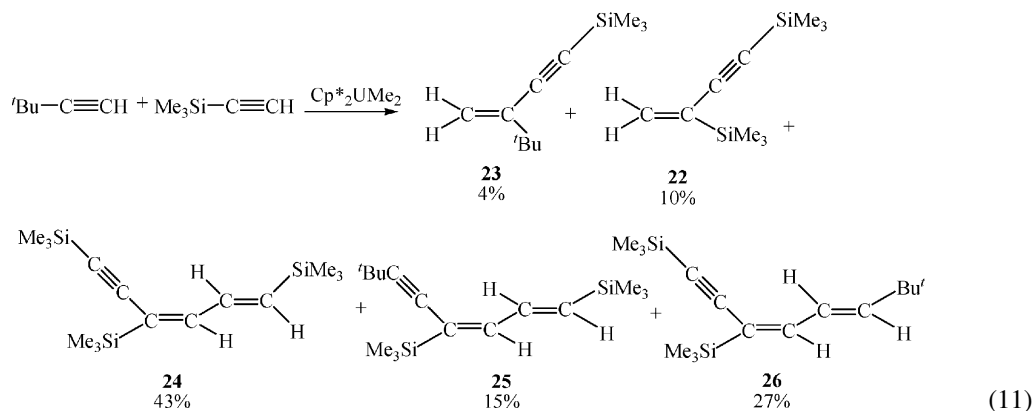
3.5. Regio-selective oligomerization of ^{t}BuC≡CH promoted by [(Et$_2$N)$_3$U][BPh$_4$] in the presence of amines

Catalytic oligomerization of the bulky alkyne ^{t}BuC≡CH with the cationic uranium complex [(Et$_2$N)$_3$U][BPh$_4$] in the presence of ethylamine was reported by Wang et al. [80]. The reaction gave mainly the *cis*-dimer and small amounts of the geminal isomer (up to 2%), with a remarkable influence of the nature of the amine on the dimerization reaction, by transposing the regio-selectivity (see Eq. (25)). With other primary or secondary amines, the *cis*-dimer was the major product although the concomitant formation of one regiospecific trimer and one regiospecific tetramer were also observed. The most remarkable result, aside from the fact that only one trimer and one tetramer were produced, was the observation that the regiochemistry of these oligomers was unpredictable, regardless of amine (Eq. (12)). The trimer and the tetramer corresponded to the consecutive insertions of an alkyne molecule into the vinylic CH bond *trans* to the bulky *tert*-butyl group.

products with *no* deuterium, indicating that ^{t}BuC≡CD was transformed into ^{t}BuC≡CH. The blank reaction for the H/D exchange between ^{t}BuC≡CH and ^{t}BuND$_2$ was found to be operative in the presence of the catalyst, to give ^{t}BuC≡CD and ^{t}BuNHD. These compounds were also observed at the early stage of the catalytic oligomerization of ^{t}BuC≡CH in the presence of ^{t}BuND$_2$, which afforded the *cis*-dimer as a mixture of mono- and non-deuterated compounds with the amount of the non-deuterated dimer always larger than that of the mono-deuterated dimer. The deuterium atom in the dimer was found only in the *trans* position relative to the ^{t}Bu group. Mixtures of non- and mono-deuterated compounds were also obtained for the trimer and tetramer having the deuterium atom always in the internal position, *trans* to the ^{t}Bu group. The presence of only one deuterium atom in the oligomers, in unique positions, strongly suggested that this D atom was introduced during the protonolysis steps of the catalytic cycle. In agreement with this fact was the increasing proportion of the trimer and tetramer, which probably results

$$(12)$$

To recognize the role of the amine and to elucidate the possibility that the initially *cis*-isomer was reactivated to yield the regio-selective trimer and tetramer, reactions with deuterated amine ^{t}BuND$_2$ and deuterated alkyne ^{t}BuC≡CD were performed (Scheme 8). The reaction of ^{t}BuC≡CD with ^{t}BuNH$_2$ gave the

from the slower cleavage of the alkenyl intermediate by the deuterated amine or alkyne, permitting further insertion of an alkyne molecule into the U−C bond.

The proposed mechanism for the regiospecific formation of the trimer and tetramer is described in Scheme 9. The early
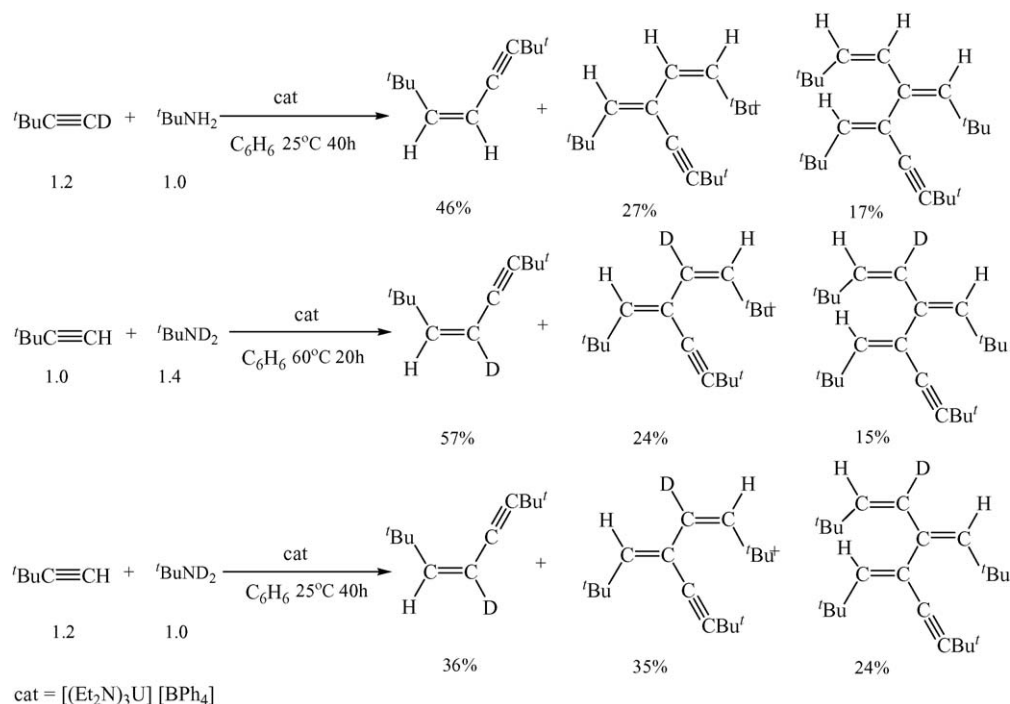
Scheme 8. Deuterium labeling experiments in the oligomerization of ^{t}BuC≡CH with ^{t}BuND$_2$ and ^{t}BuC≡CD with ^{t}BuNH$_2$ promoted by [(Et$_2$N)$_3$U][BPh$_4$] [80].
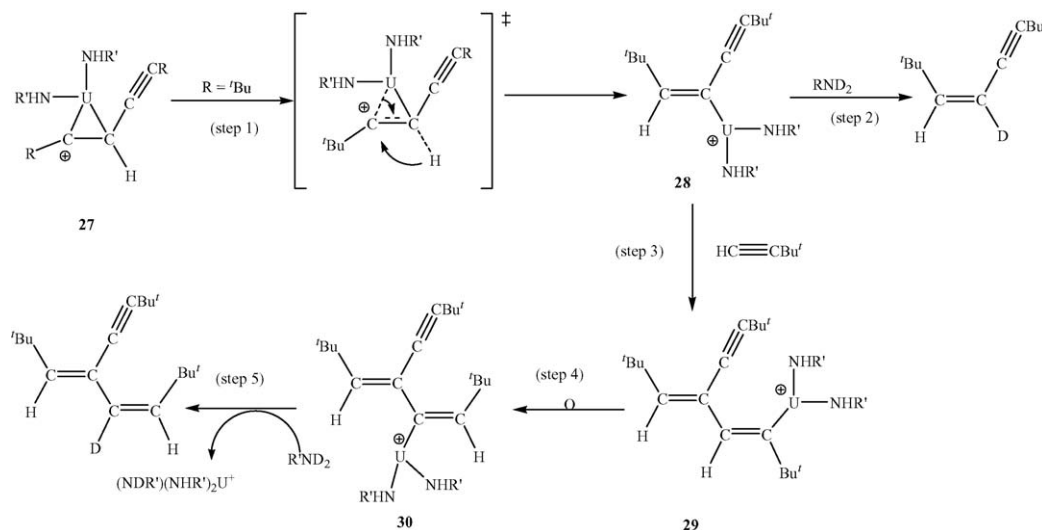
Scheme 9. Proposed mechanism for the regio-selective dimerization and trimerization of ^{t}BuC≡CH promoted by [(Et$_2$N)$_3$U] [BPh$_4$] in the presence of ^{t}BuNH$_2$.

steps of the reaction (e.g., dimer formation) will be covered in Section 4.3 (Scheme 14). Intermediate 27, which was proposed to explain the *trans–cis* isomerization of the alkenyl intermediate by the envelope mechanism (see Eq. (27)) was proposed to explain conceptually the regiospecific formation of one trimer and one tetramer. The mechanism is based on the 1,2-hydride shift isomerization of the metal–alkenyl complex **27** leading to the isomeric compound **28** (step 1). Deuterolysis at this stage liberates the deuterated dimer, regio-selectively (step 2). Insertion of an alkyne molecule into the U–C bond of **28** leads to the formation of complex **29**. The regio-selectivity of this insertion (step 3) would result from the steric hindrance between the alkyne substituent at the α-position of the metal–alkenyl chain and the incoming alkyne due to the rotation around the metal–carbon bond. The same isomerization process, as before, converts complex **29** into the *syn* complex **30** (step 4). Protonolysis of **30** regenerates the catalyst and produces the specific trimer (step 5), whereas the additional insertion of the alkyne, envelope isomerization and protonolysis yielded the specific tetramer.

4. Controlled dimerization of terminal alkynes

4.1. Dimerization of terminal alkynes promoted by Cp$_2^*$AnMe$_2$ in the presence of amines

In an interesting conceptual advance based on the proposed mechanism (Scheme 7), the oligomerization of alkynes could be controlled so as to permit the formation of a specific dimer or trimer, rather then higher oligomers. This is possible by slowing steps 4 and 5 (Scheme 7) so that the catalyst follows step 2 and 3. Haskel et al. [81] have reported a principle for the selective control on the extent of the oligomerization of terminal alkynes, by an acidic chain transfer agent. The basic approach used a chain transfer reagent not ending up in the product and not involving in subsequent elimination from the product to release the unsaturated oligomer (in contrast to, e.g., ethene oligomerization by metallocene catalysts or magnesium reagents) [82,83].

The dimerization was performed by adding an amine (primary or secondary) into the catalytic cycle, without altering much the turnover frequencies as compared with the non-controlled process. The selectivity control, which is the amount of the different oligomers obtained from the new catalytic cycle, was accomplished by considering the difference in the calculated bond-disruption energies, between an actinide–alkenyl and an actinide–amido bond, and combining non-selective catalytic pathways with individual stoichiometric reactions.

4.1.1. Stoichiometric reactivity of Cp$_2^*$AnMe$_2$ towards terminal alkynes and primary amines

The different catalytic reactivity found for structurally similar organoactinides, which is unprecedented in the chemistry of organoactinides, was the driven force for studying the stoichiometric reactivity of organoactinide complexes of the type Cp$_2^*$AnMe$_2$ (An = Th (**1**), U (**2**)) [81]. The reactivity of the actinide complexes toward alkynes or/and amines is outlined in Schemes 10 and 11 for Th and U, respectively.

Cp$_2^*$ThMe$_2$ (**1**) was found to react with terminal alkynes producing the bis(acetylide) complexes Cp$_2^*$Th(C≡CR')$_2$ (**18**) (R' = ^{t}Bu, SiMe$_3$). The reaction of these bis(acetylide) complexes with equimolar amounts of amine yielded the corresponding bisamido complexes Cp$_2^*$Th(NHR')$_2$ (**34**) and the starting bis(acetylide) complex indicating that the second amine insertion into the thorium monoamido monoacetylide complex **33** was faster than the first insertion. The reaction of **1** with an equimolar amount of amine, allowed the formation of the monoamido thorium methyl complex **32**, which upon subsequent reaction with another equivalent of amine produced the bisamido complex **34**. Heating complex **34** in THF solution afforded the elimination of an amine molecule to form the thorium imido complex **35**. This complex also was formed by eliminating methane by heating complex **32** [84]. In an excess of amine, the bisamido complex **34**, was found to be in rapid equilibrium with the bisamido–amine complex **36** [85], resembling lanthanide complexes [35,86,87] though the
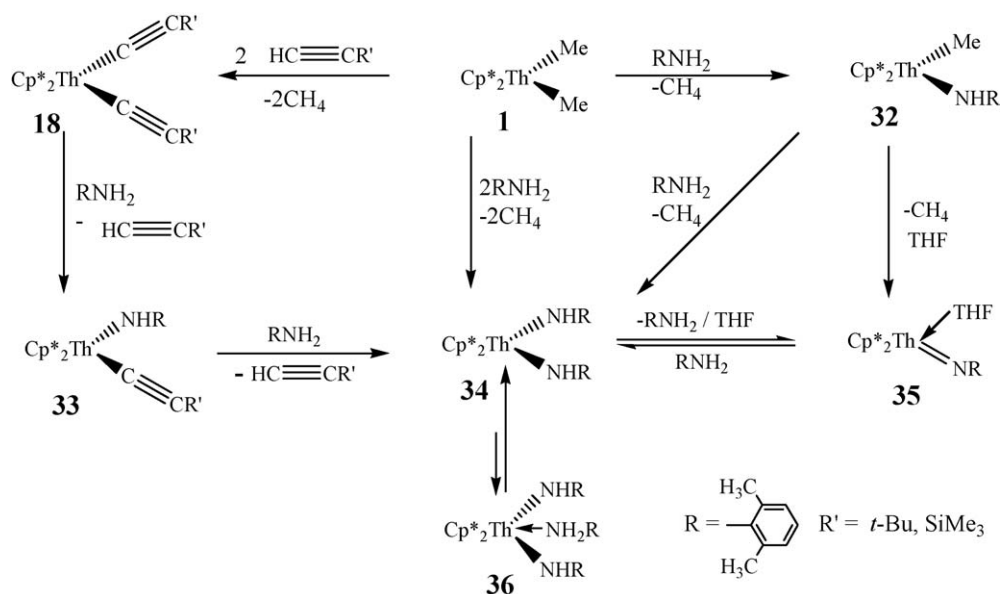
Scheme 10. Stoichiometric reactions of the complex $Cp_2^*ThMe_2$ (**1**) with primary amines and terminal alkynes [81].

equilibrium was investigated and found to favor the bisamido complex.

Complex **2** exhibits similar reactivities as complex **1** for the stoichiometric reaction with primary amines and/or terminal alkynes (Scheme 11). The reaction with alkynes produced the bis(acetylide) complexes $Cp_2^*U(C\equiv CR')_2$ (**19**) (R′ = Ph, SiMe$_3$) but in contrast to the thorium reactivity, these bis(acetylide) complexes are extremely stable and the bisamido complex **39** can be formed only by adding large excess of the amine, indicating that the equilibrium between complexes **19** and **39** lies preferentially toward the bis(acetylide) complexes, instead of either the monoamido monoacetylide **38** or the bisamido complexes **39**. Attempts to isolate the monomethyl–amido complex **37**, by

reacting one equivalent of amine with complex **2**, yielded only half equivalent of the bisamido complex **39**. Like the thorium bisamido complex **34**, in the presence of an excess of amine, complex **39** was found to be in fast equilibrium with complex **41**, with the equilibrium favoring the bisamido complex. By heating the bisamido complex **39** in THF, elimination of an amine molecule was observed allowing the formation of the corresponding uranium imido complex **40** [88].

4.1.2. Scope of the catalytic reaction

Organoactinide complexes of the type $Cp_2^*AnMe_2$ (An = Th (**1**), U (**2**)) reacted with terminal alkynes in the presence of primary amines preferentially yielding dimers (Eq. (13)) and for

Scheme 11. Stoichiometric reactions of the complex $Cp_2^*UMe_2$ (**2**) with primary amines and terminal alkynes [81].

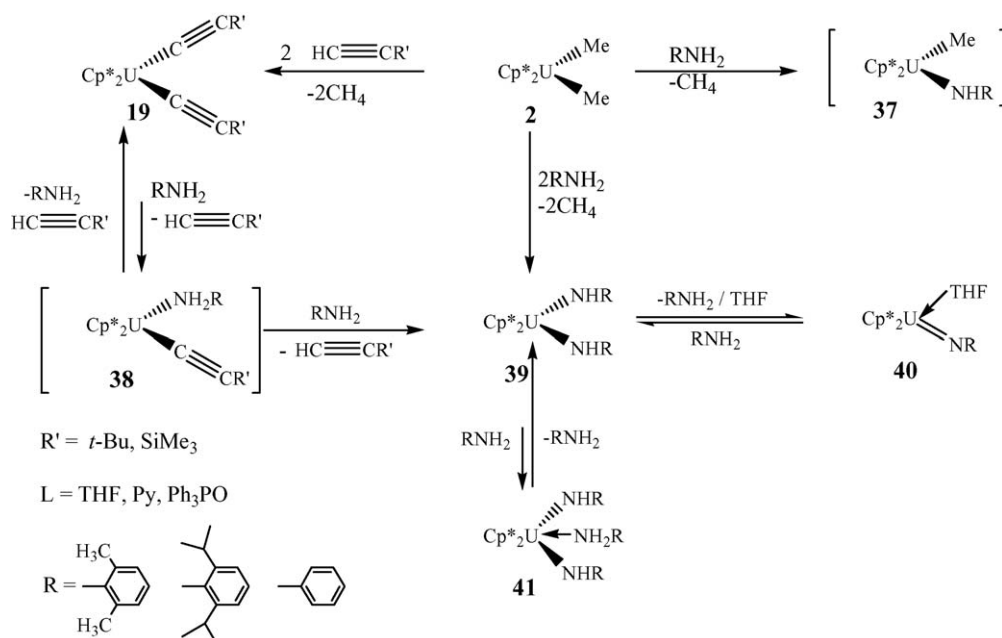specific alkynes small amounts of regio-selective trimers (Eq. (14)). This selectivity was opposite to that found in the oligomerization of alkynes, under the same conditions, in the absence of amines. In general, the initial reaction of $Cp_2^*AnMe_2$ with an alkyne yielded the bis(acetylide) complex, though in the presence of amines, for the thorium complex, the corresponding $Cp_2^*Th(NHR)_2$ (**34**) was formed. For the uranium complex, no bisamido complex is observed unless large excess of the amine was used.

$$2 \ HC\equiv CR \xrightarrow[EtNH_2]{Cp_2^*AnMe_2} \quad (13)$$

R = ^{i}Pr, ^{n}Bu, C_5H_9, ^{t}Bu-Ph, Ph, ^{t}Bu

(14)
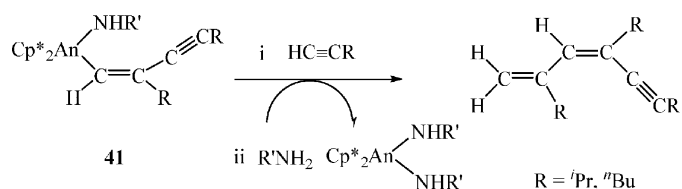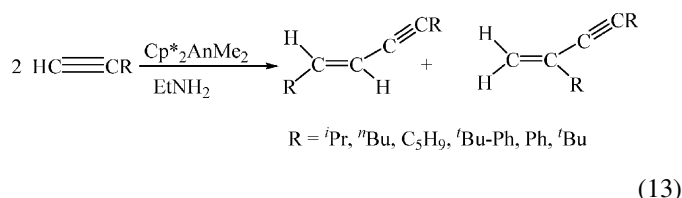
When comparing the oligomerization of terminal alkynes promoted by the thorium complex in the presence of amines to the results obtained without amines (see Section 3.3.1), a dramatic effect of reducing the extent of oligomerization was observed. When $EtNH_2$ or other primary amines were used with aliphatic alkynes, mixtures of the corresponding *geminal* and *trans*-dimer were produced, while for aromatic alkynes, just the *trans*-dimer was formed. Increasing the bulkiness of the primary amine, for aliphatic alkynes, allowed the formation of only the *geminal* dimer, and the specific trimer as represented in Eq. (14). These results indicated that the insertion of the second alkyne into the metalla–eneyne complex (**41**) and the trimer elimination (Eq. (14)), are faster than either the insertion of an alkyne into the intermediate complex **42** and/or the protonolysis of **42** by either the alkyne or the amine, eliminating the corresponding isomeric trimer and/or dimer, respectively (Eq. (15)). Reactions of the thorium precursor with secondary amines allowed the formation of higher oligomers (up to pentamers), however, in lower yields, as compared with the results obtained in the reactions in the absence of amines. It was proposed that for secondary amines, the protonolysis of the growing oligomer, from the metal, was much slower as compared to the insertion of the alkynes and cutting the oligomer chain by the alkyne itself.

(15)
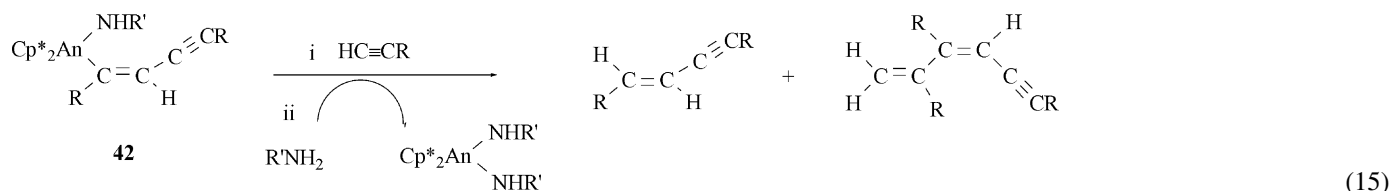
For uranium, the oligomerization of unhindered alkynes with secondary amines showed no control whereas for primary amines the intermolecular hydroamination product was exclusively obtained ($RCH_2CHN=R'$) (see Section 5.1) [84].

Dimerization of the bulky alkyne $^tBuC\equiv CH$ with no amine produced the *geminal* dimer. Adding $^tBuNH_2$ to the reaction mixture afforded only the *trans*-dimer, which suggests that the amine is attached to the metal center at the time of the alkyne insertion, allowing different regio-selectivities. Previously, for the non-controlled oligomerization reactions (Section 3.3.1), the actinide–bis(acetylide) complex was proposed as the active species in the catalytic cycle. In the controlled oligomerization reaction, the formation of the organoactinide bisamido complex, which was the predominant species, provided strong evidence that the amine was the major protonolytic agent. A novel strategy was implemented, to support the protonolytic theory, to increase the selectivity towards the trimer isomer. The process was attained by providing a kinetic delay for the fast protonolysis using deuterated amine. The kinetic effect allowed more trimer

formation, in a reaction producing both dimer and trimer (Eq. (16)). The strategy biased the chemo-selectivity of the oligomerization increasing the trimer:dimer ratio.

When the product formation was followed as a function of time the first deuterium was observed at the geminal position, but at larger conversions, more olefinic proton signals were exchanged by deuterium implicating that the alkyne and the deuterated amine were in equilibrium through a metal complex only exchanging hydrogen/deuterium atoms.

$R=^nBu$ 42%   58%

(16)
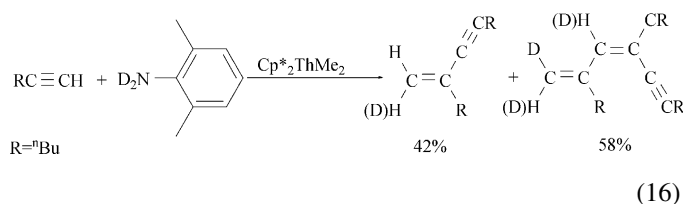
4.1.3. Kinetic, thermodynamic and mechanistic studies of the controlled oligomerization of terminal alkynes

Kinetic measurements on the controlled oligomerization reaction of $^nBuC\equiv CH$ with $^iBuNH_2$ promoted by $Cp_2^*ThMe_2$ revealed a first-order dependence of the catalytic rate on

substrate concentration, an inverse first-order in amine and a first-order dependence in precatalyst. Thus, the rate law for the controlled oligomerization of terminal alkynes promoted by

$\Delta H_{calc}(\text{step 3}) = -13 \text{ kcal/mol} \quad \Delta H_{calc}(\text{step 2}) = 15 \text{ kcal/mol} \quad \Delta H_{calc}(\text{step 1}) = -6 \text{ kcal/mol}$
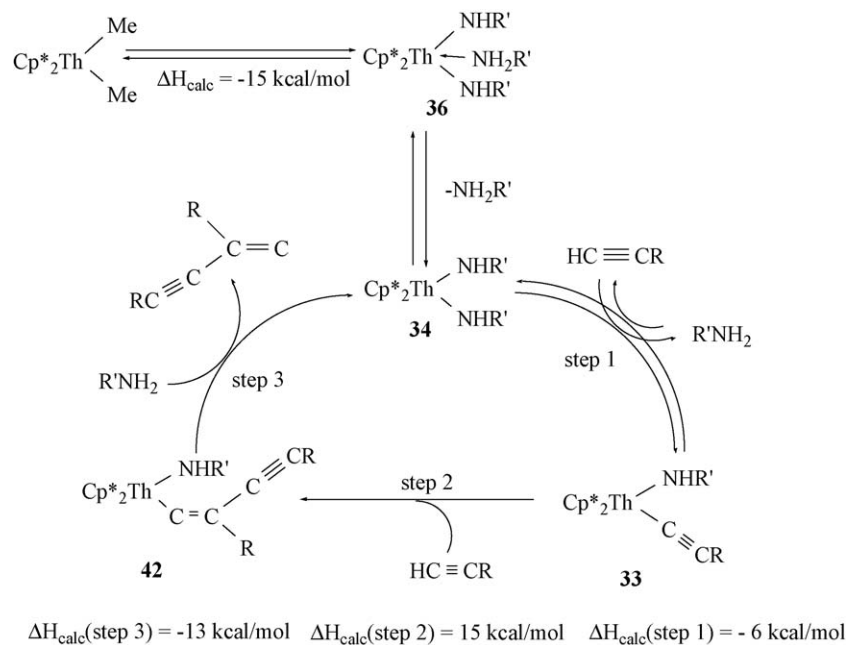
Scheme 12. Plausible mechanism for the oligomerization of terminal alkynes, in the presence of amines, promoted by organothorium complexes [85].

organoactinides can be written as presented in Eq. (17). The derived $\Delta H^{\dagger}$ and $\Delta S^{\dagger}$ values from an Eyring analysis were measured to be 15.1(3) kcal mol^{-1} and −41.2(6) e.u., respectively.

$$\nu = k[\text{Th}]^1[\text{alkyne}]^1[\text{amine}]^{-1} \qquad (17)$$

An inverse proportionality in catalytic systems is consistent with a rapid equilibrium before the rate-limiting step. For this reaction it was coherent with the equilibrium between the bisamido complex and a bisamido–amine complex, as found in the hydroamination of terminal alkynes promoted by early transition complexes [89,90] and in the hydroamination of olefins promoted by organolanthanide complexes [60,86,87].

A possible mechanism for the controlled oligomerization of terminal alkynes is described in Scheme 12. The mechanism is based on a sequence of simple reactions, such as insertion of acetylene into an M–C σ-bond and σ-bond metathesis. The starting complex Cp$_2^*$ThMe$_2$ reacts faster with amines towards the bisamido complex 34 and the concomitant formation of the bisamido–amine complex 36. These complexes were found to be in rapid equilibrium and responsible for the inverse proportionality in the kinetic dependence of the amine [85]. Complex 34, which was found to be the resting state for the catalytic species, reacted with one equivalent of alkyne, as the rate-limiting step, producing complex 33 (step 1). Comparison of the results obtained for the oligomerization of phenylacetylene in the absence of amines (with amines only a dimer was obtained), in which both dimers and higher oligomers were obtained, indicated that an amido acetylide and not the bis(acetylide) complex

is responsible for the regio-differentiation. Complex 33 reacts with an alkyne yielding the actinide–alkenyl amido complex 42 (step 2), which may undergo either a σ-bond protonolysis with the amine to yield the corresponding dimer and the bisamido complex 34 (step 3), or another insertion of an alkyne and concomitant σ-bond protonolysis by the amine, yielding the oligomeric trimer and the bisamido complex 34. Thus, the reaction rate law presented in Eq. (16) is compatible with rapid, irreversible alkyne insertion (step 2), rapid σ-bond protonolysis of the oligomer by the amine (step 3), a slow pre-equilibration involving the bisamido (34) and the monoamido–acetylide complex (33) (step 1), and a rapid equilibrium between the bisamido complex 34 and the bisamido–amine complex 36.

Controlling the length of the oligomerization was accomplished via a kinetic competition between the protonolysis by the amine (Eq. (18)) and the insertion reaction of a new alkyne molecule into the metal–alkenyl bond (Eq. (19)). The insertion reaction produces a larger metalla–oligomer complex, whereas the competing protonolysis produces the organic product and the bisamido organometallic complex. The difference in selectivity found for thorium and uranium complex was corroborated using bond disruption energy data [69,91–93]. For thorium, both reactions (18) and (19) were calculated to be exothermic by almost equal amounts allowing a control. For the corresponding uranium complex, were no real control was achieved, the formation of the bisamido complex was calculated to be endothermic encumbering the control on the degree of oligomerization.

$$\text{An = U} \quad \Delta H_{calc} = +1.5 \text{ kcal/mol}$$
$$\text{An = Th} \quad \Delta H_{calc} = -13.4 \text{ kcal/mol} \qquad (18)$$

$$\text{(19)}$$
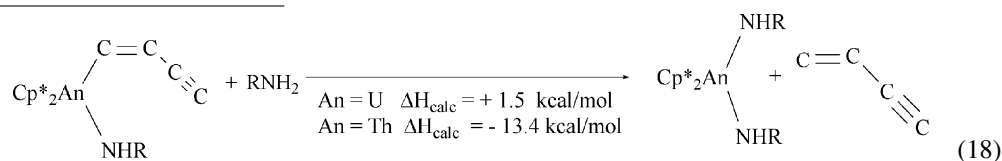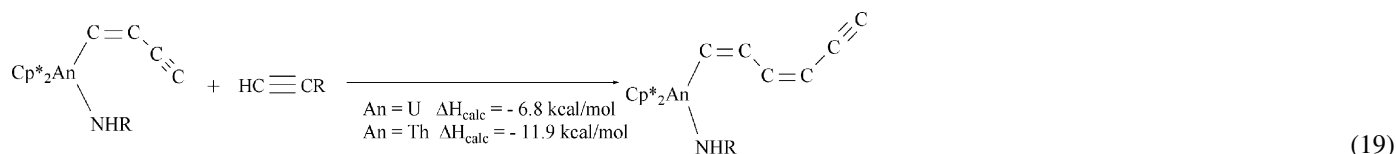
4.2. Dimerization of terminal alkynes promoted by the ansa-organothorium complex $Me_2Si(C_5Me_4)_2ThBu_2$ (3)

4.2.1. Scope of the reaction

The *ansa*-bridged organoactinide complex $Me_2Si(C_5Me_4)_2Th^nBu_2$ (**3**) was found to be an excellent precatalyst for the chemo- and regio-selective dimerization of terminal alkynes. At room temperature, head-to-tail geminal dimers were obtained whereas at higher temperature (78 °C), the geminal dimer and some minor amounts of the specific head-to-tail-to-tail trimer (up to 5%) were also observed specially for the specific alkynes $^iPrC\equiv CH$ and $^nBuC\equiv CH$ (Eq. (20)) [37]. Although no large difference was observed among similar alkyne substituents, the dimerization reaction of either $^iPrC\equiv CH$, $^nBuC\equiv CH$ with $Me_2Si(C_5Me_4)_2Th^nBu_2$ was much faster and selective than the dimerization with $Cp_2^*ThMe_2$. The most striking result regarding the dimerization/oligomerization of terminal alkynes was found for $Me_3SiC\equiv CH$. By using the bridged complex no catalytic reaction was observed, although butane was evolved, in contrast to the results obtained in the reaction of $Me_3SiC\equiv CH$ with $Cp_2^*ThMe_2$, in which the geminal dimer (10%) and the head-to-tail-to-head trimer (90%) were obtained with high regio-selectivity [76].

Fig. 1. Alkyne dependence in the dimerization of $^iPrC\equiv CH$ promoted by $Me_2Si(C_5Me_4)_2Th^nBu_2$ [88].

4.2.2. Kinetic studies of the dimerization of terminal alkynes promoted by $Me_2Si(C_5Me_4)_2Th^nBu_2$

Kinetic studies for the dimerization of $^iPrC\equiv CH$ promoted by $Me_2Si(C_5Me_4)_2Th^nBu_2$ were performed by monitoring the reaction by ^1H NMR. The results indicate that the reaction

$$\text{(20)}$$

When the dimerization of an alkene-functionalized alkyne was performed, the produced dimer 43 underwent a domino reaction—a quantitative intermolecular Diels Alder cyclization to produce compound **44** (Eq. (21)).

behaves with first-order dependence in precatalyst and a two domains behavior for the alkyne dependence was observed (Fig. 1). At low concentrations, an inverse proportionality was

$$\text{(21)}$$

observed indicating that the reaction is in an inverse first-order, but at higher concentrations, the reaction exhibited a zero order in alkyne [88]. The change from an inverse rate to a zero rate was rationalized via two equilibrium processes. In one of these equilibrium processes, the complex was routed out of the catalytic cycle (inverse order), whereas the second equilibrium was found to be the rate-determining step towards the dimer formation commensurable only at high alkyne concentrations. The derived activation parameters E_a, $\Delta H^{\ddagger}$ and $\Delta S^{\ddagger}$ from an Eyring analysis were 11.7(3) kcal mol^{-1}, 11.0(3) kcal mol^{-1} and $-22.6(5)$ e.u., respectively.

Since the alkyne approaches the organometallic moiety side-on, the highly regio-selective production of the geminal dimers was rationalized by means of the insertion of the alkyne always having the substituent away from the metal center. The methyl groups of the cyclopentadienyl spectator ligand also encumber the disposition of the alkyne substituent facing the metal center.

A plausible mechanism for the selective dimerization of $^iPrC{\equiv}CH$ promoted by $Me_2Si(C_5Me_4)_2Th^nBu_2$ is presented in Scheme 13. The initial step in the catalytic cycle is the alkyne C–H activation by the complex $Me_2Si(C_5Me_4)_2Th^nBu_2$ and the formation of the bis(acetylide) complex **45** together with butane (step 1). Complex **45** is proposed to be in equilibrium with an alkyne, forming the proposed π-alkyne acetylide complex **46**, which drives the active species out of the catalytic cycle (inverse rate dependence), or undergo, with another alkyne, a head-to-tail insertion into the thorium–carbon σ-bond, producing the substituted alkenyl complex **47** (step 2). Complex **47** goes through a σ-bond protonolysis with an additional alkyne (step 3) yielding the corresponding dimer and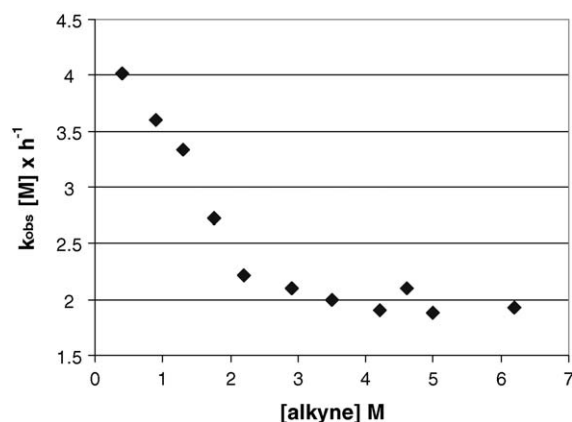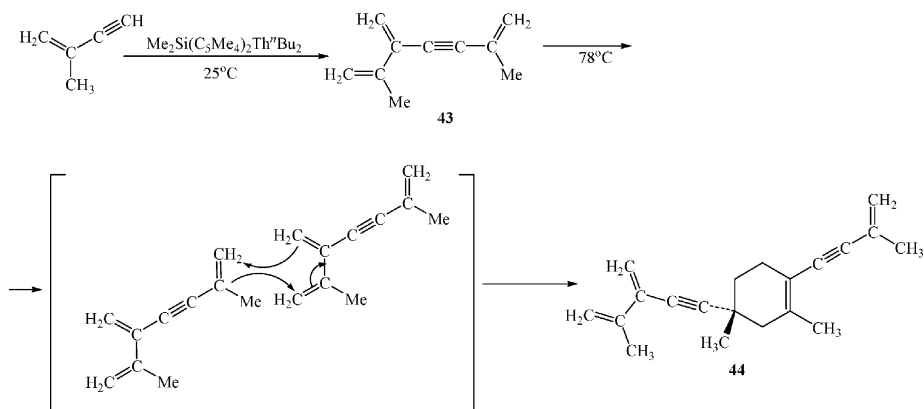 regenerating the active acetylide complex **45**. In contrast to the general expectations for organoactinides, complex **46** is the first π-olefin intermediate complex (vide infra) exhibiting new rich and versatile reactivity for actinide complexes. The turnover-limiting step for the catalytic dimerization was determined to be the insertion of the

alkyne into the thorium–acetylide complex **45** (step 2). This result suggested that the σ-bond metathesis between the complex $Me_2Si(C_5Me_4)_2Th^nBu_2$ and the alkyne (step 1), and the protonolysis of **47** by the alkyne acidic proton were faster than the insertion of the alkyne into complex **45**. Thus, the derived rate law based on the mechanism proposed in Scheme 9 for the oligomerization of terminal alkynes promoted by the complex $Me_2Si(C_5Me_4)_2Th^nBu_2$ is given by Eq. (22), fitting the kinetic data for the alkyne and catalysts.

$$\nu = \frac{k_{-1}k_2[\text{cat}]}{k_1 + k_2 - \frac{k_2k_{-2}}{k_3[\text{alkyne}]}} \tag{22}$$

4.3. Catalytic dimerization of terminal alkynes promoted by the cationic complex $[(Et_2N)_3U][BPh_4]$: first cationic f-element alkyne π-complex $[(Et_2N)_2U(C{\equiv}C^tBu)(\eta^2\text{-}HC{\equiv}C^tBu)][BPh_4]$

4.3.1. Scope of the reaction

In contrast to neutral organoactinide complexes, homogeneous cationic d^0/f^n actinide complexes have been used as catalysts for the polymerization of α-olefins [94,95], like their isolobal group four complexes. However, very little is known regarding their reactivity with terminal alkynes [96]. Reaction of the cationic complex $[(Et_2N)_3U][BPh_4]$ [45] with the terminal alkynes $RC{\equiv}CH$ (R = Me, ^nBu, ^iPr) resulted in the chemo- and regio-selective catalytic formation of the head-to-tail *geminal* dimers without the formation of the *trans*-dimer or any other major oligomers (Eq. (23)). For $PhC{\equiv}CH$, the reaction was less chemo-selective allowing the formation of some trimers (dimer:trimers ratio = 32:58). For $Me_3SiC{\equiv}CH$, besides the formation of the geminal head-to-tail dimer, the *trans*-head-to-head dimer and the regio-selective head-to-tail-to-head-trimer (E,E)-1,4,6-tris(trimethylsilyl)1-3-hexadien-5-yne, the *unexpected* head-to-head *cis*-dimer was also formed (Eq.
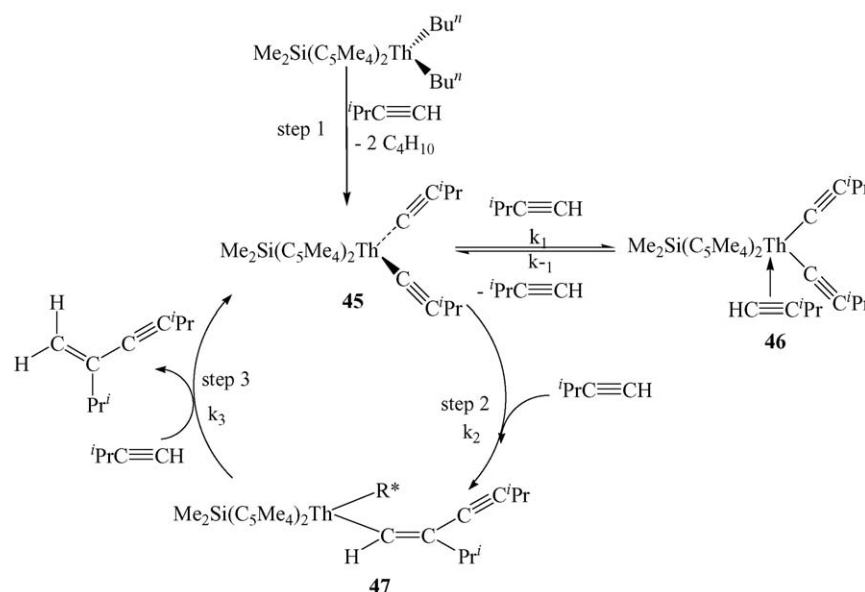
Scheme 13. Proposed mechanism for the dimerization of terminal alkynes promoted by $Me_2Si(C_5Me_4)_2Th^nBu_2$. Only one alkenyl ligation is shown in complex **47** for clarity.

(24)). For $^tBuC\equiv CH$, besides the geminal dimer also the unexpected *cis*-dimer was formed (Eq. (25)).

$$RC\equiv CH \xrightarrow[\text{toluene}]{\text{cat}} \underset{R}{\overset{RC\equiv C}{>}}C=C\underset{H}{\overset{H}{<}}$$

R = Me, ^nBu, ^iPr (23)

$$Me_3Si-C\equiv CH \xrightarrow{\text{cat}} \ (24)$$

$$^tBuC\equiv CH \xrightarrow{\text{cat}} \ (25)$$

cat = $[(Et_2N)_3U][BPh_4]$

minor   major
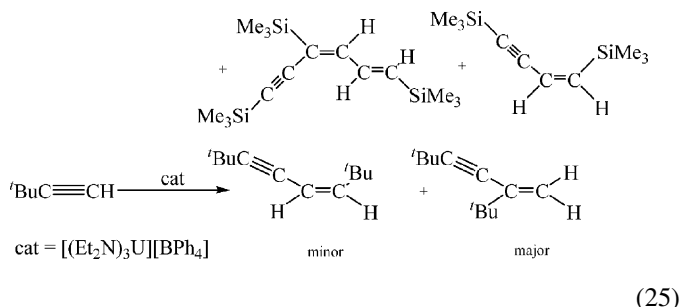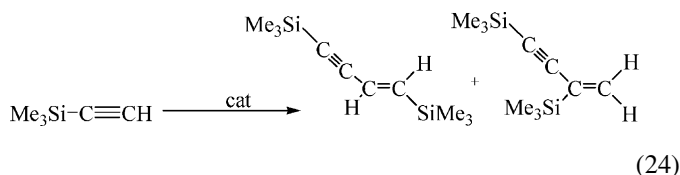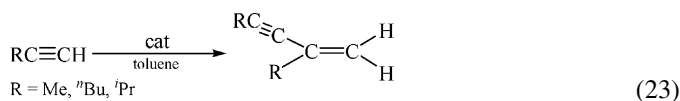
As was mentioned earlier (Section 3.1), insertion of terminal alkyne into metal–acetylide bond should follow a *syn* addition, and the resulting products should have either a *cis*-configuration or a geminal terminal end. Hence, the formation of the *trans*-dimers (Eqs. (24) and (25)) can be rationalized by an isomerization pathway before the products were released from the metal center. For comparison, in the oligomerization of terminal alkynes promoted by the cationic complexes $[Cp_2^*AnMe][B(C_6F_5)_4]$ (An = Th, U), the geminal dimer was chemo-selectively formed with no trace formation of either *cis*- or *trans*-dimers [80].

Mechanistically, in the reaction of $[(Et_2N)_3U][BPh_4]$ with terminal alkynes, one equivalent of the Et_2NH amine was released to the solution, forming the bisamido acetylide cationic complex $[(Et_2N)_2U-C\equiv CR][BPh_4]$. This reaction was shown to be in slow equilibrium and the addition of external equimolar amounts of Et_2NH to the reaction mixture led to a linear lowering of the reaction rate (Fig. 2), as expected for a Le-Chatelier equilibrium.
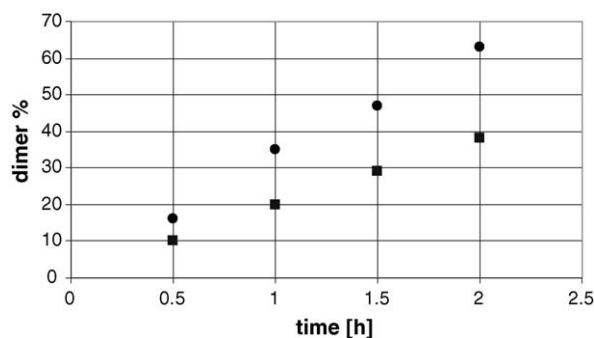
Fig. 2. Monitoring dimer formation as a function of time in the reaction of $^iPrC\equiv CH$ catalyzed by $[(Et_2N)_2U-C\equiv CR][BPh_4]$. Absence of external amine (●), presence of one equivalent of external Et_2NH (■) [97].
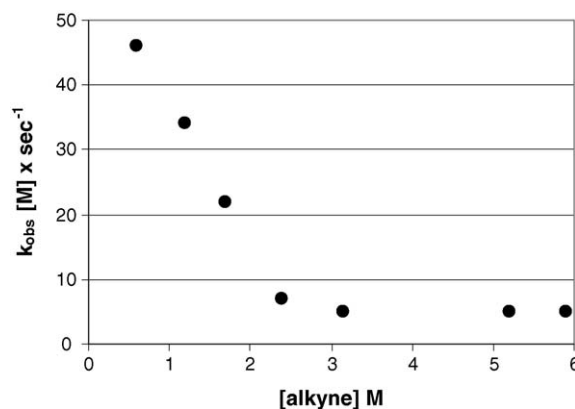
Fig. 3. Dependence of k_{obs} on the alkyne concentration in the dimerization of $^nBuC\equiv CH$ promoted by $[(Et_2N)_3U][BPh_4]$.

Considering that in the reactions of alkynes the amount of the released free amine was in stoichiometric amounts, it was deduced that the free terminal alkyne was also the major protonolytic agent. The corroboration for this protonolytic hypothesis was performed by using a kinetic delay for the presumed fast protonolysis, by the alkyne, to allow trimer formation, through replacement of the terminal hydrogen with deuterium (Eq. (26)). By using that strategy, the chemo-selectivity of the oligomerization was altered forming besides the deuterated geminal dimer, also some trimer [97].

$$MeC\equiv CD \xrightarrow{\text{cat}} \ + \ \text{trimers}$$

cat = $[(Et_2N)_3U][BPh_4]$ 92%   8%   (26)
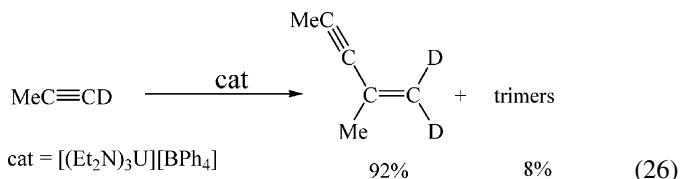
Kinetic measurements on the dimerization reaction of $^nBuC\equiv CH$ were done, indicating that the reaction behaved with a first-order dependence in precatalyst, and as a function of alkyne, the kinetic plots showed a two domain regime (Fig. 3). At low alkyne concentrations, an inverse proportionality was observed, indicating that the reaction was in an inverse first-order, and at higher concentrations, the reaction exhibits a zero order in alkyne, similar as displayed in Fig. 2. The derived activation parameters for the dimerization of $^nBuC\equiv CH$ were characterized by a small enthalpy of activation ($\Delta H^\dagger = 15.6(3)$ kcal mol^{-1}) and a negative entropy of activation ($\Delta S^\dagger = -11.4(6)$ e.u.).

The proposed mechanism for the dimerization of $^nBuC\equiv CH$ is presented in Scheme 14. The initial step in the catalytic cycle is the alkyne C—H activation by the cationic uranium amide complex and the formation of the bisamido carbyl complex $[(Et_2N)_2U-C\equiv C^nBu][BPh_4]$ (**48**) together with Et_2NH. Complex **48** can form the π-alkyne acetylide uranium complex **50** by equilibrium with an alkyne, which drives the active species out of the catalytic cycle (inverse rate dependence), however, complex **48** may undergo a head-to-tail insertion into the uranium–carbon σ-bond with an alkyne, yielding the substituted uranium alkenyl complex **49**. σ-Bond metathesis of **49** with an additional alkyne, regenerates the active carbyl complex **48** and produces the corresponding dimer.
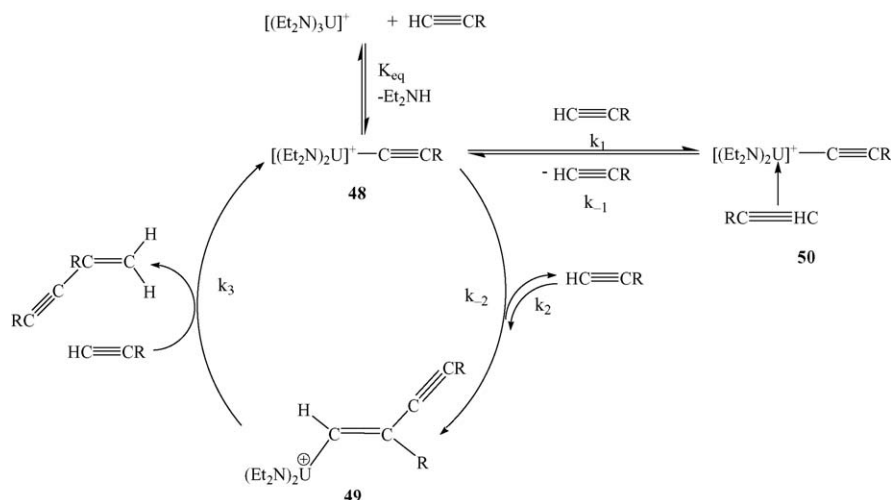
Scheme 14. Proposed mechanism for the dimerization of terminal alkynes promoted by [(Et$_2$N)$_3$U][BPh$_4$].

The structure of complex **50** (for R = ^{t}Bu) was determined by spectroscopic methods. The ^{1}H and ^{13}C NMR spectra of complex **50** showed sharp lines as found for other actinide-IV type of complexes. The ^{1}H NMR spectrum exhibited the acetylide signal ($\equiv$C–H) at $\delta = -2.14$ which correlated in the DEPT and in the 2D C–H correlation NMR experiments to the carbon having the signal at $\delta = -19.85$, with a coupling constant of $^1J = 250$ Hz. The formation of an alkyne η^2-complex, as compared to an acetylide complex or to a free alkyne was also confirmed by FT-IR spectroscopy. The C$\equiv$C stretching vibration of the free alkyne (2108 cm^{-1}) was replaced by two signals at low frequencies, as expected for η^2 transition-metal complexes, one at 2032 cm^{-1} similar to acetylide lanthanides, and the second one at 2059 cm^{-1}. The turnover-limiting step for the catalytic dimerization was found to be the insertion of the alkyne into the uranium–carbyl complex **48**, which suggested that the σ-bond metathesis between [(Et$_2$N)$_3$U][BPh$_4$] and the alkyne, and the protonolysis of **49** by the alkyne are much faster than the insertion of the alkyne into complex **48**. The results also corroborated with the formation of trimer oligomers, which are only expected if a kinetic delay in the protonolysis was operative (Eq. (26)).

For sterically demanding alkyne substituents (SiMe$_3$, ^{t}Bu), the rate of the protonolysis step is lower than that of the isomerization of the sigma–alkenyl complex **51**, producing the unexpected *cis*-dimer **53**, probably through the metalla–cyclopropyl cation (**52**), via the "envelope isomerization" (Eq. (27)) [98]. Agostic β-hydrogen interaction to the metal center was suggested as an explanation for the preference towards the *cis*-isomer [96,97].

(27)
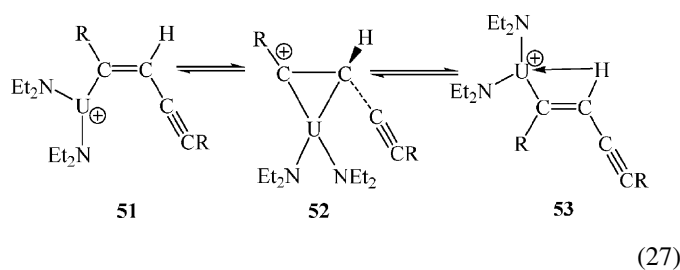
4.3.2. Effect of external amines on the dimerization of alkynes promoted by [(Et$_2$N)$_3$U][BPh$_4$]

Since the formation of the cationic complex **48** is an equilibrium reaction (Scheme 10), tailoring the regiochemistry of the dimerization might be performed by using external amines. The expectation was that the amine would be bonded to the cationic metal center causing a kinetic delay but also allowing a unique regiochemistry. As presented above, the reaction of 1-hexyne with [(Et$_2$N)$_3$U][BPh$_4$] as catalyst (Eq. (23)) affords the chemo-selective geminal dimer. However, when the reaction was carried out in a polar solvent like THF, the reaction was much slower affording besides the dimer a mixture of trimers (Eq. (28)). This result was rationalized by the lower reactivity of the THF adduct [(Et$_2$N)$_3$(THF)$_3$U]$^+$ that induced a slower protonolysis of the corresponding alkenyl intermediate [(Et$_2$N)$_2$(THF)$_3$U(C=C(H)C$\equiv$CR)]$^+$ (R = ^{n}Bu), and allowed further alkyne insertion with the formation of trimers, but with a total lack of regio-selectivity.

(28)
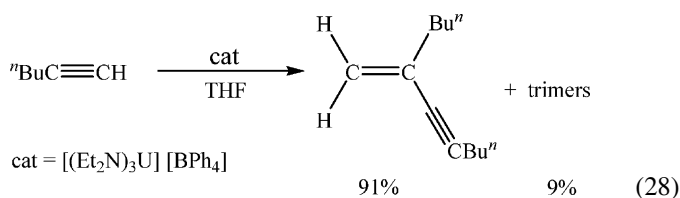
Addition of equimolar amounts of the external amine EtNH$_2$ (alkyne:amine = 1:1) to the 1-hexyne reaction mixture prevented the dimerization process. The same behavior was found for propyne. This lack of reactivity for these alkynes was proposed to be a consequence of either the formation of an inactive π-alkyne complex, similar to **50** in Scheme 14 or their inability to move the equilibrium reaction (Scheme 14) toward the formation of the acetylide complex **48** in the presence of external EtNH$_2$. When 1-hexyne was reacted in the presence of an equimolar amount of the bulkier amine ^{t}BuNH$_2$, the unexpected *cis*-dimer and the *gem* dimer were obtained (Eq. (29)) indicating that the bulky amine probably allowed the formation of the acetylide intermediate (analogue to com-

plex **48**) $[(^tBuNH_2)_x(^tBuNH)_2U(C\equiv C^nBu)]^+$ by the reaction of $^nBuC\equiv CH$ with the trisamido cation $[(^tBuNH_2)_3(^tBuNH)_3U]^+$. In turn, this acetylide complex undergoes insertion of an alkyne molecule to give the dimerization products and the corresponding alkenyl species.

$$(29)$$
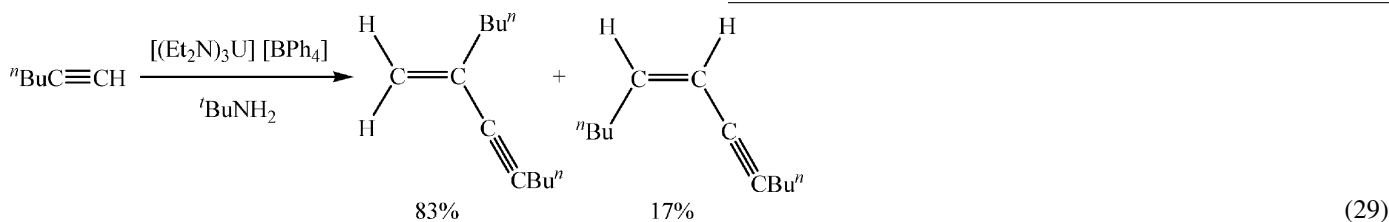
5. Intermolecular hydroamination of terminal alkynes catalyzed by neutral organoactinide complexes

5.1. Scope of the intermolecular hydroamination

The catalytic C–N bond formation is a process of cardinal importance in modern synthetic organic chemistry. The catalytic hydroamination of unsaturated substrates by addition of a N–H moiety represent a desirable atom-economic route transformation with no by-products and remains a research challenge (Eq. (30)). The hydroamination of terminal alkynes results in the formation of enamines or imines, which are important synthons in organic synthesis, bearing at least two active organic group functionalities (double bond and nitrogen lone pair).

$$(30)$$
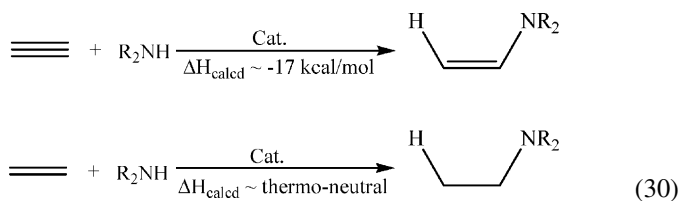
Thermodynamically, the addition process of amines to alkynes is exothermic, while addition to alkenes is close to thermo-neutral. Therefore, hydroamination of alkynes is more promising from a catalytic point of view. Since the mode of activation of organoactinides follows a four-center transition state, the negative entropy of the reaction thwarts the use of high temperatures. Organolanthanide complexes have been found to be extremely good catalysts for the intramolecular hydroamination/cyclization of aminoalkenes, aminoalkynes and aminoallenes [35,86,99–106], and enantioselective intramolecular amination have been performed using chiral organolanthanide precatalysts [35]. In addition, the intermolecular functionalization of olefins and alkynes with amines, was mentioned as one of the 10 most important challenges in catalysis [107].

The organoactinide complexes $Cp^*_2AnR_2$ (An = Th, U; R = Me, NHR'; R' = alkyl) were found to be excellent precatalysts for the intermolecular hydroamination of terminal aliphatic and aromatic alkynes in the presence of primary aliphatic amines to yield the corresponding imido compounds [84,108]. The reactivity exhibited for the thorium complexes were different, depending on the alkynes, as compared to organouranium complexes (Eqs. (31) and (32)).

The intermolecular process (Eqs. (31) and (32)) showed two hydroamination regio-selectivities depending on the precatalyst. The intermolecular hydroamination catalyzed by the thorium catalyst yielded the methyl alkyl-substituted imines in moderate yields with the concomitant formation of the alkyne *gem* dimer.

With the uranium catalyst the reaction exhibited large regio- and chemo-selectivity towards one type of imine in which the amine and alkyne substituents are disposed, almost always, in a *E* regiochemistry.

R = H; R' = Et
R = ^nBu; R' = Me, Et
R = Ph; R' = Et
R = ^iPr; R' = Ph

$$(31)$$

R = SiMe$_3$, ^tBu; R' = Me, Et, ^nPr, ^iPr, ^nBu, ^iBu
R = ^nBu; R' = Me, Et, ^nPr, ^iPr, ^iBu
R = Ph; R' = Me, Et
R = ^iBu; R' = Et
R = C$_5$H$_{11}$; R' = Et
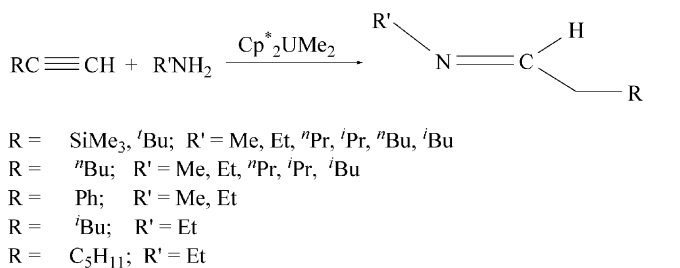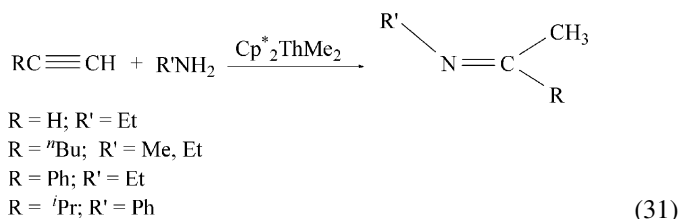
For R = SiMe$_3$ both E and Z imine isomers are obtained

$$(32)$$

When the alkyne reactions catalyzed by the uranium complexes were performed using the bulky $^tBuNH_2$ as the primary amine, no hydroamination products were obtained. The products observed were only the selective *gem* dimers corresponding to the starting alkyne. This result indicates that with $^tBuNH_2$ the proposed active species responsible for the intermolecular hydroamination was not obtained. Using this bulky amine, the observed organouranium complexes in solutions were the corresponding uranium bis(acetylide) (**19**) and the uranium bis(amido) (**39**) complexes. These two compounds were found to be in rapid equilibrium to the monoamido acetylide complex (**38**), responsible for the oligomerization of alkynes in the presence of amines (Eq. (33)).

$$(33)$$
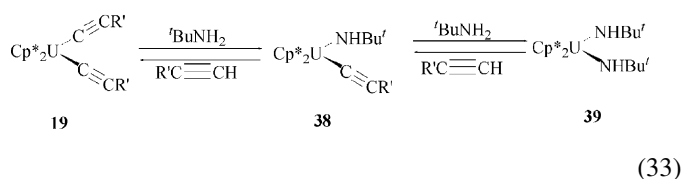
When comparing hydroamination rates, utilizing the various amines, for a specific alkyne, the bulkier the amines the lower turnover frequency, and when comparing the hydroamination rates for a particular amine (MeNH$_2$), using various alkynes, similar N$_t$ were observed. The lack of effect on the alkyne suggested no steric effect on the hydroamination process.

The intermolecular hydroamination catalyzed by the analogous organothorium complex Cp$_2^*$ThMe$_2$ exhibited similar reactivities with Me$_3$SiC≡CH and MeNH$_2$ or EtNH$_2$ as with the uranium complex (Eq. (32)). However, in the intermolecular hydroamination with ^{n}BuC≡CH or PhC≡CH and MeNH$_2$ or EtNH$_2$ a dramatic change in the regio-selectivity was obtained generating the unexpected imines (Eq. (31)). For all the organoactinides, no hydroamination products were formed by using either internal alkynes or secondary amines. With secondary amines the chemo-selective alkyne dimers and in some cases trimers were obtained.

The catalytic hydroamination of ^{n}BuC≡CH or Me$_3$SiC≡CH with EtNH$_2$ with either the organothorium complex **1** or the bisamido complex **34** gave identical results (yields, stereochemistry of the products, rate and kinetic curves) indicating that both complexes were routed through a mutual active species, parallel to the observed behavior of the different uranium complexes. It should be mentioned that when the mixture of imines **54** and **55** were obtained, **54** was found to undergo a non-catalyzed Brook silyl rearrangement to form the corresponding enamine **56** (Eq. (34)) [109]. The rearrangement followed a first-order in imine **54** to **56** leaving the concentration of **55** unaffected.
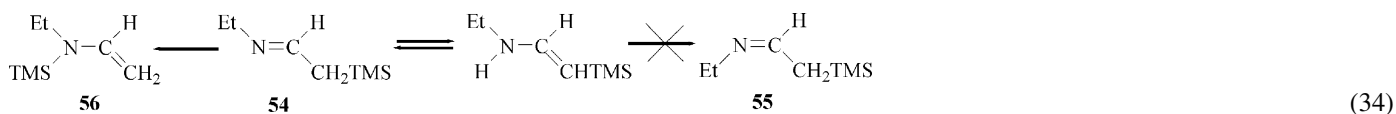
discrimination between the two most probable mechanistic pathways to find the key organometallic intermediate, responsible for the hydroamination process, was performed by kinetic and thermodynamic studies (Scheme 15). The first route proposed the insertion of an alkyne into a metal-imido (M=N) bond, as observed for early transition-metal complexes [89,110]. The second route regarded the insertion of an alkyne into a metal–amido bond, as found in lanthanide chemistry [35,86,99,100].

Kinetic measurements on the hydroamination of Me$_3$SiC≡CH with EtNH$_2$ were conducted by monitoring the reaction with ^{1}H NMR. The results revealed that the reaction has a inverse first-order dependence in amine, first-order dependence in precatalyst and zero order dependence in alkyne concentration, as presented in the rate law for the hydroamination of terminal alkynes promoted by organoactinides (Eq. (35)). The derived $\Delta H^\ddagger$ and $\Delta S^\ddagger$ parameter values from a thermal Eyring analysis (in the range 60–120 °C, error values are in parenthesis) were 11.7(3) kcal mol^{-1} and −44.5 (8) e.u., respectively.

$$\nu = k[\text{An}][\text{amine}]^{-1}[\text{alkyne}]^0 \qquad (35)$$

Since the stereochemical approach of either alkyne or amine to the organometallic moiety is expected to follow a side approach, the lack of alkyne effect on the kinetic hydroamination rate suggested that pathway 2 (Scheme 15) was not a major operative route. The zero kinetic order with respect to alkyne predicted for pathway 1 (Scheme 15), is consistent with the high

(34)

5.2. Kinetic and mechanistic studies of the hydroamination terminal alkynes with primary amines

The formation of oligomers observed in the hydroamination reactions catalyzed by the thorium complexes indicated that two different complexes were active, in solution, plausibly interconverting, causing the occurrence of two parallel processes. The

coordinative unsaturation of the imido complexes and allows fast insertion of different alkynes with indistinguishable rates. This pathway can also support the lack of reactivity when performing the reaction with bulky amines since the formation for the corresponding imido complexes is halved due to the encumbered transition state (Eq. (36)), reaching the highest steric hindrance with ^{t}BuNH$_2$.
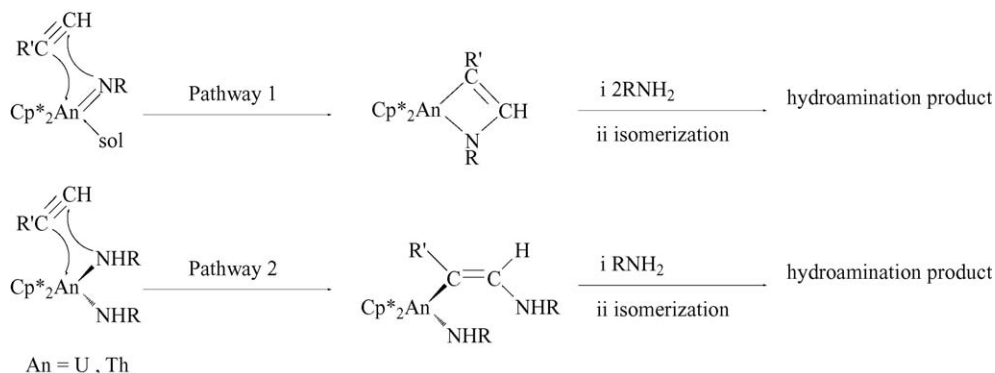
Scheme 15. Expected pathways for the organoactinide-catalyzed intermolecular hydroamination of primary amines with terminal alkynes. For thorium the approach of some alkynes was inverted before insertion.
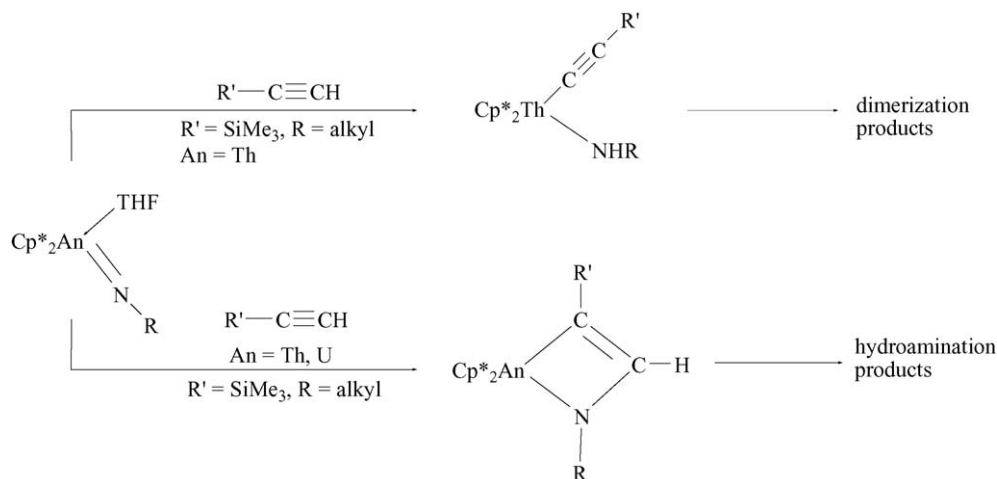
Scheme 16. Activation modes for organoactinide–imido complexes in the presence of terminal alkynes.
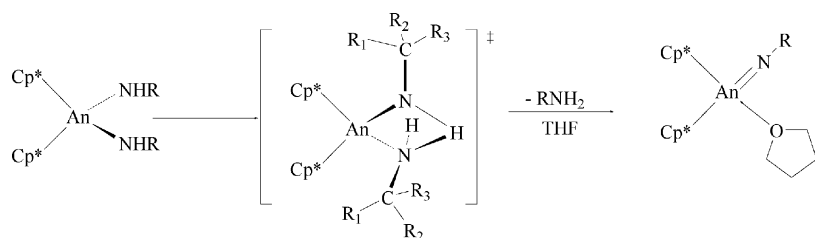
(36)

The different mode of activation for the different organoactinides is very unusual. For both organoactinide–imido complexes, a selective metathesis with the alkyne π-bond was operative (production of hydroamination products), whereas for the thorium complex a competing protonolysis reaction also occurs. This competing reaction was responsible for the selective dimerization of the terminal alkynes (Scheme 16).

The product distinction between the two organoactinide catalysts in the hydroamination reaction is a result of a contrasting stereochemistry in the metathesis of the alkyne, toward the imido complex (Scheme 17). It seems plausible that the regiochemistry of the intermolecular hydroamination was driven

Scheme 17. Opposite reactivity of organoactinide–imido complexes with terminal alkynes.

by the organometallic differences in their imido-electronic configurations rather than the difference in their thermodynamic characteristics (plausible the f^2 electrons at the uranium complex).

Scheme 18 presents a plausible mechanism for the intermolecular hydroamination of terminal alkynes promoted by the organothorium complex 1. The first step in the catalytic cycle involved the N–H σ-bond activation of the primary amine by the starting organothorium complex yielding the bisamido–amine complex $Cp_2^*Th(NHR')_2(H_2NR')$ (36) and methane (step 1). Complex 36 was found to be in rapid equilibrium with the corresponding bis(amido) complex 34 (step 2) [85,88]. An additional starting point involved a similar C–H activation of an alkyne with complex 1 yielding methane and the bis(acetylide) complex 18 (step 3). This complex may react rapidly, in the presence of amines, either with an excess (step 4) or in equivalent amounts (step 5) yielding complexes 36 or 33, respectively. Complex 34 followed two competitive equilibrium pathways. The σ-bond metathesis with a terminal alkyne yielded complex 33 (step 6), which induced the production of selective dimers (step 12). The second pathway (step 7) is the rate-limiting step, in which an amine molecule is eliminated from complex 34 to produce the corresponding imido complex 35. The imido complex followed a rapid π-bond metathesis with an incoming alkyne yielding the metallacycle 57 (step 8). Rapid protonolytic ring opening of complex 57, by an amine, yielded the actinide-enamine amido complex 58 (step 9), which in turn isomerized quickly to the actinide–alkyl(imine) amido, 59, by an

Scheme 18. Plausible mechanism for the intermolecular hydroamination of terminal alkynes and primary amines promoted by Cp*$_2$ThMe$_2$ [108].

intramolecular 1,3 sigmatropic hydrogen shift (step 10). Upon a subsequent protonolysis by an additional amine, complex **59** produced the imine and regenerated the bis(amido)complex **34** (step 11).

The larger amount of the *E* imine isomer as compared to that of the *Z* isomer was explained by the steric hindrance of the amine substituents in the isomerization pathway as described in Scheme 19.
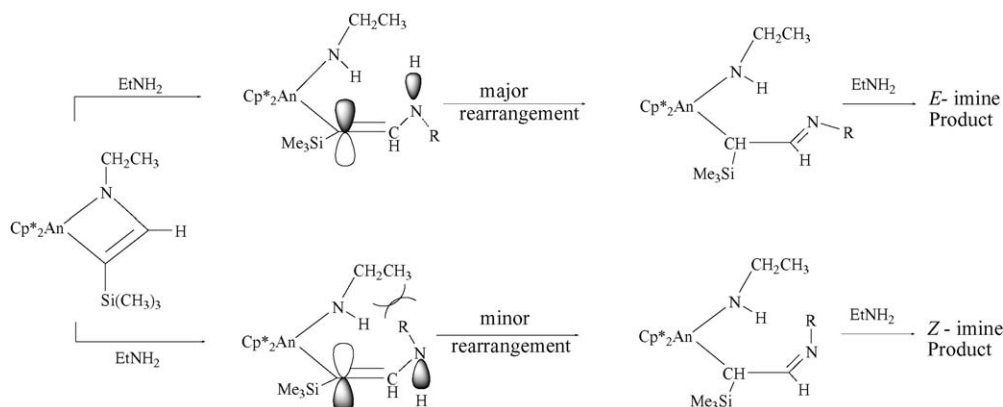
Scheme 19. Formation of *E* and *Z* imines via a 1,3-sigmatropic hydrogen shift. The curves show the steric interaction between the amine substituents present in the bottom route as compared to the top route.

6. Catalytic hydrosilylation of olefins

6.1. Catalytic hydrosilylation of terminal alkynes promoted by neutral organoactinides

The metal-catalyzed hydrosilylation reaction, which is the addition of a Si–H bond across a carbon–carbon multiple bonds, is one of the most important reactions in organosilicon chemistry and has been studied extensively for half a century. The hydrosilylation reaction is used in the industrial production of organosilicon compounds (adhesives, binders and coupling agents), and in research laboratories, as an efficient route for the syntheses of a variety of organosilicon compounds, silicon-based polymers, and new type of dendrimeric materials. The versatile and rich chemistry of vinylsilanes have attracted considerable attention in recent years as they are considered to be an important building blocks in organic synthesis [111–113].

The syntheses of vinylsilanes have been extensively studied and one of the most convenient and straightforward methods is the hydrosilylation of alkynes [114–116]. In general, hydrosilylation of terminal alkynes produces the three different isomers, *cis*, *trans* and *geminal*, as a result of both 1,2 (*syn* and *anti*) and 2,1 additions, respectively, as shown in Eq. (37). The product distribution varies considerably with the nature of the catalyst, substrates and the specific reaction conditions.

$$RC\equiv CH + R'_3SiH \longrightarrow \underset{cis}{\overset{H}{\underset{R}{>}}C=C\overset{H}{\underset{SiR'_3}{<}}} + \underset{trans}{\overset{H}{\underset{R}{>}}C=C\overset{SiR'_3}{\underset{H}{<}}} + \underset{gem}{\overset{H}{\underset{H}{>}}C=C\overset{SiR'_3}{\underset{R}{<}}}$$

(37)

6.1.1. Stoichiometric reactivity of metallocene–alkyl organoactinide complexes towards terminal alkynes and silanes

In order to detect the key organometallic intermediates in the hydrosilylation process (vide infra) which will be discussed later, a consecutive series of stoichiometric reactions were carried out by Dash et al., using the organoactinide precursor $Cp^*_2AnMe_2$ (An = Th (**1**), U (**2**)), $^iPrC\equiv CH$ and $PhSiH_3$ [117]. The reaction of $PhSiH_3$ with $Cp^*_2ThMe_2$ (**1**) produced only the dimer and the corresponding $[Cp^*_2ThH(\mu\text{-}H)]_2$, as described in the literature [63,118], while the stoichiometric reaction of $PhSiH_3$ with $Cp^*_2UMe_2$ (**2**) induced the dehydrogenative coupling of the silane ($PhSiH_3$) toward oligomers. The reaction of the organoactinide complexes, $Cp^*_2AnMe_2$ (An = Th, U) with alkynes in stoichiometric amounts was discussed in Section 3.2.

Addition of one equivalent of $PhSiH_3$, at room temperature, to a benzene solution of any of the bis(acetylide) organoactinide complexes, afforded the quantitative formation of the silylalkenyl acetylide actinide complexes $Cp^*_2An(PhSiH_2C=CH^iPr)$

($C\equiv C^iPr$) (An = U (**60**), Th (**61**)), which were found to be intermediates in the catalytic cycle for the hydrosilylation reactions (Eq. (38)).

$$\underset{An = Th\ (\textbf{18}),\ U\ (\textbf{19})}{Cp^*_2An\overset{C\equiv CPr^i}{\underset{C\equiv CPr^i}{<}}} + PhSiH_3 \xrightarrow{C_6D_6\ \ 30^oC} \underset{An = U\ (\textbf{60}),\ Th\ (\textbf{61})}{Cp^*_2An\overset{C\equiv CPr^i}{\underset{PhH_2Si}{<}}\overset{H}{\underset{Pr^i}{C=C}}}$$

(38)
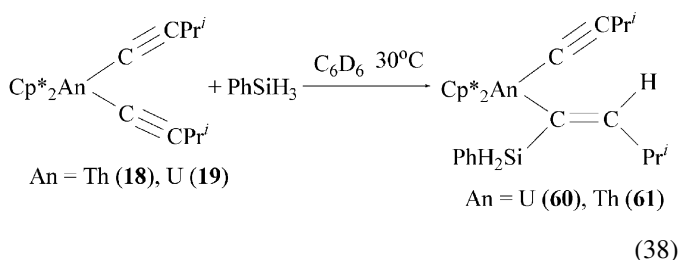
The formation of the intermediate was indicated by the change in color of the reaction from orange to dark orange-brown for complex **60** and from pale yellow to dark red for complex **61**. The structure of **60** and **61** were unambiguously confirmed by ^1H, ^{13}C and ^{29}Si NMR spectroscopy as well as by NOE experiments. The silyl group was found to be in a *cis*-configuration relative to the *iso*-propyl group of the organometallic complex. Another corroboration of the stereochemistry of **61** was found by the quenching experiment of **61** with H_2O producing the corresponding *cis*-vinylsilane product **62** (Eq. (39)).

$$\underset{\textbf{61}}{Cp^*_2Th\overset{PhH_2Si\ \ \ \ ^iPr}{\underset{C\equiv CPr^i}{\overset{C=C}{<}}}\overset{}{\underset{H}{}}} + H_2O \xrightarrow{C_6D_6\ \ 30^oC} \underset{\textbf{62}}{\overset{PhH_2Si\ \ \ \ ^iPr}{\underset{H\ \ \ \ \ \ \ H}{C=C}}}$$

(39)

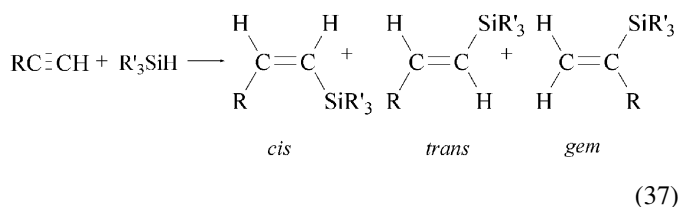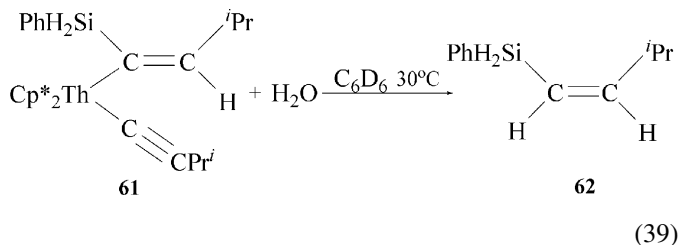Intriguingly, no further reaction was observed by the addition of an excess of $PhSiH_3$ to complex **60** or **61** which strongly suggest that at room temperature, neither the alkyne nor the silane is able to induce the σ-bond metathesis or the protonolysis of the hydrosilylated alkene or the alkyne. The addition of an excess of alkyne at room temperature to complex **61**, in the presence of $PhSiH_3$, yielded the unexpected *trans*-hydrosilylated alkyne, besides to the corresponding alkene, silylalkyne and the bis(acetylide) complex.

6.1.2. Hydrosilylation of terminal alkynes by $Cp^*_2AnMe_2$ complexes

6.1.2.1. Scope of the reaction at room temperature.
The room temperature reaction of $Cp^*_2AnMe_2$ (An = Th, U) with an excess of terminal alkynes $RC\equiv CH$ (R = ^tBu, ^iPr, ^nBu) and $PhSiH_3$ resulted in the catalytic formation of the corresponding *trans*-vinylsilanes $RCH=CHSiH_2Ph$, alkenes $RCH=CH_2$ and the dehydrogenative coupling silylalkyne product $RC\equiv CSiH_2Ph$ (R = ^tBu, ^iPr, ^nBu) (Eq. (40)) [117].

$$RC\equiv CH + PhSiH_3 \xrightarrow{Cp^*_2AnMe_2} \overset{H}{\underset{R}{>}}C=C\overset{SiH_2Ph}{\underset{H}{<}} + RCH=CH_2 + RC\equiv CSiH_2Ph$$

An = U, Th
R = ^tBu, ^iPr, ^nBu

(40)
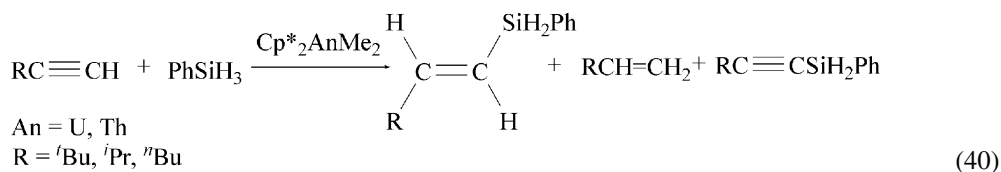
The major product in the hydrosilylation reaction was the *regio-* and stereoselective *trans*-vinylsilane, irrespectively of the alkyl substituents and the metal center, without any trace formation of the other two hydrosilylation isomers (*geminal* or *cis*). For bulky alkynes (^{t}BuC≡CH), the product distribution was nearly the same for both catalytic systems, whereas for less sterically hindered terminal alkynes, it varies from one catalytic system to another. In the hydrosilylation reaction of the alkynes with Cp${}_2^*$ThMe$_2$ and PhSiH$_3$, similar amounts of the alkene and the silylalkyne were obtained. This result suggested a mechanistic

The hydrosilylation of RC≡CH (R = ^{t}Bu, ^{i}Pr, ^{n}Bu) with PhSiH$_3$ catalyzed by Cp${}_2^*$UMe$_2$, produced in addition to the hydrosilylation products at room temperature (Eq. (41)), the corresponding *cis*-hydrosilylated compounds, *cis*-RCH=CHSiH$_2$Ph, and small to moderate yields of the *unexpected* double hydrosilylation products RCH=C(SiH$_2$Ph)$_2$, in which the two silyl moieties are attached to the same carbon atom (Eq. (43)) [117]. While Cp${}_2^*$UMe$_2$ catalyzed the hydrosilylation yielding a mixture of both *cis-* and *trans*-vinylsilane, remarkably, Cp${}_2^*$ThMe$_2$ afforded only the *trans*-vinylsilane.

$$RC≡CH + PhSiH_3 \xrightarrow[\text{THF 65°C}]{Cp^*_2UMe_2} \underset{H}{\overset{R}{\underset{SiH_2Ph}{C=C}}}{}^H + RC≡CSiH_2Ph + RCH=CH_2$$

$$R = {}^tBu, {}^iPr, {}^nBu$$

$$+ \quad \underset{H}{\overset{R}{C=C}}\overset{SiH_2Ph}{\underset{H}{}} + \underset{H}{\overset{R}{C=C}}\overset{SiH_2Ph}{\underset{SiH_2Ph}{}} \quad (43)$$
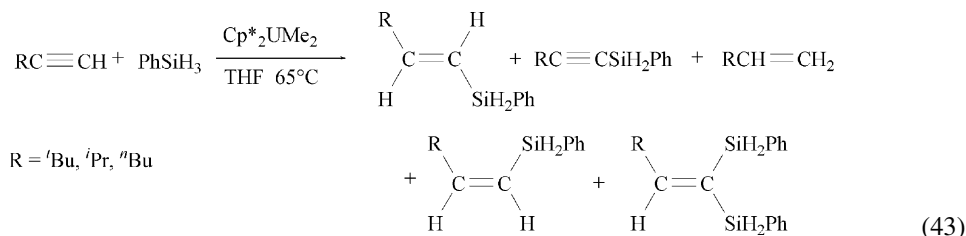
pathway involving two organometallic complexes formed, possibly in a consecutive manner, each species being responsible for each of the products.

The reaction of Cp${}_2^*$UMe$_2$ with Me$_3$SiC≡CH and PhSiH$_3$, was slow, producing the *trans*-Me$_3$SiCH=CHSiH$_2$Ph and the silylalkyne Me$_3$SiC≡CSiH$_2$Ph, respectively, whereas for the analogous Cp${}_2^*$ThMe$_2$, no hydrosilylation or dehydrogenative coupling products were observed (Eq. (41)).

6.1.3. Effect of the silane substituent and the alkyne: silane ratio on the hydrosilylation reaction

The replacement of a hydrogen atom on PhSiH$_3$ by either an alkyl or a phenyl group generated a delay in the hydrosilylation rate reaction as compared to the rate obtained utilizing phenylsilane. The selectivities of the products were appreciably

$$Me_3Si—C≡CH + PhSiH_3 \xrightarrow{Cp^*_2UMe_2} \underset{PhH_2Si}{\overset{H}{\underset{}{C=C}}}\overset{SiMe_3}{\underset{H}{}} + Me_3Si-C≡CSiH_2Ph \quad (41)$$

6.1.2.2. Scope of the reaction at high temperature.
The chemoselectivity and the regio-selectivity of the vinylsilanes formed in the organoactinide-catalyzed hydrosilylation of terminal alkynes with PhSiH$_3$ at high temperature (65–78 °C) were found to be diverse, as compared to the hydrosilylation results obtained at room temperature. In the hydrosilylation reaction of Me$_3$SiC≡CH with PhSiH$_3$ catalyzed by Cp${}_2^*$UMe$_2$, besides the *trans*-vinylsilane and the silylalkyne products, which were also obtained at room temperature (Eq. (41)), the *cis*-vinylsilane and the olefin Me$_3$SiCH=CH$_2$ were also observed (Eq. (42)). For Cp${}_2^*$ThMe$_2$, all the products formed with Cp${}_2^*$UMe$_2$ but the *cis*-vinylsilane were formed, in contrast to the room temperature reaction, in which no products were found.

different as compared to those obtained using PhSiH$_3$ as the hydrosilylating agent (Eq. (44)).

$$^iPrC≡CH + PhRSiH_2 \xrightarrow{Cp^*_2ThMe_2} \underset{H}{\overset{^iPr}{\underset{SiHRPh}{C=C}}}\overset{H}{\underset{}{}} + {}^iPrC≡CSiHRPh +$$

$$R = Ph, CH_3$$

$${}^iPrCH=CH_2 + \text{alkyne oligomers} \quad (44)$$
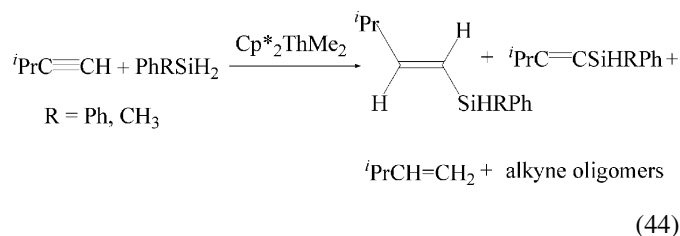
The effect of PhSiH$_3$ towards the formation of the different products was studied by performing parallel experiments. Large chemo- and regio-selectivity dependencies of the products on the silane concentrations were observed (Eq. (45)).

$$Me_3Si—C≡CH + PhSiH_3 \xrightarrow[\text{An = Th, U}]{Cp^*_2AnMe_2} \underset{H}{\overset{Me_3Si}{\underset{SiH_2Ph}{C=C}}}\overset{H}{\underset{}{}} + Me_3Si—C≡CSiH_2Ph + \underset{H}{\overset{Me_3Si}{C=CH_2}}$$

$$+ \quad \underset{H}{\overset{Me_3Si}{\underset{}{C=C}}}\overset{SiH_2Ph}{\underset{H}{}}$$

$$\text{for Cp}^*_2UMe_2 \text{ only} \quad (42)$$

(45)
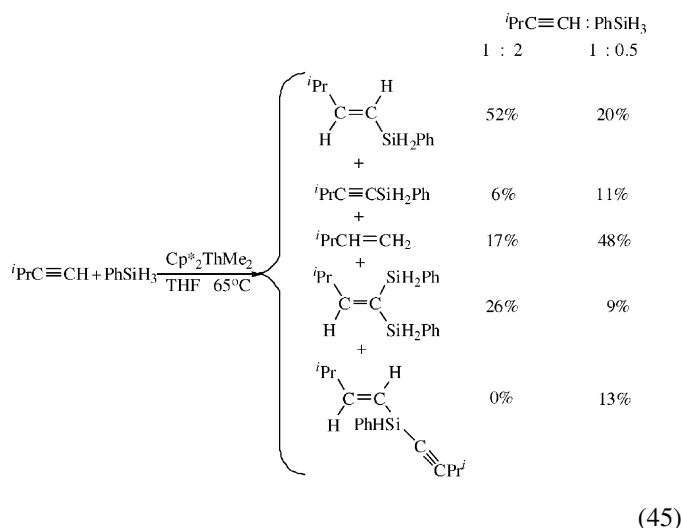
When the hydrosilylation reaction was carried out using a 1:2 ratio of ^{i}PrC≡CH:PhSiH$_3$ with Cp$_2^*$ThMe$_2$, the *trans*-vinylsilane was found to be the major product. When the reaction was conducted, with an opposite ratio between the substrates (^{i}PrC≡CH:PhSiH$_3$ = 0.5), the olefin ^{i}PrCH=CH$_2$ was found to be the major product, in addition to the other products (*trans*-^{i}PrCH=CHSiH$_2$Ph, ^{i}PrC≡CSiH$_2$Ph, the double hydrosilylated olefin, and the tertiary silane *trans*-^{i}PrCH=CHSi(HPh)(C≡C^{i}Pr)). The tertiary silane was obtained by the dehydrocoupling metathesis from the *trans*-alkenylsilane and the metal acetylide complex.

6.1.4. Kinetic studies on the hydrosilylation of ^{i}PrC≡CH with PhSiH$_3$ catalyzed by Cp$_2^*$ThMe$_2$

The kinetic study of the hydrosilylation of ^{i}PrC≡CH with PhSiH$_3$ catalyzed by Cp$_2^*$ThMe$_2$ shows the reaction has a first-order dependence in alkyne, silane and catalyst. The empirical rate law expression for the Cp$_2^*$ThMe$_2$ cat-

alyzed hydrosilylation of ^{i}PrC≡CH with PhSiH$_3$ is given by Eq. (46).

$$\nu = k[^i\text{PrC≡CH}][\text{PhSiH}_3][\text{Cp}_2^*\text{ThMe}_2] \tag{46}$$

From the Eyring analysis, the derived activation parameters, E_a, $\Delta H^\dagger$ and $\Delta S^\dagger$ values are 6.9(3) kcal mol^{-1}, 6.3(3) kcal mol^{-1} and 51.1(5) e.u., respectively.

6.1.5. Formation of active species, mechanism and thermodynamics in the hydrosilylation of alkynes

We have already seen that in the reaction of either bis(acetylide) organoactinide complex with PhSiH$_3$ the quantitative isolation of complexes **60** and **61**, for uranium and thorium, respectively, was observed (Eq. (38)). These complexes were formed by the σ-bond metathesis by the silane forming the corresponding actinide hydrides and the silylalkyne, which rapidly reinsert producing **60** or **61** (Eq. (47)).

An = Th (**61**), U (**60**)   (47)
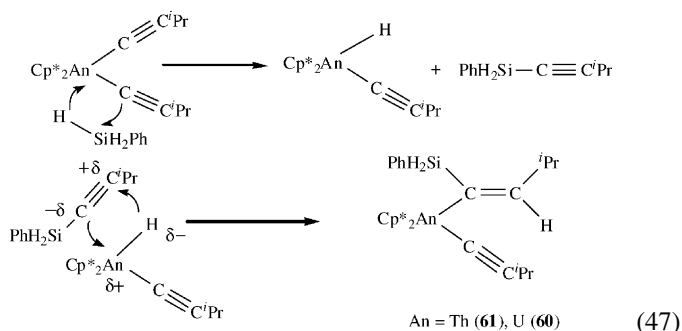
The regio-selective mode of insertion obtained for PhSiH$_2$C≡C^{i}Pr approaching the actinide hydride complex is electronically favored, as expected for the polarization of the organoactinides and the π* orbital of the alkyne [119]. In addition, since the insertion followed a four-center transition state mechanism, the *cis*-stereochemistry was expected, as corrob-
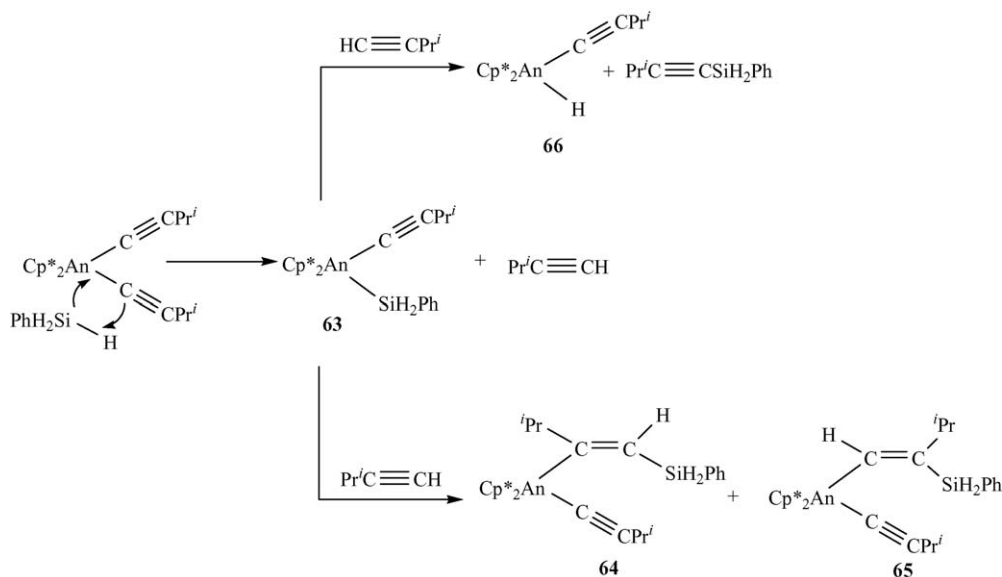
Scheme 20. Plausible organoactinide intermediates in the stoichiometric hydrosilylation of terminal alkynes via a transient organoactinide–silicon bond [117].

orated by the H_2O poisoning experiment (Eq. (39)) and the high temperature reactions with alkyne or silane. The same regio-selective insertion of $Me_3SiC\equiv CH$ to an organothorium alkenyl complex was observed in the organoactinide-catalyzed oligomerization of alkynes [76,77].

The formulation of an organoactinide-silane intermediate **63** as described in Scheme 20 was shown to be not operative due to the following arguments: (1) under stoichiometric conditions, the addition of silane did not induced the protonolysis of the acetylide–alkenylsilane complex (**60** or **61**), arguing how difficult should the production of complex **63** be, (2) the quenching experiments with water gave exclusively the *cis*-vinylsilane, (3) no geminal hydrosilylated products were obtained (to the case that the complex **65** is an intermediate), (4) no *cis* double hydrosilylated product was observed (if σ-bond metathesis occurred from complex **64** or **65**) and (5) no *cis*-hydrosilylated products can be obtained from complex **63** [117].

The reactions of complexes **60** or **61**, yielding the double hydrosilylated product (Eq. (48)) were proposed to be stereoselectively favored, due to the assumed polarization of the $PhSiH_3$ toward the metal center, as well as the preferred thermodynamics, as compared to the protonolysis by the silane producing complex **63** and the *cis*-hydrosilylated product ($\Delta H_{(Th)} = +15(4)\,\text{kcal mol}^{-1}$ and $\Delta H_{(U)} = -3(2)\,\text{kcal mol}^{-1}$).

$$\Delta H_{1h} = +2\,(3)\,\text{kcal mol}^{-1} \quad \Delta H_U = -5\,(2)\,\text{kcal mol}^{-1}$$

(48)
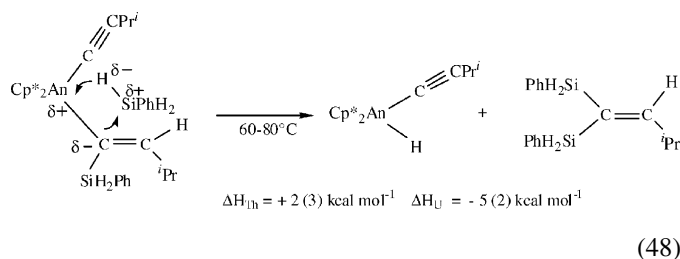
The most remarkable observation regarded the reaction products of complexes **60** or **61** with alkyne at either low or high temperature. At elevated temperatures, the expected *cis*-hydrosilylated product was obtained, but at low temperatures the unexpected *trans*-isomer was achieved. These results have been explained through an operative competitive mechanism talking

into account an equilibrium giving the different hydrosilylation products at different temperatures.

Regarding the alkynes, $Me_3SiC\equiv CH$ exhibited a total lack in reactivity with $PhSiH_3$ in the presence of $Cp_2^*ThMe_2$ at room temperature. However, at high temperature the *trans*-vinylsilane, the silylalkyne and the alkene were obtained. This type of reactivity was explained, in general, as the result of a kinetic effect suggesting another equilibrium between the organometallic complexes **67** with **68** (Scheme 21). Complex **68** was obtained by the insertion of the silylalkyne into a hydride complex. Complex **68** will be able to react with another alkyne yielding the alkene and the bis(acetylide) complex (protonolysis route) or react with a silane producing the organometallic hydride and the *trans*-product (σ-bond metathesis route). The low activity obtained for $Me_3SiC\equiv CH$ was explained via elevated activation energy to perform either the metathesis or protonolysis of complex **68**, as compared with other alkynes [117].

The ratio between the silane and the alkyne was found to govern the kinetics toward the different products. Thus, when the $PhSiH_3$:$^iPrC\equiv CH$ ratio was two, the *trans*- and the double-hydrosilylation products were the major products (metathesis route). Increasing the alkyne concentration routed the reaction towards the alkene and the bis(acetylide) complex (protonolysis route). A likely mechanism for the hydrosilylation of terminal alkynes catalyzed by $Cp_2^*ThMe_2$ was proposed and described in Scheme 22.

The mechanism presented in Scheme 22, comprises an insertion of an acetylene into a metal–hydride σ-bond, σ-bond metathesis by a silane and protonolysis by an acidic alkyne hydrogen. The precatalyst $Cp_2^*ThMe_2$ in the presence of alkyne was converted to the bis(acetylide) complex **69** (step 1). Complex **69** reacts with $PhSiH_3$ towards the silylalkyne and the organoactinide hydride **70** (step 2), which was found to be in equilibrium with the intermediate **71** after reinsertion of the silylalkyne with the preferential stereochemistry (step 6). Complex **71** was found to be the principal complex under silane and alkyne starvation. Complex **70** reacts with an alkyne producing the alkenyl acetylide–organothorium complex **72** (step 3), which is presumably in equilibrium with complex **70** (first-order

Scheme 21. High temperature hydrosilylation of $Me_3SiC\equiv CH$ with $PhSiH_3$ catalyzed by $Cp_2^*ThMe_2$, protonolysis and σ-bond metathesis routes [117].

Scheme 22. Plausible mechanism for the room and high temperature hydrosilylation of isopropylacetylene (R = ^{i}Pr) with PhSiH$_3$ promoted by Cp$_2^*$ThMe$_2$ [117].

in alkyne). Complex **72** was proposed to react with PhSiH$_3$, as the rate-determining step, regenerating the hydride complex **70** and the *trans*-hydrosilylated product (step 4). Under the catalytic conditions, complex **72** may also react with a second alkyne producing the alkene and the bis(acetylide) complex **69** (step 5). A similar insertion of the alkene into complex **70** with the concomitant reaction with an additional alkyne, will produced the double hydrogenated product, as found for isopropylacetylene. At high temperature, complex **71** may react with an alkyne (step 7) yielding complex **69** and the *cis*-isomer or with a silane (step 8) yielding complex **70** and the double hydrosilylation product. Thus, the reaction rate law (Eq. (45)) was rationalized with rapid irreversible phenylsilane metathesis with complex **69**, rapid pre-equilibrium involving the hydride and alkenyl complexes **70** and **72**, and a slow metathesis by the PhSiH$_3$. For the thorium complex, step 8 was found to be much faster than step 7 since the *cis*-product was obtained in trace amounts.

The mechanistic pathway as proposed, takes into the account comparable yields for the alkene and silylalkyne even when the alkyne concentration was in excess (the sum of the silylated products must equal to the amount of the alkene). For both the thorium and uranium complexes, the amount of the hydrosilylated product was always similar or larger than that of the alkene, indicating that a competing equilibrium should be operative, responsible for the transformation of the hydride complex back to the biscetylide complex, allowing the production of the silylalkyne without producing the alkene (Eq. (49)).

$$(49)$$

Thermodynamically, it is very interesting to compare the possible mechanistic hydride and silane intermediates towards the possible hydrosilylation *trans*-product as presented in Eqs. (50) and (51), respectively.

$$(50)$$

$$(51)$$

The calculated enthalpy of reaction for the insertion of an alkyne into an actinide hydride bond (Eq. (50)) ($\Delta H_{\text{Th}} = -33$ kcal mol^{-1} and $\Delta H_{\text{U}} = -36$ kcal mol^{-1}) or into an actinide–silane bond (Eq. (51)) ($\Delta H_{\text{Th}} = -52$ kcal mol^{-1} and $\Delta H_{\text{U}} = -34$ kcal mol^{-1}) were expected to be exothermic. However, the protonolysis by the silane yielding the An–Si bond and the *trans*-product (Eq. (51)) was for thorium an endothermic process ($\Delta H_{\text{Th}} = +15$ kcal mol^{-1}), as compared to the exothermicity of the σ-bond metathesis (Eq. (50)) of the thorium alkenyl complex by the silane ($\Delta H_{\text{Th}} = -19$ kcal mol^{-1}), yielding the corresponding Th–H bond and the *trans*-product. For the corresponding uranium complexes, the latter processes were cal-

culated to be exothermic although the σ-bond metathesis route (Eq. (50)) was more exothermic ($\Delta H_U = -26$ kcal mol^{-1}) than the protonolysis route (Eq. (51)) ($\Delta H_U = -3$ kcal mol^{-1}).

6.2. Catalytic hydrosilylation of terminal alkynes promoted by the bridged complex $Me_2Si(C_5Me_4)_2Th^nBu_2$

6.2.1. Scope of the reaction at room temperature

The hydrosilylation reaction of terminal alkynes and PhSiH$_3$ catalyzed by Me$_2$Si(C$_5$Me$_4$)$_2$Th^{n}Bu$_2$ resulted in the fast and regio-selective formation of the hydrosilylation *trans*-vinylsilane as the unique product regardless of the alkyne substituent (Eq. (52)) [37].
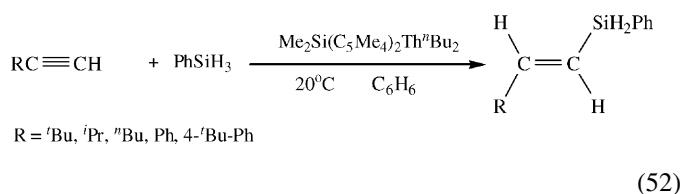
R = ^{t}Bu, ^{i}Pr, ^{n}Bu, Ph, 4-^{t}Bu-Ph

(52)

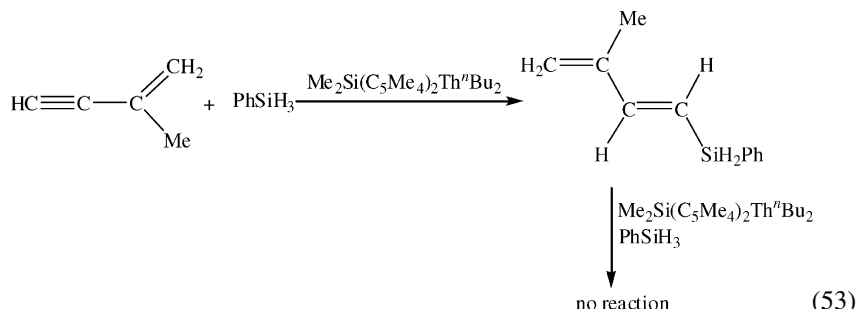When an olefin-functionalized alkyne was used for the reaction with PhSiH$_3$, the alkyne moiety was regio-selectively hydrosilylated toward the corresponding *trans*-diene (Eq. (53)). Addition of an excess of PhSiH$_3$ did not induce any subsequent hydrosilylation.

(53)

although the addition of an excess of PhSiH$_3$ to any of the vinyl-silane products did not induced further hydrosilylation, addition of a second equivalent of an alkyne to the hydrosilylation product allowed the formation of the corresponding alkene and the dehydrogenative coupling of the alkyne with the *trans*-vinylsilane (Eq. (54)) [120–123].

R' = ^{i}Pr (35%)   R' = ^{i}Pr (60%)
R' = ^{t}Bu (33%)   R' = ^{t}Bu (63%)

(54)
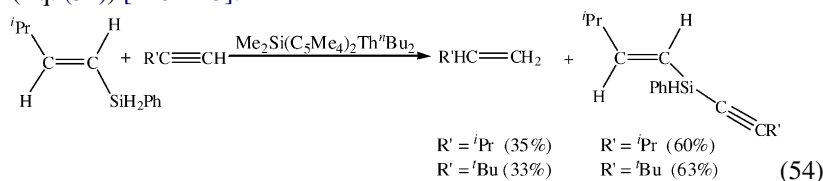
Mechanistically, in the hydrosilylation reactions of organo-f-element complexes two Chalk Harrod mechanisms has been proposed as plausible routes, except for the inclusion of a σ-bond metathesis instead of the classical oxidative addition-reductive elimination processes. The two mechanisms differ in the reactive intermediates; the hydride (M−H) route and the silane (M−SiR$_3$) route [124–135]. The use of terminal alkynes, for bridged organoactinides, was an excellent probe to investigate which of the two routes was the major followed pathway. Thus, taking into account that the alkyne was expected to insert

with the substituent group pointing away from the metal center (as observed in the dimerization) the following mechanistic insights were obtained. If the hydrosilylation reaction undergoes through a M−SiR$_3$ intermediate, the *gem*-hydrosilylated vinyl isomer will be formed, whereas through the M−H route only the *trans*-isomer will be obtained (if the insertion stereochemistry is not maintained, the *cis*-product will be observed). The exclusive selectivity obtained for Me$_2$Si(C$_5$Me$_4$)$_2$Th^{n}Bu$_2$ towards the *trans*-hydrosilylated isomer argued that the hydride route was acting as the major operative mechanistic pathway. The hydrosilylation of terminal alkynes with PhSiH$_3$ promoted by the bridged complex Me$_2$Si(C$_5$Me$_4$)$_2$Th^{n}Bu$_2$ produced regio- and chemo-selectively the *trans*-hydrosilylated vinylsilane without any other by-products. The non-appearance of silylalkynes, the dehydrogenative silane coupling products or any other geometrical isomer of the vinylsilane strongly indicated that the Th−H pathway was the major operative route in the hydrosilylation reaction.

6.2.2. Kinetic, thermodynamic and mechanistic studies of the hydrosilylation of terminal alkynes with primary silanes promoted by $Me_2Si(C_5Me_4)_2Th^nBu_2$

Kinetic measurements on the hydrosilylation ^{i}PrC≡CH with PhSiH$_3$ catalyzed by Me$_2$Si(C$_5$Me$_4$)$_2$Th^{n}Bu$_2$ shows that the reaction behaves with a first-order dependence in precatalyst and silane, and exhibited an inverse proportionality (inverse first-order) in alkyne. The inverse proportionality was consistent with a rapid equilibrium before the turnover-limiting step removing one of the key organoactinide intermediates out of the catalytic cycle (Eq. (55)).

$$v = k[Me_2Si(C_5Me_4)_2Th^nBu_2][\text{silane}]^1[\text{alkyne}]^{-1}$$ (55)

The $\Delta H^{\ddagger}$ and $\Delta S^{\ddagger}$ parameter values derived from a thermal Eyring analysis were measured to be 10.07(5) kcal mol^{-1} and $-22.06(5)$ e.u., respectively [37].
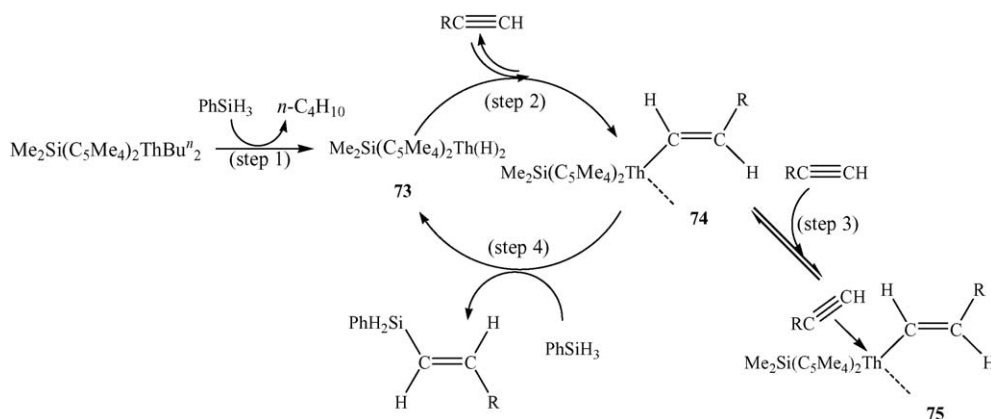
Scheme 23. Plausible mechanism for the hydrosilylation of terminal alkynes with $PhSiH_3$ promoted by $Me_2Si(C_5Me_4)_2Th^nBu_2$. For clarity, only one alkenyl group at the metal is shown [37].

It is important at this stage to mark the difference in the kinetic behavior of the alkyne in the hydrosilylation reaction as compared to the dimerization process (vide supra). In the latter process, the alkyne was operative in two parallel routes, both sensitive to the alkyne concentration. In one route, the alkyne exhibited an inverse kinetic order (removing an active component from the catalytic cycle), whereas in the second pathway the alkyne reacted in the rate-determining step. Thus, the effect at high alkyne concentrations nullifies the overall alkyne effect. In the hydrosilylation process, the alkyne was proposed to be removing an active component of the catalytic cycle and the silane is presumably reactive in the rate-limiting step. Thus, no annulment of the alkyne effect was observed. A plausible mechanism for the hydrosilylation of terminal alkynes toward *trans*-vinylsilanes was proposed and presented in Scheme 23.

The precatalyst $Me_2Si(C_5Me_4)_2Th^nBu_2$ was converted in the presence of silane and alkyne into the hydride complex **73** (step 1), as observed by the stoichiometric formation of n-$BuSiH_2Ph$. Fast insertion of an alkyne into complex **73** allows the formation of the vinylic complex **74** (step 2), which in turn was found to be in rapid equilibrium with the proposed π-complex **75** (step 3). This step was responsible for the inverse order in alkyne. Complex **74** undergoes a σ-bond metathesis with $PhSiH_3$, as the rate-determining step (step 4), regenerating complex **73** and producing selectively the *trans*-hydrosilylated vinyl product. The observation that no geometrical isomers or different products were formed by adding an excess of $PhSiH_3$ to any of the vinyl-silanes led to the conclusion that neither the hydride complex **73** nor the alkenyl complex **74** were the resting catalytic state, and pointed toward complex **75** as the resting state. However, the subsequent addition of a second equivalent of an alkyne to the reaction mixture formed the corresponding alkene and the sily-lalkyne. The formation of these two compounds was proposed to follow the mechanistic pathway as shown in Scheme 24. In the absence of a primary silane, complex **74** reacts with another alkyne (step 5) producing the corresponding alkene and the acetylide complex **76**. A σ-bond metathesis with the Si—H bond of the vinylsilane (step 6) formed the dehydrogenative coupling product and regenerated the hydride complex **73** [39].

The yield of the alkene was found to be lower than that of the silylalkyne product. Therefore, an additional equilibrium reaction was proposed operative, responsible for the transformation of complex **73** into the acetylide complex **76**, allowing the formation of the silylalkyne without forming the alkene. This pathway was also observed for non-bridged organoactinides (Eq. (49)) [14]. In the hydrosilylation process catalyzed by the bridged complex, larger turnover frequencies were measured as compared to $Cp_2^*YMe(THF)$ or other lanthanide complexes [136]. This yttrium complex induced hydrosilylation of internal alkynes, preferentially towards the *E*-isomer, although the *Z*-isomer was found in comparable amounts in some cases. Mechanistically, the active species for the yttrium hydrosilylation of internal alkynes was proposed to be the corresponding hydride [137]. The hydrosilylation of alkynes is induced either by transition-metal catalysts [138–140] or by radical initiators [141]. The radical procedure often provides a mixture of *trans*- and *cis*-hydrosilylation products, while the transition-metal catalyzed reaction proceeds with high stereoselectivity via a *cis*-hydrosilylation pathway, generally producing a mixture of two regio-isomers (terminal and internal adducts). Thus, the organoactinide process seems to complement the chemistry of other transition-metal complexes by inducing a unique chemical environment which allows the production of the *trans*-vinylsilane.

6.3. Catalytic hydrosilylation of alkynes promoted by the cationic complex $[(Et_2N)_3U][BPh_4]$

6.3.1. Scope of the reaction at room and high temperature

The hydrosilylation reaction pathways of terminal alkynes promoted by neutral organoactinides has been the motivation regarding the possibility to form a similar cationic hydride complex, as an intermediate, in the catalytic hydrosilylation of terminal alkynes, promoted by the cationic complex $[(Et_2N)_3U][BPh_4]$ [97]. The reaction of terminal alkynes $RC{\equiv}CH$ (R = ^iPr, ^tBu) and $PhSiH_3$ catalyzed by $[(Et_2N)_3U][BPh_4]$ resulted in the formation of numerous products. The products observed (to account for 100% conversion of the alkyne) were: *cis*- and *trans*-vinylsilane
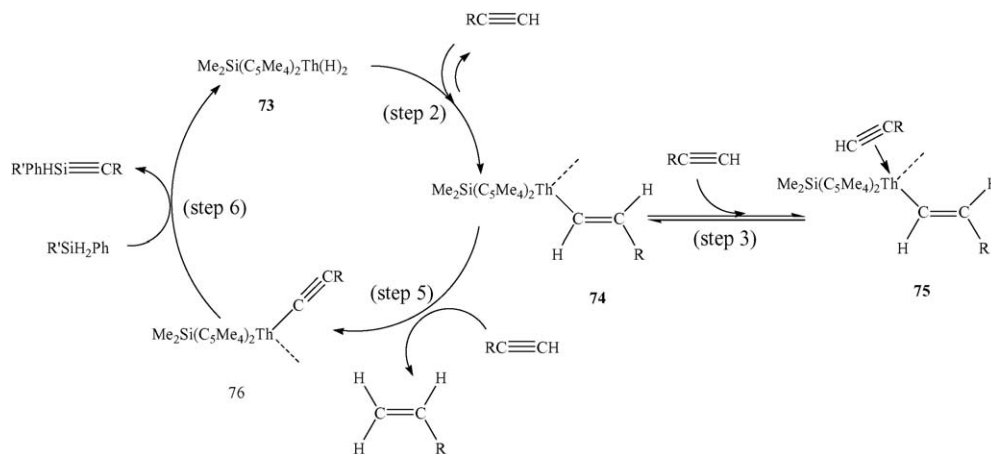
Scheme 24. Proposed mechanism for the alkene and silylalkyne formation in the presence of vinylsilanes and terminal alkynes promoted by $Me_2Si(C_5Me_4)_2Th^nBu_2$. For clarity, only one of the equatorial ligations at the metal center is shown.

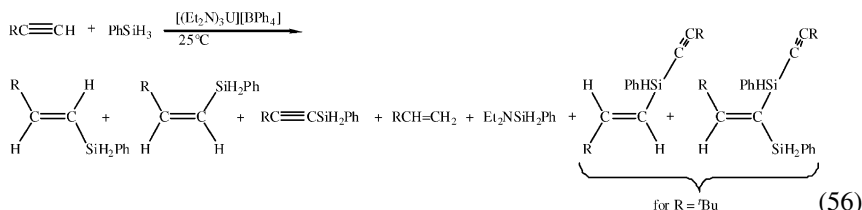(RCH=CHSiH$_2$Ph), alkenes (RCH=CH$_2$) and the dehydrogenative silylalkyne (RC≡CSiH$_2$Ph) (R = ^{i}Pr, ^{t}Bu), in addition to the aminosilane Et$_2$NSiH$_2$Ph. For the bulky alkyne ^{t}BuC≡CH, the tertiary silanes trans-^{t}BuCH=CHSi(HPh)(C≡C^{t}Bu) and ^{t}BuCH=C(SiH$_2$Ph)Si(HPh)(C≡C^{t}Bu) were also observed (Eq. (56)). Formation of the tertiary silanes can be accounted for by the metathesis reactions of the double hydrosilylated compound and the trans-alkenylsilane with the metal acetylide complex (Et$_2$N)$_2$U−C≡CR (**77**), respectively, as shown in Eqs. (57) and (58).

(56)

(56)), the corresponding double hydrosilylated compounds RCH=C(SiH$_2$Ph)$_2$, and small amounts of the corresponding geminal dimers and trimers.

(57)

(58)

6.3.2. Mechanistic studies of the hydrosilylation of alkynes promoted by the cationic complex [(Et$_2$N)$_3$U][BPh$_4$]

Based on kinetics and products distributions, a similar type of mechanism as observed for the neutral organoactinides was proposed. The formation of an active uranium hydride complex **78** was conceivable either by the reaction of the acetylide complex **77** with a silane, producing the corresponding silaalkyne or/and by the reaction of the cationic complex with a silane

At high temperature (65–78 °C), the chemo- and regioselectivity of the products formed in the cationic organouranium-catalyzed hydrosilylation of terminal alkynes with PhSiH$_3$ were found to differ from those obtained at room temperature. The hydrosilylation of RC≡CH (R = ^{n}Bu, ^{i}Pr, ^{t}Bu) with PhSiH$_3$ catalyzed by [(Et$_2$N)$_3$U][BPh$_4$] produced, in addition to the hydrosilylation products at room temperature (Eq.

molecule, giving the corresponding aminosilane (Eqs. (59) and (60), respectively).

$$[(Et_2N)_2U]^+\!-\!C\!\equiv\!CR \xrightarrow{PhSiH_3} [(Et_2N)_2U]^+\!-\!H + RC\!\equiv\!CSiH_2Ph$$
$$\underset{\textbf{77}}{} \qquad\qquad \underset{\textbf{78}}{}$$

(59)

$$[(Et_2N)_3U]^+ \xrightarrow{PhSiH_3} [(Et_2N)_2U]^+\!-\!H + PhSiH_2NEt_2$$

(60)
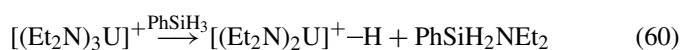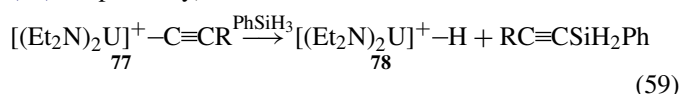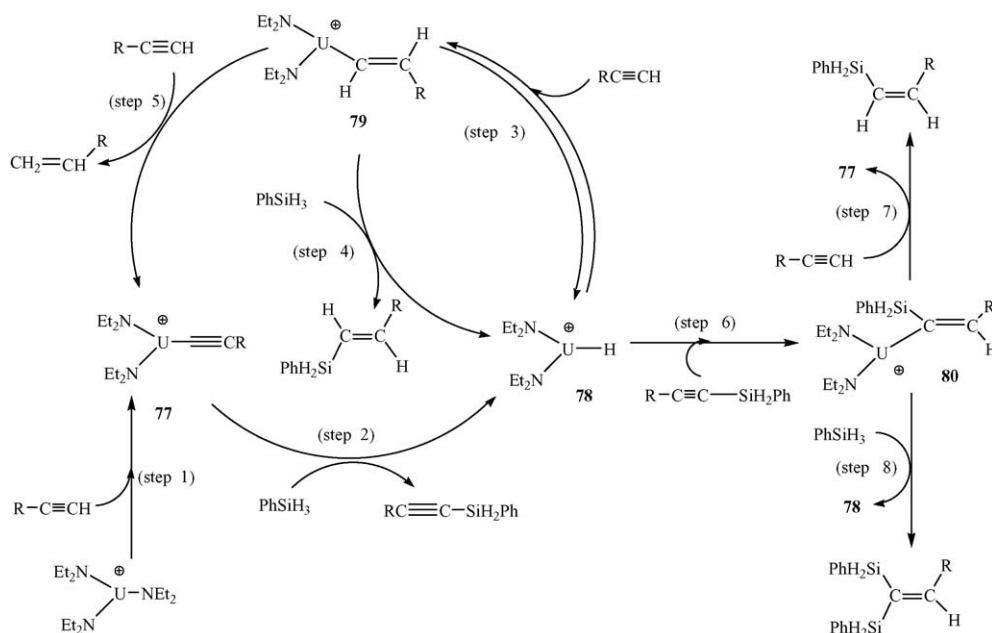
Scheme 25. Plausible mechanism for the room and high temperature hydrosilylation of terminal alkynes promoted by the cationic complex [(Et$_2$N)$_3$U][BPh$_4$] [97].

The proposed mechanism, which takes into account the formation of all the products, is described in Scheme 25 [97].

In the presence of alkyne, the precatalyst [(Et$_2$N)$_3$U][BPh$_4$] was converted to the acetylide complex **77** removing one of the amido ligands (step 1). Com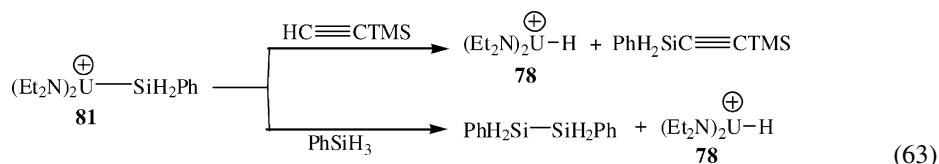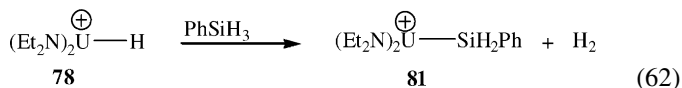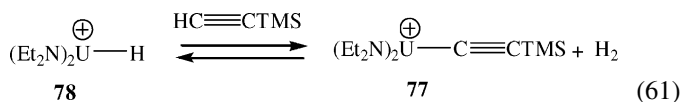plex **77** was proposed to react with PhSiH$_3$ to give the silylalkyne and the actinide hydride **78** (step 2). The hydride **78** may react with the alkyne to produce the alkenyl uranium complex **79** (step 3) or reinsert the silaalkyne forming complex **80** (step 6). Complex **79** will react with PhSiH$_3$, producing back the organouranium hydride

organometallic silyl compound [(Et$_2$N)$_2$USiH$_2$Ph][BPh$_4$] (**81**) (Eq. (62)), which would further react with RC≡CH or PhSiH$_3$ to give back the hydride **78** and PhH$_2$SiC≡CR or PhH$_2$Si−SiH$_2$Ph, respectively (Eq. (63)).

$$\underset{\textbf{78}}{(Et_2N)_2\overset{\oplus}{U}-H} \;\; \underset{}{\overset{HC\equiv CTMS}{\rightleftharpoons}} \;\; \underset{\textbf{77}}{(Et_2N)_2\overset{\oplus}{U}-C\equiv CTMS} + H_2 \qquad (61)$$

$$\underset{\textbf{78}}{(Et_2N)_2\overset{\oplus}{U}-H} \;\; \overset{PhSiH_3}{\longrightarrow} \;\; \underset{\textbf{81}}{(Et_2N)_2\overset{\oplus}{U}-SiH_2Ph} + H_2 \qquad (62)$$

$$\underset{\textbf{81}}{(Et_2N)_2\overset{\oplus}{U}-SiH_2Ph} \begin{array}{l} \overset{HC\equiv CTMS}{\longrightarrow} \underset{\textbf{78}}{(Et_2N)_2\overset{\oplus}{U}-H} + PhH_2SiC\equiv CTMS \\[2ex] \overset{PhSiH_3}{\longrightarrow} PhH_2Si-SiH_2Ph + \underset{\textbf{78}}{(Et_2N)_2\overset{\oplus}{U}-H} \end{array} \qquad (63)$$

complex **78** and the *trans*-hydrosilylated product (step 4). Under the catalytic conditions, complex **79** may also react with a second alkyne to yield the alkene and the acetylide complex **77** (step 5). Complex **80** may react with an alkyne (step 7) yielding complex **77** and the *cis*-isomer or react with a silane (step 8) yielding complex **78** and the double hydrosilylation product.

This proposed mechanism takes into account the higher yields of the alkene compound when compared with those of the silylalkyne. For Me$_3$SiC≡CH and ^{i}PrC≡CH, at high temperature, the amount of the hydrosilylated products is larger than that of the alkenes, indicating that an optional competing equilibrium route was operative. This route would involve the transformation of the hydride **78** back into the acetylide complex **77** by reaction with the alkyne (Eq. (61)), which allows the production of more silylalkyne without the production of the alkene. The hydride **78** could alternatively react with PhSiH$_3$ to give the

When ^{t}BuC≡CH was hydrosilylated at high temperature, a small amount of the dehydrogenative coupling of phenylsilane was observed. The formation of this product suggests the formation of a complex bearing a uranium–silicon bond, although not as a major operative intermediate. Considering that the silane might act as the protonolytic source, the complex [(Et$_2$N)$_2$USiH$_2$Ph][BPh$_4$] (**81**) can be theoretically postulated instead of the hydride complex **78**, either from steps 2, 4 or 8 in the catalytic cycle (Scheme 25).

6.4. Catalytic hydrosilylation of alkenes promoted by organoactinide complexes

6.4.1. Scope of the reaction

The organoactinide complexes Cp$_2^*$ThMe$_2$ and Me$_2$Si(C$_5$Me$_4$)$_2$Th^{n}Bu$_2$ were also found to be good precatalysts for the highly regio-selective hydrosilylation of alkenes. The reactions of Cp$_2^*$ThMe$_2$ and Me$_2$Si(C$_5$Me$_4$)$_2$Th^{n}Bu$_2$ with

Table 1
Results obtained for the hydrosilylation of alkenes promoted by $Cp_2^*ThMe_2$ (**1**) and $Me_2Si(C_5Me_4)_2Th^nBu_2$ (**3**)[a]

Entry	Cat.	R in RHC=CH	Temperature (°C)	Time (h)	Yield of 1-silylalkane (%)	Yield of alkane (%)	N_t[b] (h^{-1})
1	**3**	^nBu	20	12	63	35	5.5
2	**1**	^nBu	20	12	54	44	1.5
3	**3**	^nBu	78	1	62	36	64.5
4	**1**	^nBu	78	6	57	41	3.2
5	**3**	$^nC_6H_{13}$	20	12	65	33	4.6
6	**1**	$^nC_6H_{13}$	20	12	68	30	1.9
7	**3**	$PhCH_2$	78	1	71	29	83.1
8	**1**	$PhCH_2$	78	6	61	38	4.8
9	**3**	Ph	78	36	31(30)[c]	37	1.9
10	**1**	Ph	78	36	65(6)[c]	28	0.9

[a] Solvent = benzene.
[b] Turnover frequency for the hydrosilylation process.
[c] The number in parenthesis correspond to the 2,1-addition hydrosilylation product, 2-(phenylsilyl)ethylbenzene.

an excess of $PhSiH_3$ and an alkene resulted in the production of the regio-selective 1,2-addition hydrosilylated alkene and the alkane with no major differences between the two organoactinides (Eq. (64)) and Table 1 [37]. The chemo-selectivity of the reactions was moderate since the hydrogenated alkane was always encountered as a concomitant product.
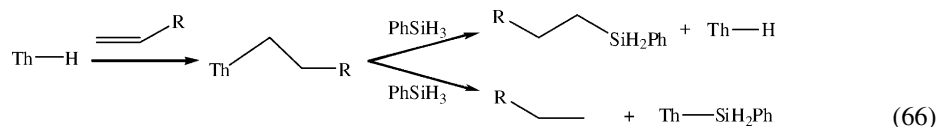
$$RHC{=\!=}CH_2 \; + \; PhSiH_3 \xrightarrow{\text{cat.}} RH_2C{-\!\!-}CH_3 \; + \; RH_2C{-\!\!-}CH_2$$
$$\overset{\hspace{3.5cm}}{\underset{\hspace{3.5cm}SiH_2Ph}{}}$$
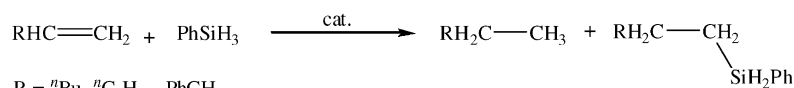
R = ^nBu, $^nC_6H_{13}$, $PhCH_2$

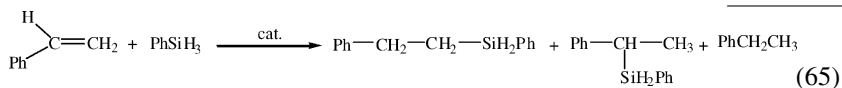cat. = $Cp^*_2ThMe_2$ or $Me_2Si(C_5Me_4)_2Th^nBu_2$

(64)

Since for the reaction of allyl benzene only one hydrosilylated product was formed, a comparison of the effect of the distance between the aromatic ring and the metal center was performed. In the hydrosilylation of styrene with each of the organoactinides (Eq. (65)), both 1,2 and 2,1 addition hydrosilylation products were obtained, in addition to ethylbenzene. For $Cp^*_2ThMe_2$ a small amount of the branched silane was obtained whereas for $Me_2Si(C_5Me_4)_2Th^nBu_2$ equal amounts of both (linear and branched) isomers were yielded (entries 9 and 10 in Table 1).

$$\overset{H}{\underset{Ph}{}}C{=\!=}CH_2 + PhSiH_3 \xrightarrow{\text{cat.}} Ph{-\!\!-}CH_2{-\!\!-}CH_2{-\!\!-}SiH_2Ph \; + \; Ph{-\!\!-}\underset{SiH_2Ph}{CH}{-\!\!-}CH_3 + PhCH_2CH_3$$

(65)

The presence of both the hydrosilylation and the hydrogenation products indicates that two parallel catalytic pathways exist. The formation of the hydrogenation products required

considering the possibility that the intermediates Th–Si/Th–H bonds were formed (Eq. (66)). Consequently, the production of alkanes might be considered as indirect evidence of the existence of complexes containing an actinide–Si bond. Metathesis of the Th–carbyl by the silane will produce the hydrosilylated compound and regenerating the hydride complex, while protonolysis of a Th–carbyl by the silane will yield the Th–Si bond and the hydrogenation product.

(66)

The reaction between $Cp^*_2ThMe_2$ and an excess of 1-octene was studied in order to exclude an additional theoretical possibility to obtain a hydrogenation product, from a Th–alkyl complex. This product might be produced by cutting the alkyl chain with an additional alkene, forming a transient vinyl complex. Although no hydrogenation product was observed, ruling out the protonolysis by an alkene, a stoichiometric reaction was observed (Eq. (67)), allowing the production of 2-methyl-1-octene, 2-nonene and 3-nonene in almost equal amounts, and the additional slow catalytic isomerization of the starting 1-octene to E-4-octene (3.8%), E-3-octene (39.4%), E-2-octene (13.0%) and Z-2-octene (41.8%) [37].
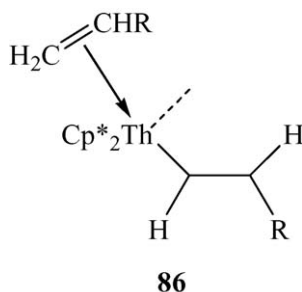

(67)
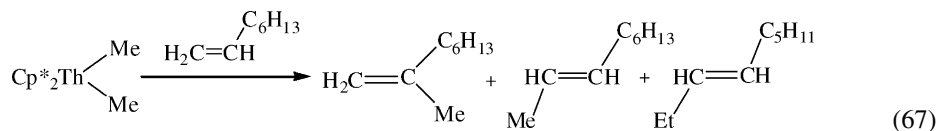
Fig. 4. Proposed structure of the π-alkene thorium–alkyl complex **86**.

the formation of these products indicates that the Th−Me bond inserts into the alkene moiety forming a Th–alkyl complex, followed by a β-hydrogen elimination to the corresponding metal–hydride (Th−H) and equimolar amounts of all three isomeric nonenes. The hydride was proposed to be the active species in the isomerization of 1-octene. The same reaction with 2-octene showed a slower reaction and different product ratios (*E*-3-octene (11.2%), *E*-2-octene (82.2%) and *Z*-2-octene (6.6%)) indicating a non-equilibrium process between 1-octene and 2-octene. Based on the hypothesis that only two complexes with either a thorium–hydride (Th−H) or a thorium–alkyl (Th−R) were expected, the following experiment was performed, in order to study the resting state of the organoactinide moiety. The isomerization reaction of 1-octene was performed until a full conversion (>98%). All the volatiles were transferred by high vacuum and new solvent was reintroduced. The ratio between the products, which remained in the reaction mixture, was measured by GC chromatography, showing full disappearance of 1-octene. By using a slight excess of D_2O, at low temperature, the reaction mixture containing the organometallic complexes was quenched. Analysis of the solution showed the presence of a mono-deuterated 1-*d*-octane, indicating that the Th–alkyl moiety was the resting organoactinide complex. The GC chromatograph after the D_2O quenching showed equimolar amounts of 1-octene, as compared to the starting amount of the metal complex. This astounding result indicated that a π-*alkene thorium–alkyl* complex (**86**, shown in Fig. 4) was the resting catalytic state of the organoactinide complex; D_2O quenching liberated the alkene and the alkane from the metal.

6.4.2. Kinetic and mechanistic studies of the hydrosilylation of alkenes with PhSiH₃

Kinetic measurements of the hydrosilylation of allylbenzene with PhSiH₃ catalyzed by Cp$_2^*$ThMe₂ were performed. The reaction follows a first-order dependence in precatalyst and silane, and an inverse first-order dependence in alkene. The inverse proportionality as described for alkynes is consistent with a rapid equilibrium before the rate-determining step, steering an intermediate out of the catalytic cycle. Consequently, the rate law for the hydrosilylation of alkenes with PhSiH₃ promoted by Cp$_2^*$ThMe₂ can be expressed as presented in Eq. (68).

$$v = k[\text{Cp}_2^*\text{ThMe}_2][\text{silane}]^1[\text{alkene}]^{-1} \qquad (68)$$

The derived E_a, $\Delta H^\ddagger$ and $\Delta S^\ddagger$ parameter values from an Arrhenius and a thermal Eyring analysis were measured to be 11.0(4), 10.3(4) kcal mol^{-1} and −45 e.u., respectively.

Comparison of the products distribution with both catalytic systems revealed that increasing the coordinative unsaturation of the organothorium complex had no special effect. The presence of the two-hydrosilylation products suggested the presence of two parallel interconnecting competing pathways. The formation of the alkane required considering the intermediate Th−H/Th−Si moieties [142,143]. The only evidence so far for the existence of a Th−Si bond, has been the formation of a metalloxy ketene via the double insertion of carbon monoxide into a Th−Si bond [144]. The proposed mechanism for the hydrosilylation of alkenes promoted by Cp$_2^*$ThMe₂ or Me₂Si(C₅Me₄)₂Th^{n}Bu₂ is presented in Scheme 26 which shows the mechanism for the former complex.

The first step in the proposed mechanism is the reaction of the precatalyst Cp$_2^*$ThMe₂ with PhSiH₃ yielding the hydride complex **82** and PhSiH₂Me (step 1). Complex **82** reacts with an alkene to produce the alkyl complex **83** (step 2), which can undergo three parallel pathways. The first path, another reaction with an alkene, produces the π-alkene complex (**86**), driving complex **83** out of the catalytic cycle (step 3). This step was found to be responsible for the inverse order in alkene. The second pathway is a protonolysis of the Th–carbyl fragment of **83** by the Si−H moiety, yielding the Th−SiH₂Ph complex (**84**) and the alkane (step 4). The last possible pathway involves the metathesis of the Th–carbyl complex by the Si−H to form the substituted silane and complex **82** (step 5). The proposed scenario also considered the formation of compounds in trace amounts. The formation of both hydrosilylation products in similar amounts for styrene has indicated comparable activation energy for both processes, diverging only in the disposition of the silane with respect to the thorium carbyl complex. The Th−SiH₂Ph bond in complex **84** can be activated by two different methods. The first method is the metathesis reaction with the Si−H bond in PhSiH₃ producing the dehydrogenative dimer and the hydride **82** (step 6). The other method is the reaction of with the Si−Ph bond, yielding Ph₂SiH₂ and a complex containing the Th−SiH₃ moiety (**85**, step 7), which will then rapidly react with an additional silane yielding the oligomeric dehydrogenative coupling of silanes and regenerating complex **82** (step 8).

In the hydrosilylation of styrene (Scheme 27), the formation of the branched isomer was rationalized by the stereochemistry in the metathesis reaction of the styrene with the metal–hydride complex that is presumably stabilized by the π-arene interaction. Thus, complex **87** is more stable then complex **88**, which results in higher yields of the branched isomer.

For alkenes, the hydrosilylation reaction promoted by organoactinides is much slower (about one order of magnitude) then the analogue organolanthanides of the types Cp$_2^*$LnR (Ln = Sm, La, Lu) or Me₂Si(C₅Me₄)₂SmR (R = alkyl). The difference is found for linear terminal alkenes, which lanthanides will hydrosilylate forming both isomers, while actinides will exclusively yield the 1,2-adduct product [123,124,136]. Mechanistically, lanthanide hydrides were postulated as the primordial pathway toward the hydrosilylated products. Thus, organoac-
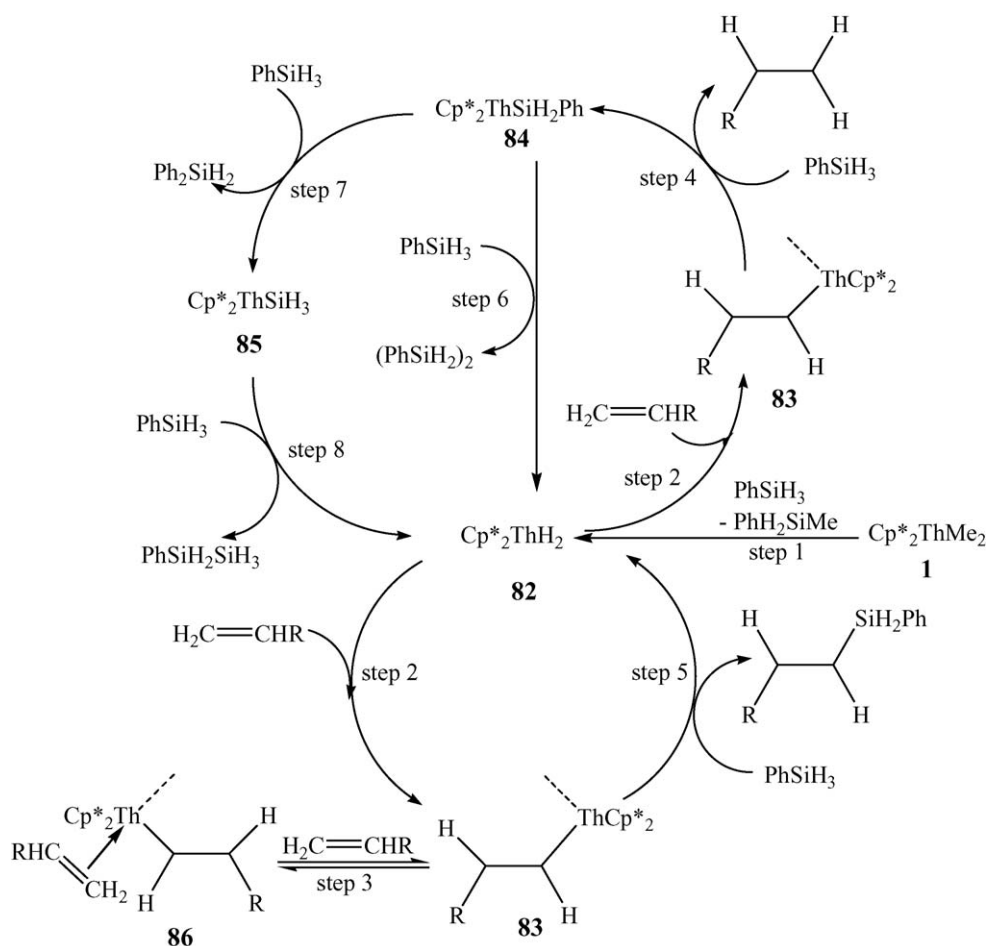
Scheme 26. Proposed mechanism for the hydrosilylation of alkenes with PhSiH$_3$ promoted by Cp$_2^*$ThMe$_2$ or Me$_2$Si(C$_5$Me$_4$)$_2$Th^{n}Bu$_2$. Only one of the equatorial ligations at the metal center is shown for clarity.
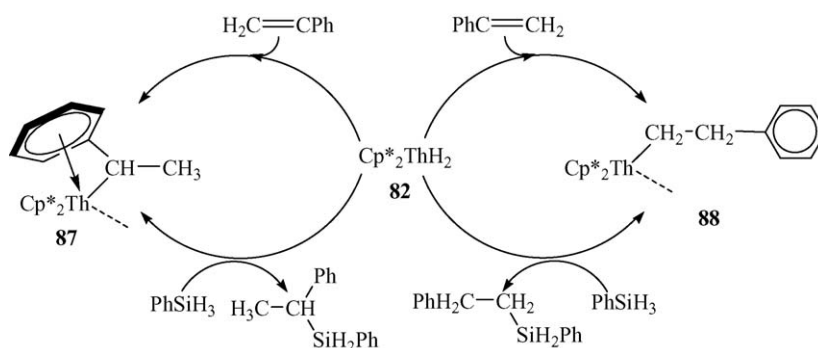
Scheme 27. Proposed mechanism for the hydrosilylation of styrene with PhSiH$_3$ promoted by Cp$_2^*$ThH$_2$.

tinides represent again complementary catalysts to organolanthanides and other transition-metal complexes for the regioselective hydrosilylation of α-olefins.

7. Dehydrocoupling reactions of amines with silanes catalyzed by [(Et$_2$N)$_3$U][BPh$_4$] (6)

Catalytic processes involving the cationic uranium amide complex, [(Et$_2$N)$_3$U][BPh$_4$], have been found to be particularly efficient in the hydrosilylation of terminal alkynes with PhSiH$_3$ (Section 6.3) and in the controlled dimerization of terminal alkynes (Section 4.3). These processes have been described through the activation of the corresponding amido uranium hydride or the amido uranium–acetylide species that were the active intermediates, respectively. A conceptual question, which rose from those studies, concerned the possibility to activate the amido ancillary ligands in [(Et$_2$N)$_3$U][BPh$_4$] with a silane molecule producing the corresponding aminosilane and an organometallic hydride complex. The ability to transform the hydride, to the starting amido complex, using another amine,

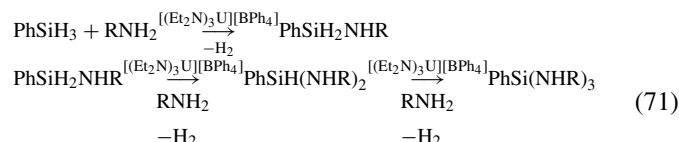with the related elimination of dihydrogen would provide a way to perform the catalytic dehydrogenative coupling of amines and silanes. Dehydrogenative coupling of amines and silanes constitute an elegant and alternative route to silazanes, attractive precursors for important silicon nitride materials, which are classically prepared by the aminolysis or ammonolysis of chlorosilanes with the disadvantageous formation of large amounts of ammonium halide by-products.

At first, stoichiometric reactions of $[(Et_2N)_3U][BPh_4]$ (**6**) with amines were investigated. The amido ligands of **6** were easily activated under mild conditions (i.e. room temperature in benzene). The reaction of **6** with *n*-propylamine yielded an organoactinide intermediate, which was quenched by water after all volatiles were removed, to yield *n*-propylamine with no traces of Et_2NH. Thus, all three amido groups were easily transaminated (Eq. (69)) [145].
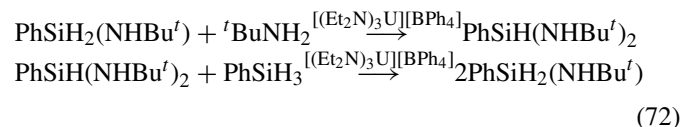

(69)

(70)
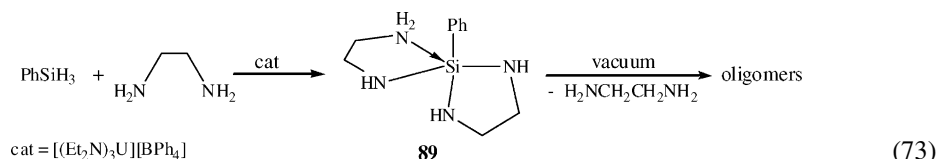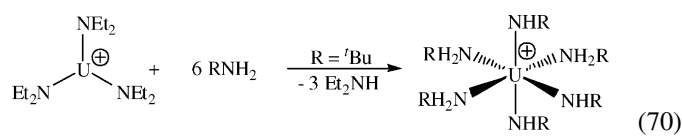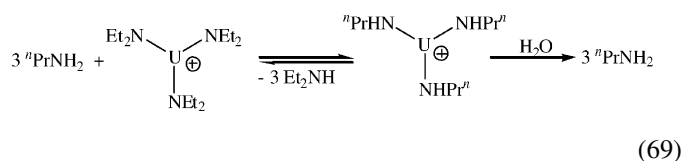
A similar reaction of $[(Et_2N)_3U][BPh_4]$ with *t*butylamine yielded the complex $[(^tBuNH_2)_3(^tBuNH)_3U][BPh_4]$ (Eq. (70)), which was characterized by X-ray crystal structure and NMR spectroscopy [80].

Theoretical thermodynamic calculations have predicted this process as plausible [21]. The dehydrogenative coupling of amines and silanes has been performed both by late transition-metal catalysts [146–148] and early transition-metal complexes [149–151]. These reactions are an alternative substitute route to silazanes, which are precursors for the synthesis of silicon nitride materials. The reaction of $^nPrNH_2$ and $PhSiH_3$ promoted by the cationic complex $[(Et_2N)_3U][BPh_4]$ produced dihydrogen and the aminosilanes $PhSiH(NHPr^n)_2$ and $PhSi(NHPr^n)_3$ (Eq. (71)). Full conversion of the silane into the di- and tri-aminosilanes was achieved by using a large excess of amine. The monoaminosilane, $PhSiH_2(NHPr^n)$, was not detected, indicating that in this compound the Si–hydride bonds were more reactive than those bonds in the starting $PhSiH_3$ [145].

$$PhSiH_3 + RNH_2 \xrightarrow[-H_2]{[(Et_2N)_3U][BPh_4]} PhSiH_2NHR$$

$$PhSiH_2NHR \xrightarrow[\substack{RNH_2 \\ -H_2}]{[(Et_2N)_3U][BPh_4]} PhSiH(NHR)_2 \xrightarrow[\substack{RNH_2 \\ -H_2}]{[(Et_2N)_3U][BPh_4]} PhSi(NHR)_3$$

(71)

$$R = {}^nPr; {}^iPr; {}^tBu$$

The reaction of $^iPrNH2$ and $PhSiH_3$ gave dihydrogen together with $PhSiH_2NHPr^i$ (33%) and $PhSiH(NHPr^i)_2$ (56%) with a total conversion of 89% for $PhSiH_3$. The use of large amine excess promoted the reaction towards the bisaminosilane $PhSiH(NHPr^i)_2$. For the bulky $^tBuNH_2$, reaction with $PhSiH_3$ yielded quantitative amounts of $PhSiH_2NHBu^t$. This monoaminosilane reacts further with the excess of amine to produce an additional equivalent of dihydrogen and the bisaminosilane $PhSiH(NHBu^t)_2$, which transforms back slowly into the monoaminosilane, $PhSiH_2NHBu^t$, after the addition of 1 equivalent of $PhSiH_3$ (Eq. (72)), which indicated that the production of aminosilanes promoted by the cationic complex $[(Et_2N)_3U][BPh_4]$ were in equilibrium.

$$PhSiH_2(NHBu^t) + {}^tBuNH_2 \xrightarrow{[(Et_2N)_3U][BPh_4]} PhSiH(NHBu^t)_2$$

$$PhSiH(NHBu^t)_2 + PhSiH_3 \xrightarrow{[(Et_2N)_3U][BPh_4]} 2PhSiH_2(NHBu^t)$$

(72)

When $PhSiH_3$ reacts with ethylenediamine ($H_2NCH_2CH_2NH_2$) in the presence of the catalyst, dihydrogen and the spiro chelated compound $PhSi(\eta^2\text{-}NHCH_2CH_2NH)(\eta^2\text{-}NHCH_2CH_2NH_2)$ (**89**) are formed quantitatively. By evaporating ethylenediamine under vacuum conditions the spiro product was transformed into a mixture of oligomers (Eq. (73)).

(73)

Secondary amines and silanes were found to be less reactive than the corresponding primary amine and silanes. The reaction of Et_2NH with $PhSiH_3$ produced a mixture of $PhSiH(NEt_2)_2$ and $PhSiH_2NEt_2$ in addition to H_2. No reaction was observed between $(^iPr)_2NH$ and $PhSiH_3$, most likely due to the steric hindrance of the amine. These results show that the reactivity of amines towards the formation of aminosilanes with $PhSiH_3$ catalyzed by $[(Et_2N)_3U][BPh_4]$ follows the order primary > secondary > tertiary. As to the effect of the silane, $^nPrNH_2$ reacted with the secondary silane $PhSiMeH_2$ producing H_2, $PhSiMe(NHPr^n)_2$ and $PhSiHMe(NHPr^n)$.

Under stoichiometric or excess amounts of $PhSiH_3$, the cationic complex $[(Et_2N)_3U][BPh_4]$ reacted to yield (in both cases) one equivalent of $[(Et_2N)_2UH][BPh_4]$ (**78**) and the corresponding aminosilane $PhSiH_2NEt_2$. When an excess of silane was used, trace formation of the homodehydrogenative coupling product of the silane was observed. These results suggest that the monohydride complex is the active intermediate, since no other amido moieties were found to react with the phenylsilane. Therefore, the synthesis of a uranium hydride was accomplished by treatment of the corresponding amide with a silane. Similar reactions were reported for a zirconium complex, with similar exchange reactions with boranes, alanes and stannanes [152–154].

PhSiH$_3$
or
PhSiH$_{4-n}$(NHR)$_{n-1}$

PhSiH$_2$(NHR)
or
PhSiH$_{3-n}$(NHR)$_n$

(step 2)

3 RNH$_2$
(step 1)

[(Et$_2$N)$_3$U]$^+$ $\xrightarrow{- 3 \text{ Et}_2\text{NH}}$ [(RHN)$_3$U]$^+$ [(RHN)$_2$UH]$^+$

90   91

(step 3)

H$_2$ RNH$_2$
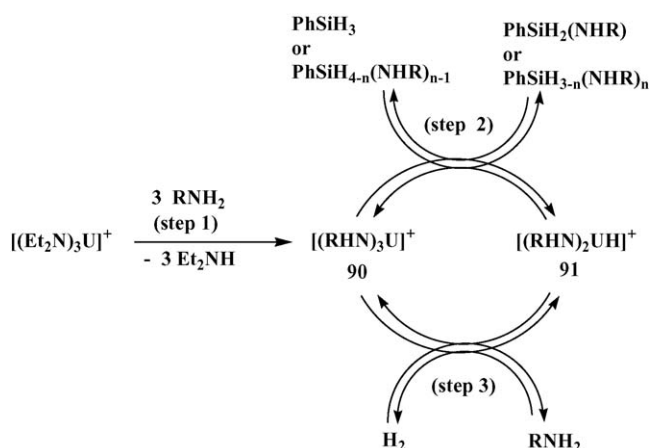
Scheme 28. Probable mechanism for the coupling of silanes with amines promoted by [(Et$_2$N)$_3$U][BPh$_4$] [145].

A probable mechanism for the dehydrocoupling of amines with silanes promoted by the cationic complex [(Et$_2$N)$_3$U][BPh$_4$] is presented in Scheme 28. The first step is the transamination reaction of [(Et$_2$N)$_3$U][BPh$_4$] with RNH$_2$ to yield [(NHR)$_3$U][BPh$_4$] (90) (step 1). Reaction of PhSiH$_3$ with complex 90 affords the hydride complex [(NHR)$_2$UH][BPh$_4$] (91) and the corresponding monoaminosilane PhSiH$_2$NHR (step 2). In the last step of the catalytic cycle 91 reacts with the amine to regenerate 90 by elimination of dihydrogen (step 3). By replacing PhSiH$_3$ with PhSiH$_{4-n}$(NHR)$_{n-1}$ in step 2, the different polyaminosilanes PhSiH$_{3-n}$(NHR)$_n$ were obtained.

Since in the presence of excess of amine the hydrogens of the silane moiety were found to be the reactive ones, the study on the reactivity of the aminosilane products towards a silane followed. The reaction of PhSi(NHPr^n)$_3$ with an excess of PhSiH$_3$, without amine, was considered in order to determine a possi-

ble equilibrium and/or a tailoring approach to specific products by activation of the amine hydrogen atoms of the aminosilane. PhSi(NHPr^n)$_3$ reacted with an excess of PhSiH$_3$ in the presence of [(Et$_2$N)$_3$U][BPh$_4$] to give a mixture of four compounds (92–95) (Scheme 29).

The explanation for the formation of only four compounds is based on the theoretical formation of all possible compounds as outlined in Scheme 30.

These results demonstrate that cationic organoactinide complex offer an alternative route for the dehydrogenative coupling of amines with silanes. The proposed mechanism for this transformation consists of activation of an amido ligand by a silane, producing the aminosilane and an organometallic hydride, which is then recycled by addition of amine.

8. Catalytic coupling of terminal alkynes and isonitriles promoted by organoactinide complexes

Isonitriles (RN≡C:) are two electron donor ligands which are known to undergo a 1,1-insertion into metal–acetylide bond of early or late transition metals, under stoichiometric conditions [155–157]. A basic conceptual question regards the use of organoactinides as catalysts for the coupling of terminal alkynes with isonitriles to form substituted 1-aza-1,3-enynes, which contain conjugated acetylenic and azomethine fragments R^{1}C≡C–CH=NR^2 (α,β-acetylenic aldimines). These species have attracted great attention as important synthons in organic synthesis since they possess three active reaction centers for constructing polyfunctional compounds [158].

The organoactinide complexes Cp$_2^*$AnMe$_2$ (An = Th (1), An = U (2)) and [(Et$_2$N)$_3$U][BPh$_4$] (6) were found to be excellent precursors for the coupling reaction of terminal alkynes and t-butylisonitrile (^{t}BuNC) [24]. The coupling reaction proceeded
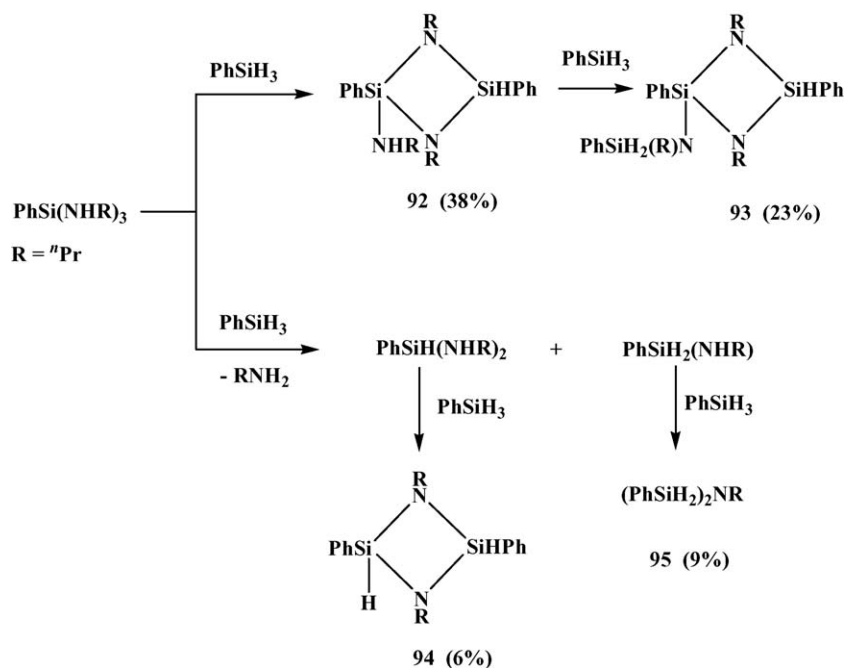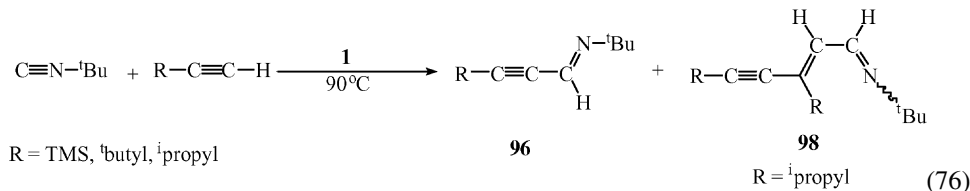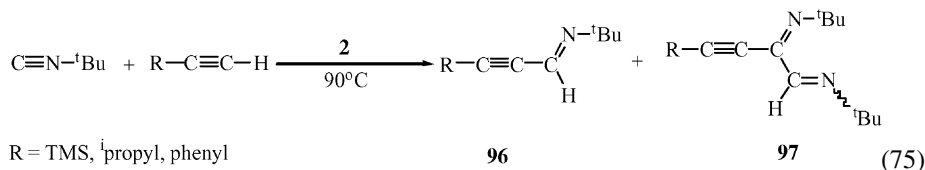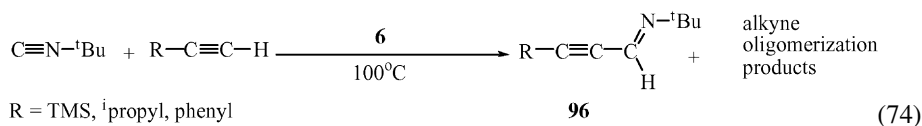
Scheme 29. Reactions of PhSi(NHPr^n)$_3$ with an excess of PhSiH$_3$ in the presence of [(Et$_2$N)$_3$U][BPh$_4$].
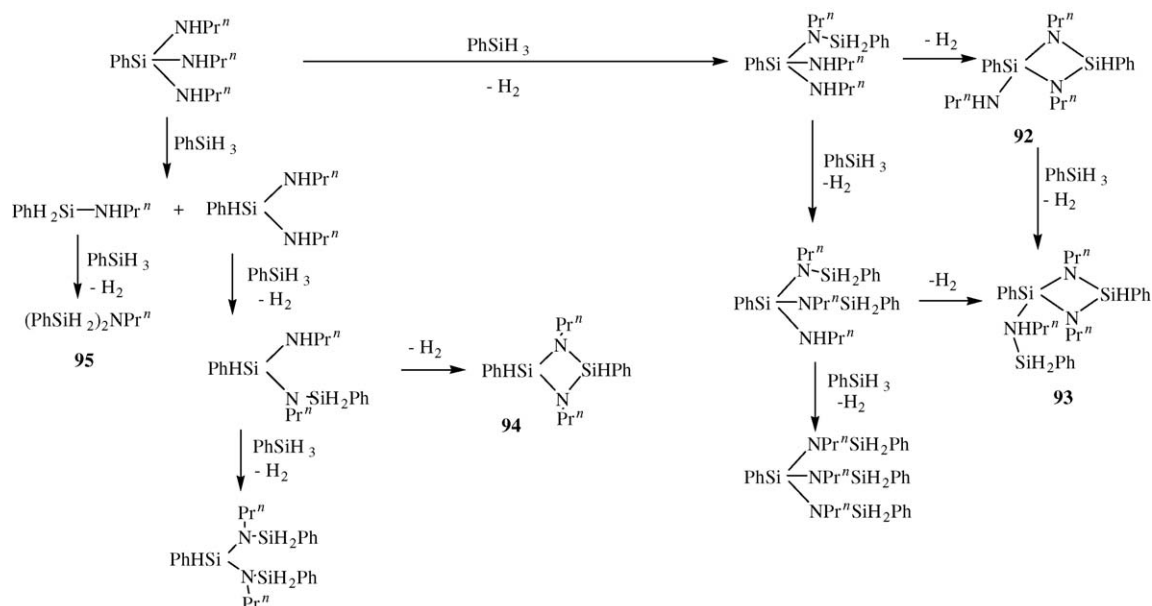
Scheme 30. Proposed routes for the formation of compounds **92–95**.

via 1,1-insertion of the isonitrile terminal carbon atom into a metal–acetylide or a metal–imine bond (Eqs. (74)–(76)). The complete conversion of the isonitrile and alkyne to 1-aza-1,3-enynes was achieved in toluene or benzene at 90–100 °C, while no reaction was observed in the absence of catalyst.

$$\text{(74)}$$

$$\text{(75)}$$

$$\text{(76)}$$

The product distribution for the coupling reaction (Table 2) was found to depend strongly on both the catalyst and the alkyne:isonitrile ratio. The cationic catalyst **6** selectively produces the (E)-acetylenic imine **96** as the major product (Eq. (74)), from the mono-insertion reaction of ^{t}BuNC into the terminal alkyne, beside some minor by-products (oligomerization of the terminal alkyne and tautomerization [159] of the isonitrile to the nitrile).

Interestingly, reaction with $Cp_2^*UMe_2$ affords product **97** in addition to compound **96** from the double insertion of two isonitrile molecules into one molecule of the terminal alkyne (Eq. (75)). The percentage of **97** was successfully raised by increasing the amount of isonitrile (Table 2, entry 7). The reaction between

bulky terminal alkynes ($R = SiMe_3$, ^{t}Bu) and ^{t}BuNC catalyzed by $Cp_2^*ThMe_2$ (Table 2, entries 9–11) produces **96** (Eq. (76)) as the major product. When the reaction is performed with smaller (unhindered) terminal alkynes, the formation of the additional

product **98** is observed. Product **98** results from the coupling of two acetylene and one isonitrile molecules (Table 2, entry 13). The variation of the molar ratio of **96** and **98** over time suggests that compound **98** is formed only after the complete formation of **96**, by coupling of the latter with the remaining alkyne. The similar behavior of the three catalytic systems strongly suggests a common mechanism (presented in Scheme 31) to obtain compound **96**, with various branches forming products **97** and **98**.

The organoactinide complexes **2** and **3** react with the terminal alkynes to yield the bis(acetylide) complex **18** (step 1). This complex undergoes a 1,1-insertion of the isonitrile into the metal–carbon bond to form the acetylenic imido complex

Table 2
Products distribution for the coupling reaction of ^{t}BuNC and terminal alkynes catalyzed by organoactinide complexes

Entry	Cat.	R^a	Cat.:^{t}BuNC: RC≡CH	Time (h)	96	97 (%)	98
1	6	Me$_3$Si	1:40:50	48	80	–	–
2	6	Ph	1:50:50	48	81	–	–
3	6	^{i}Pr	1:40:55	48	81	–	–
4	2	Me$_3$Si	1:50:30	6	56	13	–
				24	81	19	–
5	2	Ph	1:40:60	48	90	10	–
6	2	^{i}Pr	1:40:70	48	75	25	–
7	2	^{i}Pr	1:50:20	48	50	50	–
8	1	Me$_3$Si	1:100:100	23	90	–	–
9	1	Me$_3$Si	1:100:180	18	85	–	–
10	1	^{t}Bu	1:100:100	18	80	–	–
11	1	^{t}Bu	1:100:200	18	90	–	–
12	1	^{i}Pr	1:100:100	18	90	–	–
13	1	^{i}Pr	1:100:200	2	19	–	0
				17	95	–	5
				64	60	–	40
				210	47	–	53

^{a} R in RC≡CH.

99 (step 2). Protonolysis by another terminal alkyne yields the mono-insertion product **96** and regenerates complex **18** as the active species in the catalytic cycle (step 3). For complex **2**, this protonolysis step is not as rapid as for complex **1**, permitting complex **99** to undergo an additional 1,1-insertion of a second isonitrile molecule to yield the corresponding intermediate **100** (step 4). The double insertion product **97** is then obtained by the protonolysis with a terminal alkyne (step 5) regenerating the active bis(acetylide) complex **18**.

With an excess of unhindered terminal alkynes, the bis(acetylide) complex **18** (An = Th) can react with product **96** to yield complex **101**, by insertion of the triple bond of **96** into the Th–acetylide bond (step 6). Protonolysis of **101** by another terminal alkyne yields product **98** and the active species **18** (step 7). This is the first example of an insertion of an internal triple bond into an actinide–carbon bond. For organoactinides it was shown (Section 3.2) that the insertion of terminal alkynes into a metal acetylide bond produces dimers or higher oligomers, and when the reaction is performed in the presence of terminal and internal alkynes, only the products formed by the activation of the terminal alkyne are produced. Thus, the insertion of
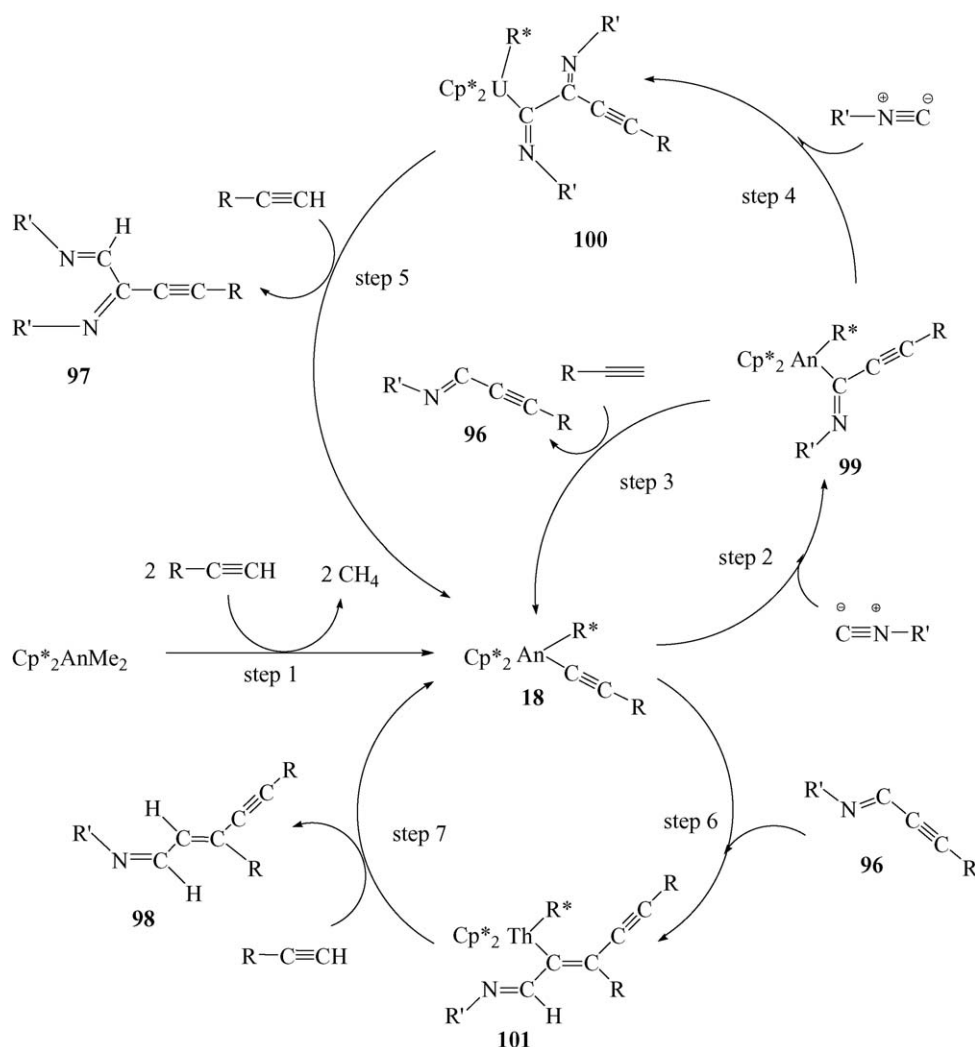

Scheme 31. Plausible mechanism for the catalytic coupling of ^{t}BuNC and terminal alkynes mediated by Cp$^*_2$AnMe$_2$. For clarity one of the equatorial ligations is presented as R* [24].

an internal triple bond must be higher in energy in comparison with terminal alkynes. In contrast, the formation of **98** indicates that even in the presence of a terminal alkyne, the insertion of the internal triple bond of **96** was preferred, presumably due to the electronic effects of the imine fragment (^{t}Bu−N=C−), which induces polarization of the internal triple bond.

Considering that complex **6** reacts with terminal alkynes to form the acetylide complex (**77**), catalysis mechanism similar to that of complexes **1** and **2** should be expected. By following steps 2–3 of the proposed mechanism, complex **77** catalyzes the coupling reaction. The protonolysis step 3 can be performed via a terminal alkyne to yield **96** and **77** or by the free amine (present in stoichiometric amounts in the reaction mixture) to produce **96** and regenerate **6**.

## 9. Polymerization of α-olefins by cationic organoactinide complexes

Since the synthesis of the cationic actinide complexes [Cp$_2^*$ThMe][BPh$_4$] and [Cp$_2^*$ThMe][B(C$_6$F$_5$)$_4$] and their study for the polymerization of α-olefins [160] other highly coordinatively unsaturated organothorium complexes have been prepared (Eq. (77)) [161].

(77)
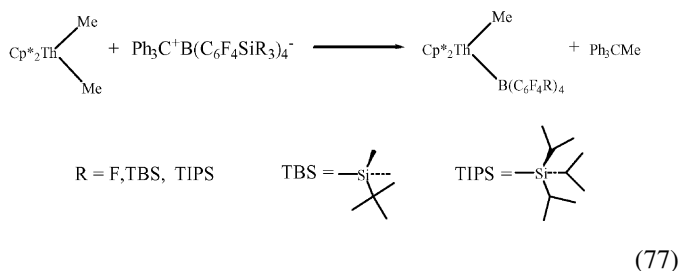
The reactivity of the newly synthesized organothorium complexes for the polymerization of ethylene follows the order [Cp$_2^*$ThMe][B(C$_6$F$_5$)$_4$] > [Cp$_2^*$ThMe][B(C$_6$F$_4$TIPS)] > [Cp$_2^*$ThMe][B(C$_6$F$_4$TBS)$_4$], though their activity is an order of magnitude lower that that observed for analogue zirconium complexes.

10. Catalytic reduction of azides and hydrazines by high-valent organouranium complexes

U(IV) metallocene compounds frequently show reactivities comparable to group IV transition-metal and lanthanide
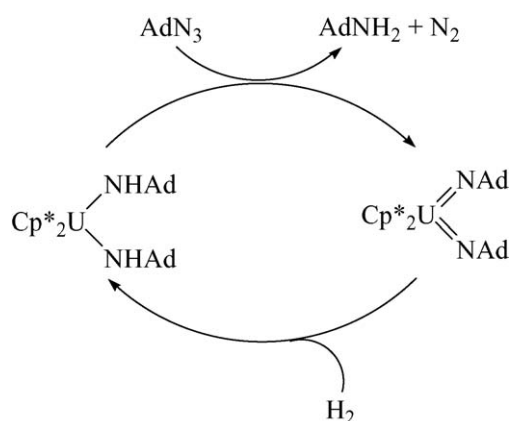

Scheme 32. Catalytic reduction of azides by organouranium complexes [162].

13, R = Ad = 1-adamantyl, **15**) to an atmosphere of hydrogen, resulted in their reduction to the corresponding bis(amide) complexes (Cp*)$_2$U(NHR)$_2$ (**14**) (R = Ph, Ad) (Eq. (78)). The rate of hydrogenation of complex **15** was found to be much faster than that of complex **13**. In addition, when AdN$_3$ was added to a solution of the bis(amide) **14**, the bis(imido) **15** and AdNH$_2$ were formed. Therefore, when complex **14** (R = Ad) was reacted with AdN$_3$ under a dihydrogen atmosphere, catalytic hydrogenation of AdN$_3$ to AdNH$_2$ was observed (Scheme 32) [162].

(78)
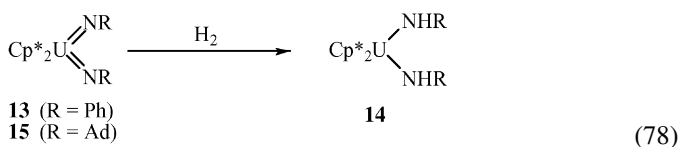
N,N'-diphenylhydrazine was also used as an oxidant for the conversion of Cp$_2^*$UMe$_2$ (**2**) to **13**. The reaction occurs by the protonation of the methyl groups, liberating methane. When Cp$_2^*$U(=NPh)$_2$ was treated with an excess of *N,N'*-diphenylhydrazine under starving hydrogen conditions, the reaction came to completion, producing aniline and azobenzene in a 2:1 ratio (Eq. (79)). This disproportionation indicated that the *N,N'*-diphenylhydrazine function as both oxidant and reductant. The formation of aniline during this reaction suggested that the U(IV) bis(amide) **14** should be present to reduce the hydrazine, although the only observed uranium species in solution throughout the reaction, was Cp$_2^*$U(=NPh)$_2$ indicating that the oxidation from U(IV) to U(VI) is faster than the subsequent reduction [160].

(79)
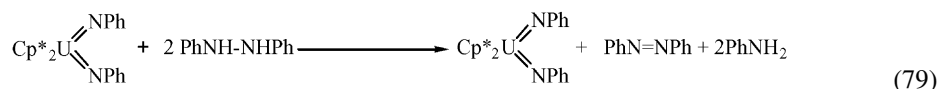
metallocenes. The similar steps in catalytic cycles, as shown above, comprise olefin insertion, σ-bond metathesis and protonolysis. In contrast to the lanthanides and group IV metals, however, uranium can also access the +6 oxidation state, giving rise to the possibility of two-electron (+4/+6) redox processes. Exposure of the complexes Cp$_2^*$U(=NR)$_2$ (R = Ph,

From a thermodynamic point of view, the reaction should be favored by both enthalpy and entropy. The calculated ΔH_f for producing two molecules of aniline and one molecule of azobenzene from two *N,N'*-diphenylhydrazine molecules is −14.6 kcal/mol. Entropy considerations also qualitatively favor product formation; two molecules of starting material are converted to three molecules of product.
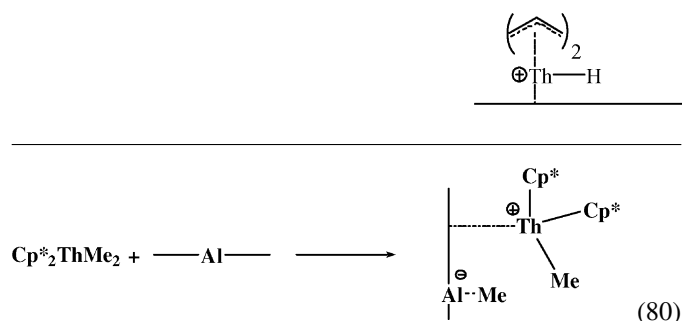
The reaction of $Cp_2^*U(=NPh)_2$ with N,N'-diphenylhydrazine was postulated to proceed via protonation of U(IV) bis(amide) by N,N'-diphenylhydrazine. Therefore, it was proposed that for the reaction of $Cp_2^*U(=NAd)_2$ (**15**) with N,N'-diphenylhydrazine, the initial product would include 1-adamantylamine and azobenzene, with the concomitant formation of $Cp_2^*U(=NPh)_2$. However, when the reaction was performed, $Cp_2^*U(=NAd)_2$, aniline and azobenzene were the only products observed, indicating that the imido ligands might operate as sites for mediating H-atom transfer. No reaction was observed in the stoichiometric reaction of **13** with 1-adamantanamine. This result rules out the possibility of U−N bond break in which compound **13** is formed and undergoes subsequent rapid reaction with 1-adamantanamine regenerating **15** [160].

The catalytic two-electron oxidation/reduction processes presented here are a novel type of reactivity for organoactinide complexes. The involvement of U(VI) species strongly argued for the requirement for f-orbital participation.

11. Heterogeneous catalysis by supported organoactinide complexes

11.1. Hydrogenation of arenes by supported organoactinide complexes, kinetic and mechanistic studies

Supporting homogeneous complexes on metal oxides, was shown to have substantial effect on their activity, when compared with solution and heterogeneous activity [163]. Large enhancements in the catalytic hydrogenation activities were observed for both early transition metals [164] and actinide hydrocarbyl [165–168] adsorbed upon metal oxide (usually alumina). The increase in the coordinative unsaturation of metollocene organometallic–f–complexes has generated a remarkable increase in the reactivity of the adsorbed complexes toward polymerization and hydrogenation of simple olefins rivaling the activity of supported rhodium [169]. However, these adsorbed complexes were not efficient for the hydrogenation of arenes. Chemisorption of organoactinides involves the transfer of an alkyl group to the acidic Al^{3+} sites and the formation of "cationic" organothorium center as shown schematically in Eq. (80) [166].

the efficient reduction of arenes, a series of complexes of the type $R^1R_3^2Th$ ($R^1 = Cp^*$; $R^2 = CH_2C_6H_5$; $R^1 = R^2 = 1,3,5$-$(Me)_3C_6H_2$; $R^1 = R^2 = \eta^3$–C_3H_5) chemisorbed on highly dehydroxilated γ-alumina (DA), were prepared [170]. Presumably, the adsorption of the latter organometallic–f–complex (**102**) is performed by transferring an allyl group from the thorium coordination to the strong Lewis acid site in the surface (Eq. (81)).

$$(81)$$
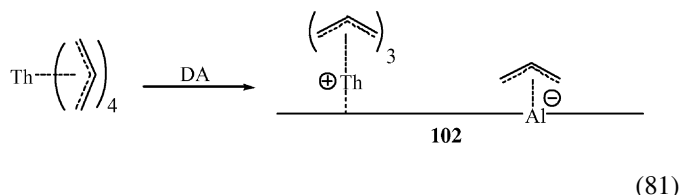
The reactivity of $Th(\eta^3–C_3H_5)_4/DA$ (**102**) towards the hydrogenation of benzene (Table 3) shows that for the complex with the higher coordinative unsaturation, the higher the reactivity of the formed adsorbate.

11.2. Estimation of the $Th(\eta^3–C_3H_5)_4/DA$ active sites percentage

The percentage of supported organoactinide sites active in the olefin hydrogenation was assessed by dosing the catalyst with measured quantities of CO in a H_2 stream, measuring the amount of CO adsorbed by the catalyst and determining the effect on subsequent catalytic activity. Similar results were found on H_2O/D_2O, and CH_3Cl poisoning experiments. The CO poisoning chemistry presumably involved migratory insertion to produce surface η^2-formyl (Eq. (82)), which may then undergo various possible following-up reactions.

$$(82)$$
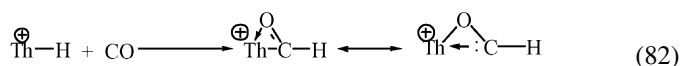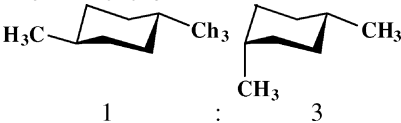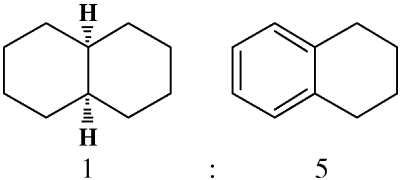
Additional corroboration, for the estimation of the number of active sites, was devised to measure the metal–hydride content by adding measured amounts of D_2O and studying the catalytic activity after each addition. This stepwise titration of active sites indicated that $8 \pm 1\%$ of the total $Th(\eta^3–C_3H_5)_4/DA$ sites present on the support were responsible for the majority of the catalysis (Eq. (83)).

$$(83)$$

$$(80)$$

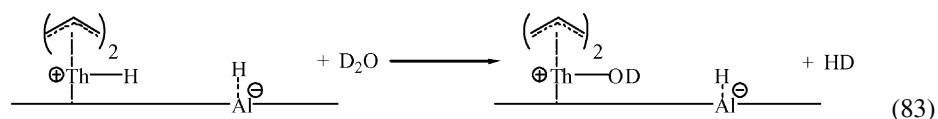To address the question of how coordinatively unsaturated an organometallic–f–element complex needs to be for

In another complementary experiment for measuring the number of hydrides the adsorbed $Th(\eta^3–C_3H_5)_4/DA$ was reacted with hydrogen and the amount of organic gas recovered from the reaction was measured. The amount of propane/thorium was found to be only 10% from the total amount expected (Eq. (84)). No propylene was released from the reaction, indicating that the hydrogenation of propylene was extremely fast. This was also demonstrated by the turnover frequency for the

Table 3
Product and kinetic data for the hydrogenation of various arenes[a] catalyzed by $Th(\eta^3-C_3H_5)_4/DA$ (**102**)

Entry	Substrate	Product	Turnover frequency (s^{-1})
1	C_6H_6	C_6H_{12}	6.80
2	C_6D_6	$C_6H_6D_6$	6.78
3	MeC_6H_5	MeC_6H_{11}	4.05[b]
4	$CD_3C_6D_5$	$CD_{3-X}H_XC_6H_6D_5$	3.98[b]
5	$1,4-(CH_3)_2C_6H_4$		0.65[b]
6	Naphthalene		8.3×10^{-3}

[a] [Arene] = 10 mmol; P_{H_2} = 190 psi; temperature = 90 °C.
[b] Values at 100% yield.

hydrogenation of propylene which was measured separately (N_t (25 °C) = 25 s^{-1}).
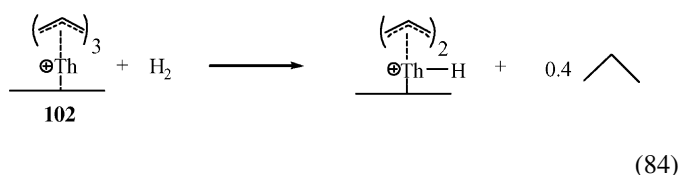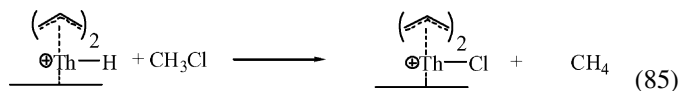

(84)

The number of thorium hydrides formed, was confirmed to be the same by reacting these hydrides with methyl chloride and measuring the amount of methane/Th that was evolved from the reaction (Eq. (85)).

(85)

The importance of these experimental poisoning results is that they indicate that only a very small fraction of the organothorium adsorbates sites on the support was responsible for the bulk of the catalytic turnover. It is likely that one or more different structures of the suggested "cationic" organothorium moieties constitute the catalytic sites on alumina, but the exact structural characteristics defining these structures remain to be revealed.

The kinetics of arene hydrogenation can be accommodated by a three consecutive two-step sequence: (i) arene insertion (olefin inserti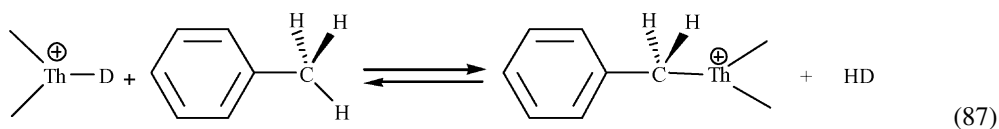on for the subsequent step) into a Th–H bond and (ii) hydrogenolysis of the resulting Th–alkyl bond. From the kinetic data measured for benzene the rate law (Eq. (86))

was deduced.

$$\nu = k[\text{benzene}]^0[P_{H_2}]^1[\mathbf{102}]^1 \qquad (86)$$

Kinetic isotope measurements for the hydrogenation of benzene by dihydrogen and dideuterium indicated that $N_t(H_2)/N_t(D_2) = 3.5 \pm 0.3$ at 90 °C and 180 psi of H_2. In the hydrogenation reaction of benzene with D_2, the product $C_6H_6D_6$ was obtained as a mixture of two geometric isomers: *all cis*:*cis, cis, trans, cis, trans* in a ratio of 1:3, respectively. The Arrhenius activation energies for the catalytic hydrogenation of benzene was measured to be 16.7 ± 0.3 kcal mol^{-1} and the corresponding thermodynamic activation parameters were $\Delta H^{\ddagger} = 16.0 \pm 0.3$ kcal/mol and $\Delta S^{\ddagger} = 32.3 \pm 0.6$ e.u. [171].

The mechanism proposed for the hydrogenation of arenes is described in Scheme 33. The process takes into account the lack of face selectivity by which the ratio of 1:3 between the geometrical isomers was formed. As a function of olefin, the relative rates of $Th(\eta_3-C_3H_5)_4/DA$-catalyzed hydrogenation of arenes was found to be in the order benzene > toluene > *p*-xylene > naphthalene.

In contrast to the results obtained in the hydrogenation of benzene, H/D scrambling was observed after fully hydrogenation of toluene-d_8 with H_2 or toluene with D_2. In these processes high C–H/C–D activations occurred during the hydrogenation. Incorporation of deuterium atoms in the starting toluene and subsequently in the cyclohexane product were observed at partial conversions. A plausible pathway for the C–H/C–D exchange proceeds through benzylic activation (Eq. (87)).

(87)

Competing reactions marked the large kinetic discrimination for the different arenes. The hydrogenation reaction of equimolar quantities of *p*-xylene and benzene yielded cyclohexane with
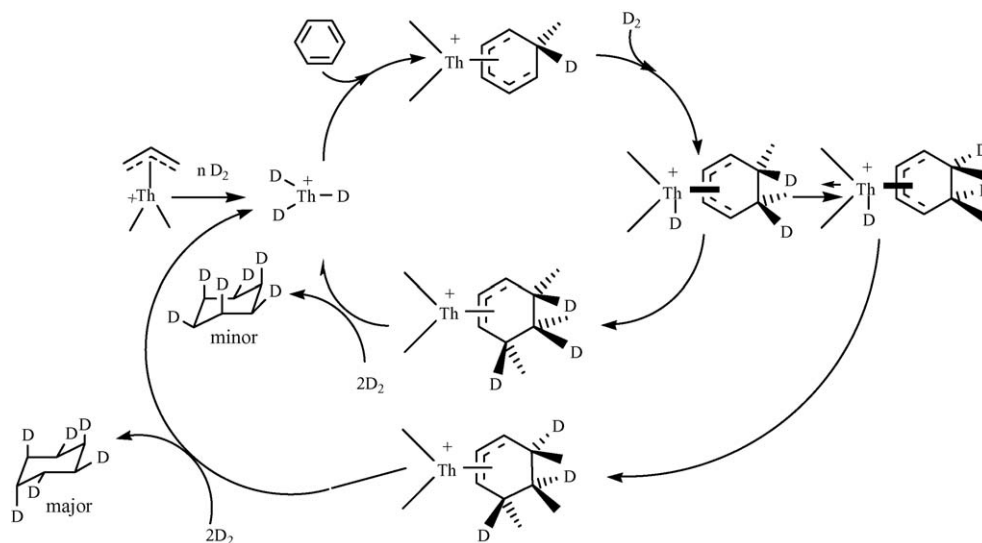
Scheme 33. Proposed mechanism for arene hydrogenation catalyzed by cationic supported organoactinide complexes [170].

Table 4
Product structure/deuterium distribution data and kinetics for $Th(\eta^3-C_3H_5)_4$/DA catalyzed C—H/C—D fuctionalization

Entry	Substrate	Deuterium distribution in product	Turnover frequency (h^{-1})
1	$CH_3(CH_2)_3CH_3$	$CH_2DCHDCHDCHDCH_2D$ 58 32 10	778
2			879
3			825
4	C_6H_{12}	$C_6H_{12-x}D_x$	1285
5			1113
6			884
7			834

Scheme 34. Proposed mechanism for the C—H activation and isomerization of alkanes catalyzed by Th(η^3-allyl)$_4$/DA [170].

almost complete selectivity (97%) and a mixture of 3:1 *cis*:*trans* 1,4-dimethylcyclohexane (3%).

11.3. Selective and facile alkane activation by supported tetraallylthorium

C—H activation processes involving alkanes are considered high-energy demanding transformations. Although significant advances have been made in the functionalization of C—H bonds by early transition-metal and f-metal complexes [166,171–174], the catalytic intermolecular activation of inert alkane molecules with favorable rates and selectivities is still a major challenge. As noted above, studies on the benzene reduction with D$_2$ revealed C—H/C—D exchange in the cyclohexane product only after benzene conversion was complete. This observation prompted detailed studies on the activation of hydrocarbons. Table 4 summarizes the results of the slurry reaction of C—H/C—D exchange for a variety of alkanes catalyzed by Th(η_3–C$_3$H$_5$)$_4$/DA (**102**) under D$_2$ atmosphere [175].

Th(η^3–C$_3$H$_5$)$_4$/DA promoted a rapid C—H/C—D exchange, with turnover frequencies comparable to or exceeding those of conventional group 9 heterogeneous alkane activation catalysts [176]. C—H functionalization occurred with substantial selectivity and in an order which does not parallel the C—H bond dissociation energies: primary > secondary > tertiary, and sterically less hindered > sterically more hindered. NMR and GC–MS measurements as a function of conversion indicated single C—H exchanges, with no evidence for multiple exchange process (e.g., non-statistical amounts of RD$_2$ species). Unexpectedly, in the C—H/C—D exchange reaction of *cis*-dimethylcyclohexanes the isomerization towards a *cis–trans* mixture was observed. Based on the same two reasonable assumptions as for the arene hydro-

genation, a plausible mechanistic scenario for the activation and isomerization of alkanes was proposed (Scheme 34). The mechanistic sequence invokes presumably endothermic Th—C bond formation and HD elimination via a four-center, heterolytic σ-bond metathesis (step 1), followed by deuterolysis to yield the *cis* deuterated product (step 2). Cycloalkane skeletal isomerization would then occur via a β–H elimination (step 3) and re-addition of the Th$^+$—H to the opposite face of the double bond (step 4). This process would involve the rapid dissociation and re-addition of the alkene, although other mechanisms have been proposed as conceivable. Insertion (step 5) and deuterolysis (step 6) produced the isomerized cycloalkane. The isotopic labeling experiments revealed negligible differences in the D label distribution of the isomerized and un-isomerized hydrocarbons and little D incorporation at the dimethylcyclohexane tertiary carbon centers. These results indicated that the ancillary ligands L and L′ in Scheme 34 are either non-D in identity (e.g., η^3-allyl or oxide) or that such Th—D functionalities were chemically stereochemically inequivalent to that formed in a β–H abstraction, since they do not compete for olefin addition.

In summary, these results demonstrate that supported organo-f-complexes are extremely active catalysts for a number of high-energy organic chemistry transformations.

12. Conclusions and future outlook

As presented through this review, the properties of the actinides and specially the catalytic chemistry of the organometallic actinides complexes are new, challenging and sophisticated. The ability to tailor a catalytic reaction with these complexes by a rational design of its electronic and steric features is an outcome of the basic reactivities of these complexes

that may stimulate similar reactivities, but different stereoselectivities, for other transition-metal complexes. The use of polar substrates in catalytic reaction is still a basic challenge that, once successful, will offer many potential returns. The use of organoactinide complexes in industrial processes is still far in the future and their incorporation will depend on public safety and economic advantages (other radioactive compounds are, however, involved in medical and industrial processes).

References

[1] M. Ephritikhine, Chem. Rev. 97 (1997) 2193.
[2] J.C. Berthet, M. Ephritikhine, Coord. Chem. Rev. 178–180 (1998) 83.
[3] F.T. Edelmann, V. Lorenz, Coord. Chem. Rev. 209 (2000) 99.
[4] F.T. Edelmann, Y. Gun'ko, Coord. Chem. Rev. 165 (1997) 163.
[5] P.C. Blake, M.A. Edelman, P.B. Hitchcock, J. Hu, M.F. Lappert, S. Tian, G. Müller, J.L. Atwood, H. Zhang, J. Organomet. Chem. 551 (1998) 261.
[6] P.B. Hitchcock, J. Hu, M.F. Lappert, S. Tian, J. Organomet. Chem. 536–537 (1997) 473.
[7] M.A. Edelman, P.B. Hitchcock, J. Hu, M.F. Lappert, New J. Chem. 19 (1995) 481.
[8] T.J. Marks, in: E.W. Abel, F.G.A. Stone, G. Wilkinson (Eds.), Comprehensive Organometallic Chemistry I, Pergamon Press, Oxford, 1982 (Chapter 21).
[9] F.T. Edelmann, in: E.W. Abel, F.G.A. Stone, G. Wilkinson (Eds.), Comprehensive Organometallic Chemistry II, Elsevier Science, Oxford, 1995, p. 12.
[10] L. Xing-Fu, X. Ying-Ting, F. Xi-Zhang, S. Peng-Nian, Inorg. Chim. Acta 116 (1986) 75.
[11] L. Xing-Fu, F. Xi-Zhang, X. Ying-Ting, W. Hai-Tung, S. Jie, L. Li, S. Peng-Nian, Inorg. Chim. Acta 116 (1986) 85.
[12] L. Xing-Fu, G. Ao-Ling, Inorg. Chim. Acta 134 (1987) 143.
[13] J. Marçalo, A. Pires de Matos, Polyhedron 8 (1989) 2431.
[14] J.P. Leal, N. Marquez, J. Takats, J. Organomet. Chem. 632 (2001) 209.
[15] J.P. Leal, J.A. Martinho Simões, J. Chem. Soc. Dalton Trans. (1994) 2687.
[16] J.P. Leal, N. Marquez, A. Pires de Matos, M.J. Caldhorda, J.A. Galvão, J.A. Martinho Simões, Organometallics 11 (1992) 1632.
[17] T.J. Marks, M.R. Gagne, S.P. Nolan, L.E. Schock, A.M. Seyam, D. Stern, Pure Appl. Chem. 61 (1989) 1665.
[18] X. Jemine, J. Goffart, M. Ephritikhine, J. Fuger, J. Organomet. Chem. 448 (1993) 95.
[19] X. Jemine, J. Goffart, J.C. Berthet, M. Ephritikhine, J. Fuger, J. Chem. Soc. Dalton Trans. (1992) 2439.
[20] W.A. King, T.J. Marks, D.M. Anderson, D.J. Duncalf, F.G.N. Cloke, J. Am. Chem. Soc. 114 (1992) 9221.
[21] W.A. King, T.J. Marks, Inorg. Chim. Acta. 229 (1995) 343.
[22] T.J. Marks, V.W. Day, in: T.J. Marks, I.L. Fragalà (Eds.), Fundamental and Technological Aspects of Organo-f-Element Chemistry, Reidel, Dodrecht, 1985 (Chapter 4).
[23] P.J. Fagan, J.H. Manriquez, S.H. Vollmer, C.S. Day, V.W. Day, T.J. Marks, J. Am. Chem. Soc. 103 (1981) 2206.
[24] E. Barnea, T. Andrea, M. Kapon, J.C. Berthet, M. Ephritikhine, M.S. Eisen, J. Am. Chem. Soc. 126 (2004) 10860.
[25] F.T. Edelmann, in: E.W. Abel, F.G.A. Stone, G. Wilkinson (Eds.), Comprehensive Organometallic Chemistry II, Elsevier Science, Oxford, 1995 (Chapter 2).
[26] G.A. Molander, Chemtracs: Org. Chem. 11 (1998) 237.
[27] R. Anwander, in: B. Cornils, W.A. Herrmann (Eds.), Applied Homogeneous Catalysis with Organometallic Compounds, vol. 2, VCH Publishers, New York, 1996.
[28] R. Anwander, W.A. Herrman, Top. Curr. Chem. 179 (1996) 1.
[29] F.T. Edelmann, Top. Curr. Chem. 179 (1996) 247.
[30] B.E. Bursten, R.J. Strittmatter, Angew. Chem. Int. Ed. Engl. 30 (1991) 1069;
B.E. Bursten, R.J. Strittmatter, Angew. Chem. 103 (1991) 1085.
[31] C.A. Fendrick, L.D. Schertz, V.W. Day, T.J. Marks, Organometallics (1988) 1828.
[32] C. Jeske, L.E. Schock, H. Mauermann, P.N. Swepston, H. Schumann, T.J. Marks, J. Am. Chem. Soc. 107 (1985) 8103.
[33] C. Jeske, H. Lauke, H. Mauermann, H. Schumann, T.J. Marks, J. Am. Chem. Soc. 107 (1985) 8111.
[34] C.M. Fendrick, E.A. Mintz, L.D. Schertz, T.J. Marks, V.W. Day, Organometallics 3 (1984) 819.
[35] M.A. Giardello, V.P. Conticello, L. Brard, M.R. Gagnè, T.J. Marks, J. Am. Chem. Soc. 116 (1994) 10241.
[36] M.R. Gagné, T.J. Marks, J. Am. Chem. Soc. 111 (1989) 4108.
[37] A.K. Dash, I. Gourevich, J.Q. Wang, J. Wang, M. Kapon, M.S. Eisen, Organometallics 20 (2001) 5084.
[38] J.W. Bruno, G.M. Smith, T.J. Marks, J. Am. Chem. Soc. 108 (1986) 40.
[39] C.S. Bajgur, W.R. Tikkanen, J.L. Petersen, Inorg. Chem. 24 (1985) 2539.
[40] R.C. Schnabel, B.L. Scott, W.H. Smith, C.J. Burns, J. Organomet. Chem. 591 (1999) 14.
[41] C.W. Eingenbrot, K.N. Raymond, Inorg. Chem. 21 (1982) 2653.
[42] M.R. Duttera, V.W. Day, T.J. Marks, J. Am. Chem. Soc. 106 (1984) 2907.
[43] R.E. Cramer, S. Roth, F. Edelmann, M.A. Bruck, K.C. Cohn, J.W. Gilje, Organometallics 8 (1989) 1192.
[44] R.E. Cramer, S. Roth, J.W. Gilje, Organometallics 8 (1989) 2327.
[45] J.C. Berthet, C. Boisson, M. Lance, J. Vigner, M. Nierlich, M. Ephritikhine, J. Chem. Soc. Dalton Trans. (1995) 3019.
[46] D.S.J. Arney, C.J. Burns, D.C. Smith, J. Am. Chem. Soc. 114 (1992) 10068.
[47] D.S.J. Arney, C.J. Burns, J. Am. Chem. Soc. 115 (1993) 9840.
[48] B.P. Warner, B.L. Scott, C.J. Burns, Angew. Chem. Int. Ed. Engl. 37 (1998) 959;
B.P. Warner, B.L. Scott, C.J. Burns, Angew. Chem. 110 (1998) 1005.
[49] J.P. Mitchell, S. Hajela, S.K. Brookhart, K.I. Hardcastle, L.M. Henling, J.E. Bercaw, J. Am. Chem. Soc. 118 (1996) 1045.
[50] E. Ihara, M. Nodono, H. Yasuda, N. Kanehisa, Y. Kai, Macromol. Chem. Phys. 197 (1996) 1909.
[51] P.F. Fu, T.J. Marks, J. Am. Chem. Soc. 117 (1995) 10747.
[52] C.J. Schaverien, Organometallics 13 (1994) 69.
[53] H.J. Heeres, J.H. Teuben, Organometallics 10 (1991) 1980.
[54] G. Jeske, L.E. Schock, P.N. Swepson, H. Schumann, T.J. Marks, J. Am. Chem. Soc. 107 (1985) 8091.
[55] P.L. Watson, G.W. Parshall, Acc. Chem. Res. 18 (1985) 51.
[56] P.W. Roesky, U. Denninger, C.L. Stern, T.J. Marks, Organometallics 16 (1997) 4486.
[57] P.W. Roesky, C.L. Stern, T.J. Marks, Organometallics 16 (1997) 4705.
[58] C.M. Haar, C.L. Stern, T.J. Marks, Organometallics 15 (1996) 1765.
[59] G.A. Molander, J. Winterfeld, J. Organomet. Chem. 524 (1996) 275.
[60] G.A. Molander, J.O. Hoberg, J. Am. Chem Soc. 114 (1992) 3123.
[61] H.J. Heeres, A. Heeres, J.H. Teuben, Organometallics 9 (1990) 1508.
[62] G.M. Smith, J.D. Carpenter, T.J. Marks, J. Am. Chem. Soc. 108 (1986) 6805.
[63] P.J. Fagan, J.H. Manriquez, E.A. Maata, A.M. Seyam, T.J. Marks, J. Am. Chem. Soc. 103 (1981) 6650.
[64] Z. Lin, T.J. Marks, J. Am. Chem. Soc. 112 (1990) 5515.
[65] J.P. Collman, L.S. Hegedus, J.R. Norton, R.G. Finke, Principles and Applications of Organotransition Metal Chemistry, University Science, Mill Valley, CA, 1987 (Chapters 6.3, 10, 13).
[66] C. Elschenbroich, A. Salzer, Organometallics, VCH, Weinheim, Germany, 1989 (Chapter 17).
[67] L.S. Hegedus, in: G. Wilkinson, F.G.A. Stone, E.W. Abel (Eds.), Comprehensive Organometallic Chemistry II, vol. 12, Pergamon Press, Oxford, 1995.
[68] S.P. Nolan, D. Stern, D. Hedden, T.J. Marks, ACS Symp. Ser. 428 (1990) 159.

[69] J.A. Marthino Simões, J.L. Beauchamp, Chem. Rev. 90 (1990) 629.
[70] For recent olefin and alkyne d^0/f π complexes see Refs. [37,96].
[71] Q. Shen, D. Zheng, L. Lin, Y. Lin, J. Organomet. Chem. 391 (1990) 307.
[72] W.J. Evans, D.K. Drummond, T.P. Hanusa, J.M. Olofson, J. Organomet. Chem. 376 (1989) 311.
[73] K.H. Den Haan, Y. Wielstra, J.H. Teuben, Organometallics 6 (1987) 2053.
[74] W.J. Evans, I. Bloom, W.E. Hunter, J.L. Atwood, Organometallics 2 (1983) 709.
[75] T.J. Marks, in: J.J. Katz, G.T. Seaborg, L.R. Morss (Eds.), The Chemistry of the Actinide Elements, second ed., Chapman and Hall, London, 1986 (Chapters 23 and 24).
[76] T. Straub, A. Haskel, M.S. Eisen, J. Am. Chem. Soc. 117 (1995) 6364.
[77] T. Straub, A. Haskel, A.K. Dash, M.S. Eisen, J. Am. Chem. Soc. 121 (1999) 3014.
[78] J.Q. Wang, M.S. Eisen, unpublished results.
[79] A. Ohff, V.V. Burlakov, U. Rosenthal, J. Mol. Catal. 108 (1996) 119.
[80] J. Wang, A.K. Dash, M. Kapon, J.C. Berthet, M. Ephritikhine, M.S. Eisen, Chem. Eur. J. 8 (2002) 5384.
[81] A. Haskel, J.Q. Wang, T. Straub, T. Gueta-Neyroud, M.S. Eisen, J. Am. Chem. Soc. 121 (1999) 3025.
[82] J.F. Pelletier, A. Mortreux, X. Olonde, K. Bujadoux, Angew. Chem. Int. Ed. Engl. 35 (1996) 1854.
[83] E.G. Samsel, Patent Application EP 574,854 (1993).
[84] A. Haskel, T. Straub, M.S. Eisen, Organometallics 15 (1996) 3773.
[85] T.R. Straub, W. Frank, M.S. Eisen, J. Chem. Soc. Dalton Trans. (1996) 2541.
[86] M.R. Gagné, C.L. Stern, T.J. Marks, J. Am. Chem. Soc. 114 (1992) 275.
[87] M.R. Gagné, L. Brard, V.P. Conticello, M.A. Giardello, C.L. Stern, T.J. Marks, Organometallics 11 (1992) 2003.
[88] M.S. Eisen, T. Straub, A. Haskel, J. Alloys Compd. 271–273 (1998) 116.
[89] P.J. Walsh, A.M. Baranger, R.G. Bergman, J. Am. Chem. Soc. 114 (1992) 1708.
[90] A.M. Baranger, P.J. Walsh, R.G. Bergman, J. Am. Chem. Soc. 115 (1993) 2753.
[91] G.M. Smith, H. Susuki, D.C. Sonnenberg, V.W. Day, T.J. Marks, Organometallics 5 (1986) 549.
[92] M.A. Giardello, W.A. King, S.P. Nolan, M. Porchia, C. Sishta, T.J. Marks, in: J.A. Martinho Simões (Ed.), Energetics of Organometallic Species, Kluwer, Academic Press, Dodrecht, The Netherlands, 1992, p. 35.
[93] J.W. Bruno, T.J. Marks, L.R. Morss, J. Am. Chem. Soc. 105 (1983) 6824.
[94] Y.X. Chen, M.V. Metz, L. Li, C.L. Stern, T.J. Marks, J. Am. Chem. Soc. 120 (1998) 6287.
[95] L. Jia, X. Yang, C.L. Stern, T.J. Marks, Organometallics 16 (1997) 842.
[96] J.Q. Wang, A.K. Dash, J.C. Berthet, M. Ephritikhine, M.S. Eisen, Organometallics 18 (1999) 2407.
[97] A.K. Dash, J.Q. Wang, J.C. Berthet, M. Ephritikhine, M.S. Eisen, J. Organom. Chem. 604 (2000) 83.
[98] J.W. Faller, A.M. Rosan, J. Am. Chem. Soc. 99 (1977) 4858.
[99] P.W. Roesky, C.L. Stern, T.J. Marks, Organometallics 16 (1997) 4705.
[100] S. Tian, V.M. Arredondo, C.L. Stern, T.J. Marks, Organometallics 18 (1999) 2568.
[101] G.A. Molander, E.D. Dowdy, J. Org. Chem. 64 (1999) 6515.
[102] Y. Li, T.J. Marks, J. Am. Chem. Soc. 120 (1998) 1757.
[103] M.R. Buergstein, H. Berberich, P.W. Roesky, Organometallics 17 (1998) 1452.
[104] Y. Li, T.J. Marks, Organometallics 15 (1996) 3770.
[105] V.M. Arredondo, S. Tian, F.E. McDonald, T.J. Marks, J. Am. Chem. Soc. 121 (1999) 3633.
[106] V.M. Arredondo, F.E. McDonald, T.J. Marks, Organometallics 18 (1999) 1949.
[107] J. Haggin, Chem. Eng. News 17 (1993) 23.
[108] T. Straub, A. Haskel, T.G. Neyroud, M. Kapon, M. Botoshansky, M.S. Eisen, Organometallics 20 (2001) 5017.
[109] A.G. Brook, A.R. Bassindale, Rearrangements in Ground and Exited States, vol. 2, Academic Press, New York, 1980.
[110] P.J. Walsh, F.J. Hollander, R.G. Bergman, Organometallics 12 (1993) 3705.
[111] I. Fleming, J. Dunogues, R.H. Smithers, Org. React. 37 (1989) 57.
[112] T.H. Chan, Acc. Chem. Res. 10 (1977) 442.
[113] E.W. Colvin, Silicon Reagents in Organic Synthesis, Academic Press, London, 1988.
[114] M.A. Esteruelas, O. Nurnberg, M. Olivian, L.A. Oro, H. Werner, Organometallics 12 (1993) 3264.
[115] R. Takeuchi, N. Tanouchi, J. Chem. Soc. Perkin Trans. 1 (1994) 2909.
[116] N. Asao, T. Sudo, Y. Yamamoto, J. Org. Chem. 61 (1996) 7654.
[117] A.K. Dash, J.Q. Wang, M.S. Eisen, Organometallics 18 (1999) 4724.
[118] C. Aitken, J.P. Barry, F.G. Gauvin, J.F. Harrod, A. Malek, D. Rousseau, Organometallics 8 (1989) 1732.
[119] Y. Apeloig, in: S. Patai, Z. Rappoport (Eds.), The Chemistry of Organic Silicon Compounds, Wiley-Interscience, New York, 1989, p. 57.
[120] C.M. Forsyth, S.P. Nolan, T.J. Marks, Organometallics 10 (1991) 2543.
[121] T.D. Tilley, Acc. Chem. Res. 26 (1993) 22.
[122] J.Y. Corey, J.L. Huhmann, X.H. Zhu, Organometallics 12B (1993) 1121.
[123] J.F. Harrod, in: R.M. Lain (Ed.), Inorganic and Organometallic Polymers with Special Properties, Kluwer Academic Publishers, Amsterdam, 1991 (Chapter 14).
[124] I. Ojima, Z. Li, J. Zhu, in: Y. Appeloig, Z. Rappoport (Eds.), The Chemistry of Organic Silicon Compounds, Willey, New York, 1998 (Chapter 29) and references therein.
[125] J. Reichl, D.H. Berry, Adv. Organomet. Chem. 43 (1998) 197.
[126] B. Marciniec, J. Gulinsky, W. Urbaniak, Z.W. Kornetka, in: B. Marciniec (Ed.), Comprehensive Handbook on Hydrosilylation, Pergamon, Oxford, UK, 1992.
[127] A.J. Chalk, J.F. Harrod, J. Am. Chem. Soc. 87 (1965) 16.
[128] J.F. Harrod, A.J. Chalk, J. Am. Chem. Soc. 87 (1965) 1133.
[129] R.S. Tanke, R.H. Crabtree, Organometallics 10 (1991) 415.
[130] R. Takeuchi, H. Yasue, Organometallics 15 (1996) 2098.
[131] F. Seitz, M.S. Wrighton, Angew. Chem. Int. Ed. Engl. 27 (1988) 289; F. Seitz, M.S. Wrighton, Angew. Chem. 100 (1988) 281.
[132] S.B. Duckett, R.N. Perutz, Organometallics 11 (1992) 90.
[133] J. Ruiz, P.O. Bentz, B.E. Mann, C.M. Spencer, B.F. Taylor, P.M. Maitlis, J. Chem. Soc. Dalton Trans. (1987) 2709.
[134] B.M. Bode, P.N. Day, M.S. Gordon, J. Am. Chem. Soc. 120 (1998) 1552.
[135] S. Sakaki, N. Mizoe, M. Sugimoto, Organometallics 17 (1998) 2510.
[136] H. Schumann, M.R. Keitsch, J. Demtschuk, G.A. Molander, J. Organomet. Chem. 582 (1999) 70.
[137] G.A. Molander, E.E. Knight, J. Org. Chem. 63 (1998) 7009.
[138] T. Hiyama, T. Kusumoto, in: B.M. Trost, I. Fleming (Eds.), Comprehensive Organic Synyhesis, vol. 8, Pergamon Press, Oxford, 1991.
[139] W.P. Weber, Silicon Reagents for Organic Synthesis, Springer–Verlag, Berlin, 1983.
[140] T. Sudo, N. Asao, V. Gevorgyan, Y. Yamamoto, J. Org. Chem. 64 (1999) 2494.
[141] T.J. Selin, R. West, J. Am. Chem. Soc. 84 (1962) 1860.
[142] M.S. Eisen, in: Y. Appeloig, Z. Rappoport (Eds.), The Chemistry of Organosilicon Compounds, vol. 2, John Wiley, Chichester, 1998, p. 2038 (Part 3).
[143] M.S. Eisen, Rev. Inorg. Chem. 17 (1997) 25.
[144] N.S. Radu, M.P. Engeler, C.P. Gerlach, T.D. Tilley, A.L. Rheingold, J. Am. Chem. Soc. 117 (1995) 3621.
[145] J.X. Wang, A.K. Dash, J.C. Berthet, M. Ephritikhine, M.S. Eisen, J. Organomet. Chem. 610 (2000) 49.
[146] W.D. Wang, R. Eisenberg, Organometallics 10 (1991) 2222.
[147] C. Biran, Y.D. Blum, R. Glaser, D.S. Tse, K.A. Youngdahl, R.M. Laine, J. Mol. Catal. 48 (1988) 183.
[148] Y. Blum, R.M. Laine, Organometallics 5 (1986) 2081.
[149] H.Q. Liu, J.F. Harrod, Organometallics 11 (1992) 822.

[150] J. He, H.Q. Liu, J.F. Harrod, R. Hynes, Organometallics 13 (1994) 336.

[151] F. Lunzer, C. Marschner, S. Landgraf, J. Organomet. Chem. 568 (1998) 253.

[152] X. Liu, Z. Wu, Z. Peng, Y.D. Wu, Z. Xue, J. Am. Chem. Soc. 121 (1999) 5350.

[153] M.F. Lappert, P.P. Power, A.R. Sanger, R.C. Srivastava, Metal and Metalloid Amides: Synthesis, Structures, and Physical and Chemical Properties, Ellis Horwood-Wiley, Chichester, New York, 1980 (Chapters 12 and 13).

[154] D.S. Hays, G.C. Fu, J. Org. Chem. 62 (1997) 7070.

[155] A.M. Martins, J.R. Ascenso, C.G. De-Azevedo, A.R. Dias, M.T. Duarte, J.F. Da-Silva, L.F. Veiros, S.S. Rodrigues, Organometallics 22 (2003) 4218.

[156] F. Takei, K. Yanai, K. Onitsuka, S. Takahashi, Chem. Eur. J. 6 (2000) 983.

[157] W. Ahlers, G. Erker, R.J. Fröhlich, Organomet. Chem. 571 (1998) 83.

[158] M.D. Stadnichuk, A.V. Khramchikhin, Y.L. Piterskaya, I.V. Suvorova, Russ. J. Gen. Chem. 69 (1999) 593.

[159] M. Meier, B. Muller, C. Ruchart, J. Org. Chem. 52 (1987) 648.

[160] X. Yang, C.L. Stern, T.J. Marks, Organometallics 10 (1991) 840.

[161] J. Lia, X. Yang, C.L. Stern, T.J. Marks, Organometallics 16 (1997) 842.

[162] R.G. Peters, B.P. Warner, C.J. Burns, J. Am. Chem. Soc. 121 (1999) 5585.

[163] Y. Iwasawa, B.C. Gates, CHEMTEC 3 (1989) 173.

[164] Y.I. Yermakov, B.N. Kuznetsov, V.A. Zakharov, Catalysis by Supported Complexes, Elsevier, Amsterdam, 1981.

[165] T.J. Marks, Acc. Chem. Res. 25 (1992) 57.

[166] R.D. Gillespie, R.L. Burwell, T.J. Marks, Langmuir 6 (1990) 1465.

[167] W.C. Finch, R.D. Gillespie, D. Hedden, T.J. Marks, J. Am. Chem. Soc. 112 (1990) 6221.

[168] R.L. Burwell, T.J. Marks, in: R.L. Augustine (Ed.), Catalysis of Organic Reactions, Marcel Dekker Inc., New York, 1985, p. 207.

[169] M.Y. He, G. Xiong, P.J. Toscano, R.L. Burwell, T.J. Marks, J. Am. Chem. Soc. 107 (1985) 641.

[170] M.S. Eisen, T.J. Marks, J. Am. Chem. Soc. 114 (1992) 10358.

[171] R.H. Crabtree, J. Chem. Soc. Dalton Trans. 17 (2001) 2437.

[172] P.L. Watson, in: J.A. Davies, P.L. Watson, J.F. Liebman, A. Greenberg (Eds.), Selective Hydrocarbon Activation, VCH, New York, 1990 (Chapter 4).

[173] A.D. Ryabov, Chem. Rev. 90 (1990) 403.

[174] A.E. Shilov, Activation of Saturated Hydrocarbons by Transition Metal Complexes, D. Reidel, Hingham, MA, 1984.

[175] M.S. Eisen, T.J. Marks, Organometallics 11 (1992) 3939.

[176] J.B. Butt, R.L. Burwell, Catal. Today 12 (1992) 177.